CIVIL ENGINEERING STUDIES

STRUCTURAL RESEARCH SERIES NO. 318

FATIGUE OF PLATES AND WELDMENTS IN HIGH STRENGTH STEELS

By

J. B. RADZIMINSKI

R. W. HINTON

D. F. MEINHEIT

H. A. OSMAN

W. H. BRUCKNER

and

W. H. MUNSE

A REPORT OF AN INVESTIGATION CONDUCTED

by

THE CIVIL ENGINEERING DEPARTMENT
UNIVERSITY OF ILLINOIS

in cooperation with

The Naval Ship Systems Command, U. S. Navy

Contract NObs 94232

Project Serial No. SF-020-01-05, Task 729-0

UNIVERSITY OF ILLINOIS
URBANA, ILLINOIS
FEBRUARY, 1967

FATIGUE OF PLATES AND WELDMENTS IN HIGH STRENGTH STEELS

Final Report

by

J. B. Radziminski
R. W. Hinton
D. F. Meinheit
H. A. Osman
W. H. Bruckner

and

W. H. Munse

A Report of an Investigation Conducted

by

THE CIVIL ENGINEERING DEPARTMENT
UNIVERSITY OF ILLINOIS

in cooperation with

The Naval Ship Systems Command, U. S. Navy
Contract NObs 94232
Project Serial No. SF-020-01-05, Task 729-0

University of Illinois
Urbana, Illinois
February 1967

ABSTRACT

An evaluation of the axial fatigue behavior of transverse butt-welded joints in HY-100 steel is presented. Welding procedures, using MIL-12018 and MIL-11018 electrodes, have been developed in which the defect density is held to a minimum. Specimens welded in accordance with these procedures initiated fatigue failures on the surface at the stress raiser created by the geometry at toe of the weld. For these members, the S-N curve for the life range from 10^4 to 10^6 cycles is presented for a stress cycle of zero-to-tension. Radiographic and ultrasonic inspections were used to study fatigue crack initiation and propagation originating at an internal weld flaw.

A preliminary investigation of the axial fatigue behavior of MIG weldments in HY-130/150 steel is reported. The majority of the transverse butt-welded specimens prepared at each of three laboratories initiated fatigue failures at a variety of internal defects when subjected to a cyclic maximum stress of approximately half the ultimate strength of the base metal. Several alterations in the standard MIG welding procedures were studied in an effort to improve the weld quality; however no modification has been entirely successful in eliminating all the defects which have proven to be critical points for fatigue crack nucleation.

TABLE OF CONTENTS

TABLE OF CONTENTS (continued)

LIST OF TABLES

LIST OF TABLES (continued)

LIST OF FIGURES

LIST OF FIGURES (continued)

LIST OF FIGURES (continued)

I. INTRODUCTION

1.1 Object of Study

The investigation reported herein was divided into two phases. The first phase consisted of examining the fatigue behavior of axially loaded, transverse butt welds in HY-100 steel using the MIL-12018 electrode. In addition, specimens with intentional internal defects were examined by radiographic and ultrasonic means both prior to and during fatigue cycling. These studies provided information concerning the crack initiation and propagation stages of fatigue failure. The fatigue lives of these specimens were then compared to the fatigue lives of sound welds to determine the effect of internal defects on fatigue life.

The second phase was concerned with the fatigue behavior of axially loaded plain plates and transverse butt welds in HY-130/150 steel. Before examining the fatigue properties of the welded joints, it was necessary to develop and qualify several welding procedures for MIG welding of the HY-130/150 plates using currently available welding wires. Four of the most promising of these procedures were then used to prepare butt-welded specimens which were tested under cyclic loading conditions. The fatigue test results from the joints prepared at the University of Illinois were then compared to the fatigue data for similar specimens welded at other research laboratories. Preliminary studies of crack initiation and propagation were also conducted and are reported.

1.2 Scope of Investigation

The studies reported for the HY-100 steel were conducted on transverse butt-welded joints with a 3/4 in. base metal thickness. The welded specimens were tested in two conditions: as welded, and with the weld reinforcement removed. The majority of the specimens tested were welded using either procedure P100-12018-A or P100-12018-C, (MIL-12018 electrode); a few

specimens were prepared using the MIL-11018 electrode for purposes of data comparison. All members were tested at a stress cycle of zero-to-tension. Two intentionally defective weldments, tested with the reinforcement removed, were examined radiographically and ultrasonically during cycling to determine the time to initiation, and the subsequent propagation of a fatigue crack.

The tests reported for the HY-130/150 steel were conducted with a base metal having a thickness of 1 inch. Both transverse butt-welded joints and plain plates were tested at a stress cycle of zero-to-tension. The butt-welded joints were examined in both the as-welded condition and with the reinforcement removed; the plain plates were tested in the as-received state and with the mill scale planed off. For comparison purposes welded specimens were prepared also at the laboratories of United States Steel Corporation and United States Naval Applied Science Laboratory and fatigue tested at the facilities of the University of Illinois.

The tests reported herein were conducted during the period from October, 1965 to October, 1966.

1.3 Acknowledgments

The tests reported in this study are the result of an investigation conducted in the Civil Engineering Department of the University of Illinois. The program was carried out with funds provided by the Naval Ship Systems Command, U. S. Navy, under Contract NObs 94232, Project Serial No. SF-020-01-05, Task 729-0.

This investigation constitutes a part of the structural research program of the Department of Civil Engineering, of which Dr. N. M. Newmark is the Head. The program is under the general direction of W. H. Munse, Professor of Civil Engineering; the fatigue research was conducted by

D. F. Meinheit and H. A. Osman, Research Assistants in Civil Engineering, under the direct supervision of J. B. Radziminski, Assistant Professor in Civil Engineering. The metallurgical studies were conducted by R. W. Hinton, Research Assistant, under the direction of W. H. Bruckner, Professor of Metallurgical Engineering.

The authors wish to express their appreciation to the many people on the staff of the University who so ably assisted in the investigation.

II. DESCRIPTION OF TEST PROGRAM

2.1 Material

The present study was conducted on two grades of quenched and tempered steel, HY-100 and HY-130/150. The HY-100 plate thickness was 3/4 in. while 1 in. thick plate material was used for the HY-130/150 specimens. The mechanical properties and chemical compositions of both steels are presented in Tables 2.1 and 2.2, respectively.

Fabrication of the HY-100 welded joints included use of both MIL-11018 and MIL-12018 electrodes. The electrodes were conditioned in accordance with current Navy Specifications.[1] To fabricate welded joints in the HY-130/150 material, various metal inert gas (MIG) welding procedures were used employing two welding wires; Linde X-150 and Airco AX-140. The chemical compositions of these MIG wires, obtained from ladle analyses, are presented in Table 2.3.

2.2 Fabrication of Specimens

The details of the test specimens are presented in Fig. 2.1. The fabrication technique for all specimens was similar except for differences in the welding procedures. Specimen blanks, 9 in. by 48 in., were first flame cut from larger 3/4 in. HY-100 and 1 in. HY-130/150 steel plates. For the transverse butt-welded specimens, the blanks were saw cut in half (9" x 24") and the saw cut edges were beveled by machining to provide a double "V" groove for the weld metal. The included angle of the groove was 60° for all procedures examined. All welding was performed in the flat position with the specimens loosely clamped in a special jig which could be rotated about a horizontal axis (the longitudinal axis of the weld). The

standard procedures for welding of the HY-100 and HY-130/150 plates are presented in Chapters III and IV, respectively.

After the welding was completed, holes were drilled in the ends of the specimens as shown in Fig. 2.1. The test section was then milled so that a 5 in. long straight section remained in the center of the specimen. No material in the region of the test section was removed by flame cutting. The width of the test section was governed by the test load range and the capacity of the fatigue testing machine, the width being made as large as possible within the capacity of the machine.

As a final stage of fabrication, the edges of the specimen in the test section were ground smooth and any sharp burrs filed off. For those butt joints tested with the reinforcement removed, the specimen faces were first planed, and then rough polished with a belt sander to a standard average roughness of approximately 32. The polishing was continued until all visible surface scratches were removed except those left by the polishing operation; the remaining scratches were thus all parallel to the direction of subsequent loading.

2.3 Fatigue Testing Equipment and Procedure

All fatigue tests were conducted using the University of Illinois' 250,000 lb. and 200,000 lb. lever type fatigue machines. The operating speeds of the machines are 100 and 180 cycles per minute, respectively.

The essential features of the fatigue machines are shown schematically in Fig. 2.2. The lever system provides a force multiplication ratio of approximately 15 to 1. The load range is adjusted through the throw of the eccentric, while the maximum load is controlled by the adjustable turnbuckle mounted just below the dynamometer.

The testing procedure was similar for all specimens. After the load had been set and the machine started, a micro-switch was set so that the machine would automatically shut off when a crack had propagated partially through the specimen.* The load was maintained within limits of ± 0.5 ksi by periodic checks, with adjustments made when necessary. Fatigue failure was assumed to have occurred when the micro-switch shut off the machine. The cycling was then continued until complete fracture occurred so that the fracture surfaces of the specimen could be examined.

2.4 Non-Destructive Testing Equipment and Procedures

Prior to fatigue testing, all welded specimens were subjected to radiographic examination using a sensitivity level of 2 percent. For those specimens used in the crack initiation and propagation studies, the x-ray equipment was assembled on a portable table, as pictured in Fig. 2.3, and placed directly against the test specimen mounted in the fatigue machine. A lead-shielded enclosure was built around the x-ray equipment to prevent any contamination of the laboratory from stray radiation. Using this equipment, radiographs were taken periodically during a fatigue test; the radiograph thus obtained offered a quantitative measurement of the length of a crack extending from an internal flaw well before the crack was visible on the specimen surface. The results of this investigation are presented in Section 3.4.

---

* For several of the HY-130/150 welded joints tested at high stress levels complete fracture occurred abruptly and with a loud report before the micro-switch was tripped.

Several of the transverse butt-welded specimens (with the reinforcement removed) were also examined ultrasonically both before and during fatigue cycling. The equipment used in conducting the ultrasonic traces is shown in Fig. 2.4. A complete description of this equipment and its use is presented in Section 3.4.

2.5 Metallurgical Studies

Metallurgical examinations of the fatigue fractures were performed for specimens welded using each of the HY-100 procedures. As a result of the metallurgical investigations, a number of alterations in the welding techniques were suggested, which led to improvements in the quality of the transverse butt-weldments in HY-100 steel. One alteration of particular significance was the use of a carbide wheel to grind the root pass and, when grinding was needed, for other subsequent passes during the deposition of the weld metal. Use of the carbide grinding wheel resulted in a very low concentration of internal pores near the fusion line of the root pass; such flaws had frequently been the points of fatigue crack initiation in specimens where bonded metal oxide grinding wheels had been used to grind the root pass. A complete discussion of this investigation is presented in Section 3.2.

Several welding procedures and MIG wires for use with the HY-130/150 steel were examined to develop a suitable welding procedure for transverse butt welds. The MIG welding procedures were evaluated by standard metallographic techniques to determine the type and concentration of internal defects; the most promising of the procedures were then used in the preparation of fatigue specimens.

The techniques of electron microfractography were used to observe the fracture surfaces exposed by fatigue and static tension tests in welded joints of HY-100 steel, and in both plain plates and welded joints of HY-130/150 steel. Both a two stage plastic replication process and a direct carbon replication process involving a chemical extraction of the carbon film were used to observe in detail the contours of the fracture surfaces at a high magnification with the electron microscope.

III. STUDIES OF HY-100 MATERIAL

3.1 Introductory Remarks

Prior to the present study, several series of tests were conducted on specimens of 3/4 in. thick HY-100 steel to evaluate the fatigue behavior of transverse butt joints fabricated using various welding procedures developed for the MIL-11018 coated electrode.[3] The original procedure, P100-11018-J (Fig. 3.1), was identical to that used earlier to weld similar joints in HY-80 steel. However, with the HY-100 base material, specimens prepared using this procedure often developed fatigue failures initiating at internal defects rather than at the external geometry of the butt weld. In an attempt to improve the quality of the HY-100 weldments, two additional procedures were developed, P100-11018-J30 and P100-11018-J50, Figs. 3.2 and 3.3, respectively. The results of subsequent fatigue testing indicated that these modifications to the original welding procedure provided no substantial improvement in fatigue behavior.[3]

As a result of the poor initial axial fatigue behavior obtained for welded joints of HY-100 steel plates containing transverse butt welds made with the MIL-11018 electrode, a study was undertaken to evaluate the behavior of similar weldments using the higher strength MIL-12018 electrode. The early test results using the MIL-12018 electrode again did not show the expected increase in fatigue resistance, and fatigue failures which initiated internally were still commonplace. Thus, a complete re-evaluation of the existing welding procedures and techniques was undertaken as a part of the current investigation. Discussion of the new techniques developed and of the fatigue performance of the latest weldments is presented in the following section.

3.2 Evaluation of Welding Procedures for HY-100 Steel

As mentioned above, early studies of the fatigue behavior of HY-100 plates welded with the MIL-11018 electrode indicated that internal crack initiation and a corresponding wide scatter in fatigue lives often were obtained for tests conducted at a particular stress level; this was especially evident for specimens tested with the reinforcement removed.[3] The relatively low lives and the scatter in the results were attributed to an undermatching of the weld metal strength relative to that of the base material, and to the presence of the small internal weld flaws which were critical points for fatigue crack initiation.

In an effort to improve the fatigue resistance and to effect greater consistency in fatigue lives, an investigation into the use of the MIL-12018 electrode in HY-100 weldments was initiated. Two separate welding procedures were studied. The procedures, P100-12018-A and P100-12018-C, are illustrated in Figs. 3.4 and 3.5, respectively. Both welding procedures have been qualified in accordance with Navy Specifications currently in effect for HY-80 steels.[1] The qualifications included reduced section tension tests, side bend tests, macro-etch specimens, and radiographic examination, all of which satisfactorily passed. In addition, microhardness traces were taken of the P100-12018-A weldment on a typical cross-sectional plane transverse to the long axis of the weld beads. The results of this survey are compared in Table 3.1 with the weld metal hardnesses obtained for several procedures using the MIL-11018 electrode. Details of the MIL-11018 electrode welding procedures are presented in Ref. (3) and Figs. 3.1, 3.2, and 3.3. It was found that the hardness of the weldment using procedure P100-12018-A was increased relative to the hardness of the MIL-11018 electrode weldments except at the very center of the weld.

When the first of the HY-100 specimens prepared using procedure P100-12018-A were tested in fatigue, no appreciable difference in lives was observed relative to specimens using the MIL-11018 electrode and tested at the same stress level. Internal weld failures at small isolated pores were again obtained at the higher stress levels, even when the reinforcement was left in place. It was concluded, therefore, that the presence of the small pores, and not the electrode strength per se, was responsible for the lower lives obtained in the HY-100 weldments.

For specimens prepared with both the MIL-11018 and MIL-12018 electrodes, it was noted that the internal flaws, located near the center of the weld, were created after deposition of either the first or second weld pass. Since a bonded metal oxide grinding wheel was used to grind the surface of the first weld pass before depositing the second pass, it was thought that particles from the wheel itself (possibly the metal oxide or the resin fiber bonding material) were becoming embedded in the weld and then decomposing during subsequent welding to produce the observed pores. In an attempt to eliminate pores formed in this manner, a carbide grinding wheel was used in the preparation of several welded specimens using procedure P100-12018-A.

Sections transverse to the weld axis were then cut at random locations from a number of weldments prepared using both the metal oxide and the carbide wheels to obtain a quantitative measure of the amount of porosity resulting from the use of each of these wheels. Comparisons of the porosity observed at the cut sections are presented in Table 3.2. (Although both the MIL-11018 and MIL-12018 electrodes were used in the weldments, as noted in Table 3.2, the alloy composition and electrode coatings were quite similar for these electrodes; thus, the reported

differences in porosity have been attributed primarily to the type of grinding wheel used in grinding of the root pass.) When the bonded metal oxide grinding wheel was used, about half of the sections examined had at least one measureable pore. On the other hand, no pores greater in diameter than 0.02 mm (minimum pore size recorded) were found in any of the ten sections cut from the weldments in which the root pass was ground using a carbide grinding wheel. The higher quality of weldments prepared with the carbide wheel was further substantiated by the fatigue results reported in Section 3.3.1 for specimens which were welded in accordance with procedure P100-12018-A. The majority of these specimens failed at the toe of the weld rather than by initiating failure at an internal pore, as was prevalent in earlier fatigue specimens which employed the bonded metal oxide grinding wheel.

With this evidence of improved weld quality for specimens prepared with the MIL-12018 electrode and using the carbide grinding wheel, a number of additional specimens were welded in accordance with procedure P100-11018-J (MIL-11018 electrode), also using the carbide wheel. These specimens also showed a lower density of pores in comparison to similar joints prepared with an oxide grinding wheel. Thus it is apparent that HY-100 weldments of consistently high quality (i.e., low defect density) and, as reported later, with comparatively good fatigue properties, can be obtained by using carbide grinding and by employing carefully regulated welding techniques.

In addition to the 6 pass weldments discussed above, several samples of HY-100 steel were joined in accordance with procedure P100-12018-C, Fig. 3.5, in which 12 weld passes (MIL-12018 electrode) were used in the same 3/4 in. thick material. The values of microhardness of the weld metal

at a number of indentations located along the mid-thickness, the near surface, and the center line of the 12 pass weldment, shown in Table 3.1, are not significantly different from the 6 pass welds using the MIL-12018 electrodes. The increase in microhardness of the as-deposited weld metal of MIL-12018 electrodes compared to the hardness of the as-deposited weld metal of MIL-11018 electrodes is also shown in Table 3.1.

3.3 Fatigue Test Results

3.3.1 Test Results for Standard Weldments

3.3.1.1 Tests of As-Welded Transverse Butt Joints

As discussed in the previous section, a study was initiated to develop procedures using the MIL-12018 electrode in an effort to improve the fatigue behavior of as-welded joints in HY-100 steel. The fatigue test results comparing specimens welded in accordance with procedures P100-12018-A (MIL-12018 electrode) and P100-11018-J (MIL-11018 electrode) are presented in Table 3.3 and plotted in Fig. 3.6. (It should be noted that a metal oxide grinding wheel was used in the preparation of all specimens shown in Fig. 3.6.) A typical fatigue fracture surface, showing failure initiation at internal defects, is shown in Fig. 3.7a. The low fatigue lives reported in Table 3.3 for tests conducted at the higher cyclic stress levels led to the re-evaluation of the welding procedures outlined in Section 3.2.

After it had been ascertained that the metal oxide grinding wheel was at least partially responsible for the introduction of porosity in the early weldments using both electrodes, several specimens were prepared in which the carbide wheel was used to grind the root pass. The first carbide wheel used did eliminate the internal porosity but its width (3/8 in. radius face) did not allow complete back grinding of the root pass which, in turn,

resulted in a lack of fusion in some weldments. A narrower (1/4 in. radius face) wheel was then used and weldments of consistently high quality were obtained in later specimens prepared with the MIL-12018 electrode.

The test results for specimens prepared using carbide grinding and tested in fatigue are presented in Table 3.4 and plotted in Fig. 3.8. The three specimens, tested at 0 to +80.0 ksi, that failed in the weld were prepared with the first (3/8 in.) grinding wheel, which resulted in crack initiation in regions where lack of fusion was evident in two of the specimens. The other specimens were prepared using the 1/4 in. carbide wheel which produced sound weldments and resulted in the correspondingly longer fatigue lives associated with the externally-initiated failures, Table 3.4 and Fig. 3.8. Further, comparison of the latter test results with the data of Table 3.3 (oxide grinding of welds) again indicates the substantially improved fatigue resistance attained, at the higher stress levels examined, when failure originated at the toe of the weld rather than at the previously encountered internal defects. This behavior clearly points to the necessity, in HY-100 steel, of introducing stringent weld quality requirements if the fatigue resistance of welded joints is to be increased commensurate with the static strength of this material.

After the improved fatigue behavior was established for specimens welded with the MIL-12018 electrode and ground with the carbide wheel, several additional specimens, using the MIL-11018 electrode and also ground with the carbide wheel, were fabricated. Two of these specimens, HY-84 and HY-85, classified as sound weldments under radiographic examination, were then tested in fatigue at a stress level of 0 to +80.0 ksi; the results are given in Table 3.4 and plotted in Fig. 3.8. Both specimens initiated failure at the toe of the weld and had lives within the same range as the sound

specimens prepared with the MIL-12018 electrode. A typical fracture surface for a specimen prepared using a carbide grinding wheel and failing in fatigue at the toe of the weld is shown in Fig. 3.7b.

To determine an S-N curve for specimens tested in the as-welded condition, the data for all sound HY-100 transverse butt-welded joints were analyzed using the procedure detailed in Ref. 4; the computed fatigue strengths are presented in Table 3.5. Only those specimens which did not initiate failure at an internal flaw, regardless of radiographic rating, were considered as "sound" weldments. Since failure of these weldments initiated at the toe of the weld and because the heat affected zones of weldments using both the MIL-11018 and MIL-12018 electrodes are similar, specimens prepared with both electrodes were considered in the calculations of fatigue strength.

The data and computed S-N curve (K = 0.422) for the sound HY-100 weldments are plotted in Fig. 3.9 together with the S-N curve for sound HY-80 joints (3/4 in. thick base material) tested at the same zero-to-tension stress cycle.[5] No explanation can be offered at this time for the somewhat lower fatigue strengths of the HY-100 weldments relative to the strengths in the joints of HY-80 steel, especially since the HY-80 specimens also used the MIL-11018 electrode. One possible explanation could be a difference in the joint geometry (and, consequently, the stress concentration factors) at the toe of the weld which, in both materials, was the location for fatigue crack initiation. The geometries for these weldments have been preserved in plaster casts made of the surfaces of the joints; an analysis of the casts may provide more pertinent information.

3.3.1.2 Tests of Transverse Butt Joints with Reinforcement Removed

Several experimental welding procedures using the MIL-11018 electrode were investigated in an early attempt to improve weld quality over that first obtained with procedure P100-11018-J. Fatigue specimens were prepared using procedures P100-11018-J30 and P100-11018-J50 as well as P100-11018-J; the weldments were then tested with the reinforcement removed to force crack initiation at any internal defects which were present. The data which are presented in Table 3.6 and Fig. 3.10 show that the procedures resulted in lives no better than those of the as-welded plates, Figs. 3.6 and 3.8. For purposes of comparison, the S-N curve for "sound" HY-80 weldments tested with the reinforcement removed is also shown in Fig. 3.10.

The MIL-12018 electrode was then introduced in anticipation of better fatigue behavior in the reinforcement removed condition. Specimen HY-61, with the reinforcement removed, was prepared using this electrode and tested at 0 to +50.0 ksi. Although the life of this specimen, 607,600 cycles, was above the average for the corresponding specimens welded with the MIL-11018 electrode, failure still initiated at an internal pore, Table 3.6. It should be noted that the bonded metal oxide wheel was used in HY-61 to grind the root pass. When the carbide grinding wheel was used in the preparation of subsequent weldments, however, the improvement in fatigue behavior of specimens tested with the reinforcement removed became quite evident, as seen in the data presented in Table 3.7 and in Fig. 3.11. Note also that none of the three specimens listed in Table 3.7 initiated failure at an internal defect. No S-N curve is plotted since the three specimens tested did not represent sufficient data for fatigue strength computations. Fracture surfaces for specimens typical of those reported

in Tables 3.6 and 3.7 are shown in Figs. 3.2 a and b, respectively.

Although no specimens have been tested in the condition in which the reinforcement was removed for welded joints made with the MIL-11018 electrode and ground with the carbide grinding wheel, an improvement in the fatigue life would be expected similar to that obtained in the as-welded specimens when carbide grinding replaced the metal oxide grinding disc.

It can be seen that there is no significant improvement in fatigue resistance when the early tests in which the reinforcement was removed are compared with the corresponding early tests of samples in the as-welded condition, as shown in Tables 3.3 and 3.6. This was to be expected since specimens in both conditions generally failed at internal flaw locations. After a welding procedure was developed to produce sound welds with the MIL-12018 electrode and carbide grinding wheel, the fatigue lives of specimens both in the as-welded condition and with the reinforcement removed were found to be more consistent and generally longer than those of the joints which contained defects. One might also compare the sound specimens with the reinforcement removed to the sound as-welded specimens (Tables 3.5 and 3.7) and note that the increase in fatigue resistance of welds with the reinforcement removed, as anticipated by the removal of the stress raiser associated with the external weld geometry, is quite pronounced.

3.3.1.3 Concluding Remarks

The improved fatigue behavior obtained for the butt-welded joints of HY-100 steel when a carbide grinding wheel was used in the weld preparation shows the necessity of using such a wheel to eliminate, or at least decrease, the amount of internal defects in the HY-100 weldments. This

increased fatigue resistance is indicative not only of sound weldments using the higher strength MIL-12018 electrode but also of high quality weldments using the MIL-11018 electrode. The longer fatigue lives obtained for specimens using the carbide wheel in the weld preparation were invariably associated with failures initiating at the toe of the weld reinforcement, indicating that the geometrical stress raiser at the toe is less severe than the internal porosity or lack of fusion which caused earlier crack initiation in those specimens containing such defects.

The computed fatigue strengths for the sound weldments of HY-100 steel are compared in Table 3.8 with the fatigue strengths of the plane plates of HY-100 steel and with the corresponding strengths of plain plates and butt-welded joints in the HY-80 steel.[5,6] It was observed in this investigation that the fatigue resistance of the plane plate samples of HY-100 steel which were tested in the as-received condition possessed about the same fatigue resistance as that for the corresponding HY-80 plain plates. In contrast the fatigue resistance of the butt-welded joints of HY-100, as mentioned previously, was somewhat lower than the fatigue resistance of the welded joints of HY-80 steel over the range of lives examined. All fatigue strengths reported in Table 3.8 are for tests conducted at a stress cycle of zero-to-tension.

3.3.2 Test Results for Butt-Welded Joints Containing Intentional Defects

To determine the effect of relatively gross internal flaws (i.e., defect density or percent reduction in area, based on a radiograph of the welded joint, which was unacceptable according to Navy radiographic standards) on the fatigue resistance of HY-100 transverse butt-welded joints, several specimens were prepared containing intentional porosity and/or slag inclusions

in the weld. In the welding of the fatigue specimens containing intentional porosity, the preparation of the weld groove in the base plate was identical to that employed for all other specimens tested in the current study. The normal welding procedures, P100-11018-J (specimens HY-54, HY-55) and P100-12018-A (specimens HY-86, HY-87), were followed in welding the first pass. In order to introduce porosity into the second pass, the welder removed a one in. section of the electrode coating. This one in. section of bare wire, when introduced into the weld puddle caused a porosity cluster to be formed. The bare section was so positioned on the electrode that the porosity was located at about the midpoint of the fatigue samples. After the weld reinforcement was removed by milling and subsequent rough polishing of the surface, examination of these welded joints by standard radiographic techniques clearly showed the intentional porosity clusters. The rating for each specimen is given, according to current Navy radiographic standards,[7] in Table 3.9.

After the specimens were welded and the reinforcement removed as described above, they were tested in fatigue at a cyclic stress level of 0 to +50.0 ksi. The test results for the two latest specimens (HY-86 and HY-87) are presented in Table 3.9 together with the data for specimens HY-54 and HY-55, which are reported in Ref. 3. The results presented in Table 3.9 are plotted in Fig. 3.13. Figure 3.13 also shows the range of lives obtained for specimens containing unintentional weld defects and tested with the weld reinforcement removed (Table 3.6). Although two of the intentional defect specimens had lives below the minimum for those reported in Table 3.6, the overlapping of the data indicates that even small isolated pores (in most instances not detected by standard radiographic techniques) can at times be as critical in fatigue as the gross porosity clusters found in the four specimens represented in Fig. 3.13.

3.4 Fatigue Crack Initiation and Propagation

3.4.1 Locations for Fatigue Crack Initiation

3.4.1.1 Standard Weldments

The weldments made with the MIL-11018 and MIL-12018 electrodes, ground using a metal oxide wheel, and tested in the as-welded condition, showed a prevalent tendency toward internally initiated fatigue failures. As witnessed by the results reported in Table 3.3, the failures consistently initiated at single isolated pores when the specimens were tested at high stress levels. These single isolated pores were relatively small flaws, ranging in size from approximately 0.01 in. in diameter to 0.06 in. in diameter.

It is interesting to note that when the same type specimen was tested at a lower stress cycle (i.e., 0 to +30.0 ksi) the specimens exhibited a different fatigue behavior. The majority of the fatigue failures initiated at the edge of the weld reinforcement, indicating that, at the lower stress levels, the surface conditions are apparently more critical for crack initiation than are internal defects. These test results suggest that at the lower cyclic loads, the stresses in the weld probably remain elastic in the vicinity of the defects (the defects perhaps located in a region of compressive residual stress) whereas the stress raiser associated with the geometry of the weld toe (in a region of tensile residual stress) provides the critical condition for fatigue crack initiation.

Several butt-welded specimens were also tested in the reinforcement removed condition, as tabulated in Table 3.6; the data show that when oxide grinding was used, all failures initiated internally (except HY-57 which had extensive weld undercutting). For these specimens, except for

HY-57, the lack of a critical surface stress raiser together with the presence of internal defects forced the failure into the weld metal regardless of the test stress level.

When carbide grinding was first introduced in the welding procedure using the MIL-12018 electrode, two of the four as-welded joints initiated failure at areas where lack of fusion was evident. As noted in Section 3.2 this was attributed to the use of a grinding wheel which was too wide to permit complete grinding of the root pass. The second, narrower (1/4 in. radius face), wheel was then tried and found to generally eliminate both the lack of fusion and small isolated pores (see Table 3.4). By removing both the fusion and porosity problem, fatigue initiation was again brought back to the geometrical stress raiser at the toe of the weld reinforcement in the as-welded joints tested at the higher stress levels.

Further evidence that the narrower carbide grinding wheel eliminated these weld defects was found when a few specimens were tested in fatigue with the reinforcement removed (Table 3.7). Two of these specimens initiated failure on the mill scale surface of the plain plate in the transition radius, well removed from the weld. The third failed in the specimen pull-head.

3.4.1.2 Weldments Containing Intentional Defects

Two specimens with intentional defects (HY-86 and HY-87) were tested with the reinforcement removed. The results of the defect examination and the fatigue data are presented in Table 3.9 together with the data for two tests conducted previously.[3] In each of the specimens the point of fatigue crack initiation occurred at internal defects. The effect of the defect severity (measured quantitatively by the percent reduction

in the area detected by radiography) in reducing the fatigue resistance of these specimens in comparison to the fatigue lives obtained for sound weldments tested at the same stress cycle, Table 3.7, is prounounced. As can be seen from these results, various types and sizes of defects, when encountered in HY-100 weldments, can have a severly detrimental influence on the fatigue life of such joints. At the 0 to +50.0 ksi stress level the fatigue lives of the defective weldments were approximately an order of magnitude less than the life of the sound weldment HY-81, which was also tested with the reinforcement removed. No precise quantitative comparison can be made however, because the available data are quite minimal.

3.4.2 Crack Initiation and Propagation Studies

3.4.2.1 Examination Techniques

To study crack initiation and propagation, two separate techniques were employed. The first utilized a portable x-ray machine which was mounted for the purposes of this phase of the investigation, on a transportable table. The equipment and table are shown in Figs. 2.3 a and b. Each of the welded fatigue specimens was x-rayed prior to testing to determine the size and planer location of internal weld defects. After the specimen had been secured in the fatigue machine and subjected to a number of repeated loadings (the number of cycles being set as a certain percentage of the total expected life), the machine was shut off and the specimen was placed under maximum tensile test load. With the specimen in this stressed condition the x-ray equipment was moved up to the specimen and the x-ray film holder attached as shown in Fig. 2.3a. After loading of the film holder a lead shielding was secured in place behind the film (see Fig. 2.3b) to prevent any danger to personnel from stray radiation. The radiograph was

then taken of the region containing the butt weld; following this, fatigue cycling was restarted and continued to the time for the next reading. This process was then repeated for the remainder of the life of the specimen or until such time as a fatigue crack, which had initiated internally, propagated to the specimen surface and could be visually observed thereafter.

The second method used to detect initiation utilized the ultrasonic flaw detection equipment shown in Figs. 2.4a and b. The probe used was a commercial 5 megahertz minature 45^{o} angle transducer. A special unit was constructed to hold and manipulate the probe across the fatigue specimen surface in a consistent and highly reproducible manner. The probe support consists of a movable table which supports the probe housing and permits mechanical control of horizontal and vertical movements across the specimen face. The probe itself is held against the specimen by the force of a spring mounted in a ball bushing. The spring presses the face of the probe flush against the specimen with a constant pressure and thus insures reproducibility in readings. Linear transducers are attached to the traveling table which supports the probe; the transducers are connected in turn to an X-Y recorder. The detector screen is suitably scaled so that the position of a flaw echo indicates directly the depth of the flaw within the weld. Once the flaw echo is located on the oscilloscope, the position of the echo together with the output of the transducers enables the operator to record on the X-Y plotter the horizontal and vertical location of the flaw in a plane parallel to the specimen surface.

Figure 2.4b shows the ultrasonic equipment in position for testing with the probe support secured to the lower pull-head of the fatigue machine and the probe bearing against the test surface. The support device can be clamped to the testing machine pull-head on either side of the specimen.

The ultrasonic examinations were performed with the test specimen in the fatigue machine and under the maximum tension used for the particular fatigue test in question. All specimens examined contained transverse butt welds with the reinforcement removed. The specimen faces were polished smooth to prevent excessive wear on the probe and to improve the sensitivity. Light machine oil was used as an acoustic couplant between the probe and the specimen surface. As shown in Fig. 3.14, the weld area (including the heat affected zone) was scanned by traversing horizontally across the specimen face below the weld and in 1/8 in. vertical increments until one-half of the weld area had been scanned. The probe was then placed on the opposite side of the specimen to scan the other half of the weld. An appropriate test range was selected and the detector screen adjusted so that the echo trace between the first reflection from the rear surface and the second reflection from the front surface was visible (see Fig. 3.14).

Oscilloscope readings which exceeded a preselected minimum response level were assumed to indicate defects. Once a flaw (usually a small, isolated pore but often closely spaced pores forming a cluster) was detected, the peak response was pinpointed by moving the probe both horizontally and vertically until the maximum echo height was seen on the detector screen. The projected position of the flaw on a plane parallel to the face of the specimen was then automatically plotted on the X-Y recorder. The depth of the flaw beneath the surface was determined from the position of the flaw echo on the oscilloscope screen and was manually recorded together with the magnitude of the echo. Once the position of the peak response had been located, the probe was again moved horizontally and vertically until the magnitude of the echo fell beneath the selected

minimum response level. These limits were indicated on the X-Y plots by crosses extending from the peak response in directions parallel and transverse to the long axis of the test section.

3.4.2.2 Results of Flaw Detection Study

Two butt-welded specimens with the reinforcement removed, HY-86 and HY-87, were examined using the procedure outlined above. Specimen HY-87 was inspected ultrasonically both before testing and periodically during the course of fatigue cycling. After the specimen had failed, those flaws visible on the fracture surface were compared with the location and magnitude of the ultrasonic responses which were recorded at the time of the various cyclic readings. The results are presented in Fig. 3.15. These plots represent the projection of all the ultrasonic responses onto a cross-sectional plane through the weld perpendicular to the longitudinal axis of the fatigue specimen. The crosses in Fig. 3.15 indicate the limits of the probe scan for which the echo amplitude remained above the selected minimum rejection level. The letter designation is used to indicate the vertical position of the flaw along the longitudinal axis of the specimen. The sketch of the fatigue fracture surface shown in Fig. 3.15 represents a projection of the flaws visible on the fracture surface onto a similar plane perpendicular to the long axis of the specimen.

The number of the internal defects found in specimen HY-87 were so numerous that it was impossible to locate exactly each individual defect within the porosity cluster. Further difficulty was encountered when the ultrasonic readings, taken at various cyclic intervals, were analyzed in an attempt to pinpoint fatigue crack initiation by a rise in a particular ultrasonic response. In the massive number of high amplitude responses,

the one response that indicated initiation or fatigue crack growth was difficult to distinguish among the responses associated with the remainder of the defects found in the cluster. From this experience it appears that, when dense concentrations of porosity and/or slag are present in a welded joint the ultrasonic technique used in this investigation is not as adaptable for observing fatigue crack propagation as it was when single isolated pores were examined, Ref. 3.

The radiographic weld examination procedure described in Section 3.4.2.1 was also used to determine initiation and propagation of fatigue cracks in HY-100 joints. Figure 3.16 represents a sequence of radiographs taken of specimen HY-87 at several cyclic intervals during the fatigue life of the specimen. Close examination of the radiograph taken at 10,000 cycles reveals that a fatigue crack had initiated at the extremity of the weld defect. This represents crack nucleation within twenty percent of the total life of the specimen (see column 6, Table 3.10). Since only one such test was performed during this study, the ratio of 20 percent should by no means be considered typical for specimens containing other defect types and sizes (c.f., results obtained for HY-80 butt-welded joints, Ref. 8). Column 4 of Table 3.10 indicates the number of cycles at which the fatigue crack, measured on the radiographs, was equal in length to the specimen thickness. Thus, this number could also approximately be considered to represent, for a roughly circular fatigue crack, the number of cycles for which a crack originating at the very center of the weld could first be seen on the specimen surface. This ratio of cycles at initiation to cycles at which a centrally initiated crack intersects the specimen surface might truly be a more indicative measure of the maximum useful propagation life of a particular

structural component under axial loading, especially if failure is considered emminent when a crack has progressed through the entire thickness of the member.

After the fatigue crack had reached the surface of specimen HY-87, the mode of propagation changed from that of radial growth to crack propagation along planes oblique to the loading direction, exhibiting so-called "shear-type" crack growth behavior. The rate of crack propagation during both the early "fatigue" crack growth stage and the later "shear-type" growth stage, is presented in normalized form in Fig. 3.17 and is compared to the results obtained earlier for similar HY-80 welded joints.[8] Note, for some specimens of both materials, the slow, rather erratic manner of propagation, occupying between 60 and 80 percent of the total specimen lifetime, followed by the short period of continuously increasing rate of growth which culminated in complete specimen fracture. It must be mentioned, however, that other specimens did not initiate a fatigue crack (visible by radiography) until some 70 to 80 percent of the specimen lifetime had been reached. The rate of early crack propagation in these specimens was also much higher than for the others, as seen in Fig. 3.17. This condition could be quite critical for service structures, especially where periodic inspection intervals must be established.

3.5 Concluding Remarks

As discussed in the preceeding sections, it was ascertained that the use of a narrow carbide grinding wheel in the preparation of butt-welded joints in HY-100 steel greatly improved both the weld quality and the resultant fatigue behavior of such joints relative to the quality and fatigue behavior of similar joints prepared with a bonded metal oxide wheel.

Additionally, for those specimens prepared with the carbide wheel, fatigue failure was not of internal origin, but rather initiated at the external geometrical stress raiser created by the weld reinforcement. This behavior was evident for specimens prepared with both the MIL-12018 and MIL-11018 electrodes. However, the fatigue lives for these sound HY-100 welded specimens were still somewhat below the lives of similar as-welded HY-80 joints tested at the same zero-to-tension stress levels.

The initiation and propagation studies were not particularly successful, mainly as a result of the type of internal defect examined. It appears that the ultrasonic techniques of weld inspection are excellent in detecting the exact position and growth of a fatigue crack initiating at an isolated flaw or pore;[3] however, when a cluster of pores and/or slag inclusions are present, it becomes virtually impossible to locate every defect and to determine fatigue crack initiation and propagation originating at one of these defects. The radiographic examination data did provide useful, though limited, crack propagation information which was directly comparable to results obtained previously for HY-80 weldments.

IV. STUDIES OF HY-130/150 MATERIAL

4.1 Introductory Remarks

Studies were conducted as part of a continuing investigation to evaluate the axial fatigue behavior of HY-130/150 steel plates and weldments. The test specimens were cut from 1 in. thick plate material and were examined in fatigue at a stress cycle of zero-to-tension. The fatigue behavior of the 1 in. thick plain plate has been compared to that for 1/2 in. plain plate specimens tested previously;[3] the results are reported in Section 4.2. Various MIG welding procedures suitable for use with the 1 in. thick HY-130/150 steel plates have been investigated. Initially, two welding procedures were developed using the available MIG welding wires. Using specimens welded in accordance with these procedures, preliminary fatigue tests were conducted and the fracture surfaces examined for type of defect and point of crack nucleation. After evaluation of the two initial welding techniques, based on the specimen fatigue behavior and the location and appearances of the fatigue fractures, it was decided that additional changes in the procedures were necessary to obtain weldments of consistently higher quality. The fatigue test results for specimens prepared using the adjusted welding procedures, together with the data for specimens welded at other laboratories and tested in the facilities of the University of Illinois, are presented and compared in Section 4.4.

4.2 Fatigue Test Results for Plain Plates

The results of two fatigue tests on the 1 in. thick as-received HY-130/150 plain plates were found to be comparable to the previous behavior observed for the 1/2 in. as-received material.[3] The fatigue lives

are presented in Table 4.1 and plotted with the earlier data in Fig. 4.1. Note that the current results lie within the same life range as the 1/2 in. plates for the 0 to +80.0 ksi stress cycle examined. The fatigue strengths for all of the as-received specimens are computed in Table 4.1 and averaged for selected lifetimes. The fatigue diagram shown in Fig. 4.1 has a slope, K, equal to 0.22.

The fatigue strengths of the quenched and tempered HY-130/150 plates are compared to the equivalent fatigue strengths for both HY-80 steel[5,6] and HY-100 steel,[8] in Table 4.2. The S-N curve for each of these materials is also plotted in Fig. 4.1. In general, the specimens of HY-130/150 steel exhibited a slightly greater fatigue resistance than the other steels, notably at the higher stress levels examined. When the same steels are compared on the basis of the ratio of fatigue strength to ultimate strength, however, (Table 4.3 and Fig. 4.2) the HY-80 steel exhibits the best fatigue behavior relative to its static strength while the HY-130/150 steel plates show considerably less favorable resistance. This difference in relative behavior becomes more pronounced when the comparison is made between fatigue strength and yield strength, rather than ultimate strength, Table 4.4 and Fig. 4.3.

It was observed that the plain plates of HY-130/150 steel contained a thin exterior mill scale surface which easily flaked off during fatigue cycling at nominal stresses as low as 30% to 40% of the yield strength. As this thin mill scale flaked off, a rough oxidized layer was exposed which may have acted as a severe geometrical stress raiser under continued cycling. (In several instances, initiation of the fatigue crack occurred on the specimen surface rather than at the radius of the test

section, Table 4.1.) To determine if this condition was significantly affecting the total fatigue resistance of the HY-130/150 steel, four control specimens were prepared with the mill scale milled off and the test section polished parallel to the long axis of the specimen. Two of these specimens were tested at 0 to +100.0 ksi, and two at 0 to +80.0 ksi. The results are presented in Table 4.5 and compared to the data for the as-received specimens in Fig. 4.4. Based on these few tests, it is evident that removing the mill scale from the plate surface will considerably increase the life expectancy of a specimen tested in axial fatigue, at least at the stress levels examined. Caution must be exercised in using such results, however, as most actual structures are seldom polished in this manner before being placed in operation.

4.3 Development and Evaluation of MIG Welding Procedures for HY-130/150 Steel

4.3.1 Welding Procedures

The metal inert gas (MIG) welding process has been used to fabricate all of the butt-welded joints of HY-130/150 steel described in this study. Two commercially available MIG welding wires have been examined; the chemical compositions of these are given in Table 2.3. A variety of defects have been observed in the MIG weldments prepared using these wires; the welding procedures were therefore altered in an attempt to eliminate or at least reduce the severity of the defects. The causes of the defects in the weldments and the subsequent corrective measures taken to improve the weld quality are described in detail below.

a) Mill Scale Removal: In the first few practice welds, large spherical porosity was located in the surface beads because the molten metal came into contact with the mill scale on the base plate directly

adjacent to the milled double "V" groove. Therefore, the first welding procedure examined in the study, P150-X150-A, stipulated a requirement for removal of the mill scale adjacent to the weld groove. Details of the procedure are shown in Fig. 4.5.

b) Wire Feed: After a number of samples were welded using procedure P150-X150-A and examined radiographically, three transverse butt-welded joints, NB-6, NB-7, and NB-8, were prepared and tested in fatigue. Fatigue cracks in these three weldments all initiated failure within the weld metal resulting in shorter fatigue lives than anticipated from the behavior of the plain plates of HY-130/150 steel. The fatigue crack initiated in specimen NB-6 at small internal pores. In specimen NB-7, the fatigue failure is believed to have nucleated at a cold crack, whereas the fatigue crack in specimen NB-8 initiated along a line showing a lack of fusion which extended over the entire 2-1/4 in. long axis of the weldment. Transverse sections cut from the weld in NB-8 showed that some weld beads had not been positioned properly to give complete fusion. Radiographs taken of these sections also showed that the fusion was complete in some areas and incomplete in other areas of the same weld bead. This led to the conclusion that the fusion problem was caused mainly by improper straightening of the weld wire just before it entered the molten pool. The motor of the first wire straightener used had insufficient power to properly pull the stiff high-strength wire through the straightener; thus, the bent wire could change the arc position by a slight rotation of the wire in the feed mechanism and cause the observed lack of fusion. Therefore, fatigue samples NB-6, NB-7, and NB-8, which were made under the above conditions, undoubtedly all had some areas where fusion was not complete. This

incomplete fusion was usually located at the edge of a previously deposited bead in the bottom of the "V" groove or cusp area formed by the wall of the groove or by adjacent weld beads.

Procedure P150-X150-B, shown in Fig. 4.6, was used to create a better joint geometry in the "V" groove. However, this procedure was developed before the lack of fusion was discovered in the earlier specimens and was not designed to improve the fusion problem.

Three as-welded fatigue specimens, NB-2, NB-3, and NB-4 were prepared using procedure P150-X150-B. Again, two specimens initiated fatigue cracks along lines showing a lack of fusion which were 0.45 in. and 2.75 in. long. The causes of the lack of fusion may be traced to the same source described above for procedure P150-X150-A.

Using the information gained from the above weldments, a third welding procedure, P150-AX140-C (Fig. 4.7), was specified. The main objective was to penetrate the previous bead to such an extent that the cusp area is completely fused with the new bead. Therefore, procedure P150-AX140-C has been designed so that the arc is positioned directly over each cusp made by prior weld beads. Procedure P150-AX140-C further differs from procedures P150-X150-A and P150-X150-B in that a second MIG welding wire (AX-140) is used in place of the previously used X-150 wire. It has been found that the AX-140 wire is soft enough to be satisfactorily straightened by the wire feed unit first employed. Nonetheless, a weld wire straightener with greater capacity was obtained to insure the proper positioning of the arc when using either of the available MIG wires.

A fourth welding procedure, P150-AX140-D (Fig. 4.8), was designed to insure better penetration of the weld bead in the root pass. Procedure

P150-AX140-D is similar to P150-AX140-C except that in the former, no land is used and the plates to be welded are butted together without a root opening in the double "V" groove, Fig. 4.8. Furthermore, in procedure P150-AX140-D, an argon gas shield is used on the underside of the root pass during deposition. This shield keeps the weld metal soft for grinding and prevents excessive oxidation from occurring on the machined edges of the "V" groove on the underside of the root pass during the deposition of the root pass. Qualification tests, described in MIL-STD-418A,[9] have been conducted on samples prepared using P150-AX140-D. The weldments passed the side bend and tensile qualification tests, as well as the macrosection and radiographic standards for porosity.

c) As a result of the lack of fusion observed in the initial HY-130/150 weldments, discussed above, an attempt was made to remove the sharp notch created between the edge of the weld bead and the side of the "V" groove by grinding this cusp area after the deposition of each bead. The grinding wheel used consisted of an oxide abrasive backed with a resin fiber. This wheel had been used to prepare all early weldments tested in the current study. Two transverse butt-welded fatigue specimens, NB-9 and NB-10, were ground after each pass to eliminate the cusp area. The excessive grinding required of this technique is thought to have contributed to the large amount of porosity found throughout the weldments in both specimens. The grinding was probably responsible for embedding metal oxide particles and resin fibers in the ground metal surfaces, and the weld bead placed above this may have become porous due to the arc decomposition of the oxide particles or the vaporization of the resin fiber.

P150-AX140-D is similar to P150-AX140-C except that in the former, no land is used and the plates to be welded are butted together without a root opening in the double "V" groove, Fig. 4.8. Furthermore, in procedure P150-AX140-D, an argon gas shield is used on the underside of the root pass during deposition. This shield keeps the weld metal soft for grinding and prevents excessive oxidation from occurring on the machined edges of the "V" groove on the underside of the root pass during the deposition of the root pass. Qualification tests, described in MIL-STD-418A,[9] have been conducted on samples prepared using P150-AX140-D. The weldments passed the side bend and tensile qualification tests, as well as the macrosection and radiographic standards for porosity.

c) As a result of the lack of fusion observed in the initial HY-130/150 weldments, discussed above, an attempt was made to remove the sharp notch created between the edge of the weld bead and the side of the "V" groove by grinding this cusp area after the deposition of each bead. The grinding wheel used consisted of an oxide abrasive backed with a resin fiber. This wheel had been used to prepare all early weldments tested in the current study. Two transverse butt-welded fatigue specimens, NB-9 and NB-10, were ground after each pass to eliminate the cusp area. The excessive grinding required of this technique is thought to have contributed to the large amount of porosity found throughout the weldments in both specimens. The grinding was probably responsible for embedding metal oxide particles and resin fibers in the ground metal surfaces, and the weld bead placed above this may have become porous due to the arc decomposition of the oxide particles or the vaporization of the resin fiber.

To eliminate the entrapment of the oxide particles, a carbide grinding wheel was used to grind only the root pass in an additional sample. The sample weldment used the latest procedure, P150-AX140-D, Fig. 4.8. (It should be noted also that the HY-130/150 plate material used in the sample was from the NC series, Tables 2.1 and 2.2, which had a higher aluminum content than did the material used earlier to fabricate specimens in the NB series.) A low level of porosity was observed in the two transverse sections taken from this trial weldment, but when fatigue tests were subsequently conducted on specimens fabricated using this procedure (carbide grinding), crack initiation was still found to occur at internal defects including, on occasion, porosity. A more complete discussion of this behavior is presented in Section 4.5.

4.3.2 Microhardness Survey of Welded Joints

Microhardness traces were made on sections that were cut transverse to the long axis of welds made with procedures P150-X150-A and P150-X150-B. These hardness traces are shown in Figs. 4.9 through 4.12. The near surface trace was made on the transverse section parallel to the rolled surface and 1.25 mm below that surface. The mid-thickness trace was made parallel to the rolled surface and at the geometric mid-thickness of the welded joints. In these diagrams it can be seen that the weld metal is extremely hard with a large variation in the hardness of the untempered bead. A summary is listed in Table 4.6 of the average microhardness of the untempered and of the tempered beads. Note that the untempered beads have an average hardness of about 400 Diamond Pyramid Hardness (DPH) in procedure P150-X150-A and 380 DPH in procedure P150-X150-B, while the

tempered beads have an average hardness of about 360 DPH in both procedures. The weld metal appears to be very heterogenous according to the microhardness traces shown in Figs. 4.9 through 4.12; the standard deviation for both the tempered and untempered beads of these traces is given in Table 4.6.

Only the maximum hardness in the heat affected zone (HAZ) approaches the hardness of the untempered bead. In the HAZ near the fusion line, where large prior austenite grain boundaries are expected, the microhardness is quite low. However, the hardness in the HAZ gradually increases as the prior austenite grain size becomes smaller, resulting in a sharp hardness peak rather than the 2-3mm wide region of high HAZ hardness observed in many other hardenable steels. The tendency for over tempering of the base metal in a narrow region of the heat affected zone is evident in Figs. 4.9 through 4.12, but the minimum hardness of this over tempered region is only about 10 DPH less than the average hardness of the base metal. The maximum interpass temperature used to make both of these welds was 225^{o} F; this was considered the maximum desirable to protect against excessive over tempering.

A third microhardness survey was made for the weld metal deposited using the AX-140 MIG welding wire and procedure P150-AX140-C. Complete traces over the base metal and the HAZ were not made because the heat input and travel speed used for this procedure were very similar to those used in the procedures previously discussed. The average microhardness values for the weld metal are listed in Table 4.6. Only the microhardness indentations in the untempered bead were used to give the average hardness of the near surface trace. This untempered bead had an average hardness of 390 DPH or nearly the same as the untempered bead hardness obtained when the X-150MIG welding wire was used. The tempered bead at the mid-thickness had an

average hardness of 365 DPH or about the same as the tempered bead of the other wire, but the degree of tempering may not have been the same in both cases.

Center line traces or microhardness surveys taken through the center of the weld metal from bead surface to opposite bead surface are also listed in Table 4.6 for the weld metals and procedures just discussed. The standard deviation of this average hardness gives an indication of the difference between the tempered and untempered beads. The average center line hardness should also be the average between the center line and near surface weld metal trace. This is not the case for some of the center line traces, however, because the mid-thickness trace frequently intersects the bottom of the second weld pass where tempering is less pronounced than at some other regions of the multibead weld.

A microhardness survey was made of the weld metal in a specimen that had been tested to failure in fatigue at a stress level of 0 to +80.0 ksi. The results of the survey are presented in Table 4.6. Welding procedure P150-X150-A was used in the preparation of this fatigue specimen. The individual traces at the mid-thickness and the near surface positions appeared softer than in the as-welded (i.e., not tested in fatigue) samples but, as noted above, these traces are dependent on the exact position at which the bead is intersected. When the microhardness of the weld metal was averaged over the center line trace, which is a better measure of the weld metal hardness, the average hardness and standard deviation of the weld metal tested in fatigue were found to be in good agreement with that observed in the as-welded samples.

4.3.3 Hot Cracking

Some hot cracking was observed in samples welded using both procedures P150-X150-A and P150-B. Hot cracking along dendrites was not observed for welded joints of HY-130/150 made with procedure P150-AX140-C, but in one instance a crack was observed at the center line of a lobe of one weld bead in an as-welded specimen. Typical hot cracks observed for weld beads deposited in accordance with procedures P150-X150-A and P150-X150-B are shown in Fig. 4.13. It has been suggested that the high copper in the particular heat of X-150 wire used may have been responsible for the cracking by the process of hot short cracking due to copper segregation between the dendrites. If this is the case, and since the copper content is lower in the AX-140 wire currently being examined, hot cracking may not be a problem in future program work.

The hot cracks which were observed did not appear to extend for any great distance along the longitudinal axis of the weld bead, i.e., the cracks were always shorter than the 1/4 in. thickness of the transverse sections cut from the weldment. These hot cracks were not thought to be responsible for the early fatigue failures of the NB series specimens, reported in Section 4.4.1. The incomplete fusion which was caused by the poor control of the unstraightened weld wire described earlier was considered more detrimental to the fatigue life of that series of HY-130/150 specimens.

4.3.4 Comparison of Weldments Prepared by NASL, USS, and U of I

Welded joints of HY-130/150 steel (using the same plate stock and the same heat of AX-140 weld wire) were prepared by both the U.S. Naval Applied Science Laboratory (NASL), and the U.S. Steel Corporation (USS), for comparison with specimens welded at the University of Illinois. Several

transverse sections of the weldments from the three laboratories were cut and examined; one such section of a sample from each laboratory is shown in Fig. 4.14. The results of this examination indicated that the weldments were similar except for the greater separation of the surface beads, which resulted from the bead positioning, in the weldments prepared at the University of Illinois. For the three different weldments, the amount of weld metal in each bead was approximately the same. The positions of the corresponding beads in each of the weldments, except for the surface beads, were also similar.

In general, the MIG weld beads have the characteristic shape of a large bead with a small lobe underneath; this is most clearly evident in the surface beads of Fig. 4.14c. A crack in one of these small lobes was observed at some transverse sections of the Illinois weldment; this crack extended along the center line of the lobe in the longitudinal direction of the weld. The position of the crack is indicated by the arrow in Fig. 4.14c. In Fig. 4.14b, the arrow marks the location of weld metal in the USS weldment containing hot cracks.

In addition to the observations of cracking in the USS and the Illinois specimens, porosity of a size that can be detected by standard radiographic techniques was found in all of the welded joints (NASL, USS, and U of I).

The average of the center line hardness readings (surveys taken through the center of the weld metal from exterior bead surface to opposite exterior bead surface) ranged from 365 to 380 Diamond Pyramid Hardness (DPH) for the weldments from the three laboratories, as shown in Table 4.6. The similarity in hardness traces was to be expected since the welding

equipment settings, the preheat and interpass temperatures, etc., were about the same in each instance. A comparison of these variables is presented in Table 4.7 for weldments from each of the three sources. The major differences in the welding procedures were in the welding gun manipulations; the USS and the Illinois joints had 12 weld passes deposited using a MIG wire gun track with a mechanically regulated travel speed; the NASL weldments contained 17 weld passes and were manually deposited.

4.4 Fatigue Test Results for Welded Joints

4.4.1 Tests of As-Welded Transverse Butt Joints

The fatigue results for eighteen transverse butt-welded joints tested in the as-welded condition are given in Tables 4.8 and 4.9, and are plotted in Fig. 4.15. All of the specimens were tested in fatigue at a stress cycle of zero-to-tension. Before cycling, each of the specimens was radiographed; the radiographs were used to rate the welds in accordance with Navy Specifications.[7] The radiographic ratings and defect descriptions are also presented in Tables 4.8 and 4.9. The wide scatter of fatigue results is attributed to differences in the severity of the several types of internal defects encountered in these specimens, most of which exhibited fatigue crack initiation internally rather than at the geometrical stress raiser associated with the toe of the weld reinforcement. Although four different welding procedures, Figs. 4.5 through 4.8, were used in the preparation of the fatigue specimens, none was successful in eliminating all of the defects which have continually proved critical for the initiation of fatigue cracking at stress levels

of 0 to +50.0 ksi and above. It becomes quite evident, therefore, that if consistently good fatigue behavior is to be attained in welded joints of HY-130/150 steel, it will be necessary to impose very tight restrictions on the quality of these weldments when they are to be subjected in service to large cyclic reversals of axial stress. A more complete description of the types of failures encountered in the present series of fatigue tests is presented in the following paragraphs.

It can be seen in Fig. 4.15 that the latest procedures developed, P150-AX140-C and P150-AX140-D, have improved, on the average, only slightly upon the scatter of results obtained with the earlier procedures. The fusion problem present in many of the earlier welds (NB series specimens) has essentially been overcome by using the wire straightener with a higher power and the narrower grinding wheel. However, with the exception of NC-16, the initiation of fatigue failure in the NC specimens still occurred at internal defects, in most cases at either lack of fusion, porosity, or in a region of metallurgical weakness in the structure of the lobe of the weld bead. Typical examples of fatigue failures initiating at porosity, and in a weak area of the weld structure are shown in Figs. 4.16a and b, respectively. Failure occurring in such a "zone of metallurgical weakness" refers to the fact that no physical discontinuity was observed at the point of crack nucleation in these specimens. (Specimens failing in this manner are designated in Table 4.9 as having failed "in weld metal.") Further discussion of this zone of weakness and its subsequent development into a fatigue crack is given in Section 4.5. The two specimens reported in Tables 4.8 and 4.9 that failed at the toe of the weld were also found to contain porosity, but the internal arrangement and size of the pores was less critical than the external geometrical stress raiser.

In general, for the as-welded HY-130/150 joints tested in fatigue during this study, no conclusions can be drawn concerning the effect of the amount of porosity in a specimen (as indicated by percent area reduction in Tables 4.8 and 4.9) on the resultant specimen fatigue life at a given stress level. This is due mainly to the existence in these specimens of several other types of internal defects, which were generally more critical than the porosity as locations for fatigue crack nucleation.

The butt-welded joints of HY-130/150 prepared by the two other laboratories, U. S. Naval Applied Science Laboratory (NASL), and U.S. Steel Corporation (USS), were tested in fatigue for comparison with those specimens welded at the University of Illinois. The three specimens from each of the other laboratories were also found, under radiographic examination, to contain various amounts of porosity. The results of fatigue tests of these specimens are presented in Table 4.10 and plotted in Fig. 4.17. Examination of the results shows that the average life of the USS specimens was 7,900 cycles, of the NASL specimens 18,600 cycles, and of the Illinois specimens 11,700 cycles at a stress level of 0 to +80.0 ksi. It should be noted that both the USS and NASL data are within the range of fatigue lives obtained from the Illinois specimens. The Illinois data are composed of all results using the various procedures developed at the University. Table 4.10 indicates that all the USS and the NASL specimen fatigue failures initiated in the weldment. For the four specimens designated as having failed "in weld metal", no physical discontinuity (defect) was observed at the crack origin. As noted above, probable causes of such failures will be examined in Section 4.5. In general, the weldments of HY-130/150, prepared by each of the three separate laboratories, are

approximately equivalent, both in quality (soundness of weldment) and in the directly related axial fatigue behavior, at least at the 0 to +80.0 ksi stress level investigated. Typical fracture surfaces for specimens prepared at NASL and USS are shown in Fig. 4.18.

4.4.2 Tests of Transverse Butt Joints With Reinforcement Removed

The standard welding procedure used for fabricating the transverse butt welds tested with the reinforcement removed was P150-AX140-D. Details of this welding procedure are given in Fig. 4.8. After a fatigue specimen was welded, the reinforcement and adjacent mill scale surface on the test section was first machined off and then rough polished to remove the surface stress concentrations and to force fatigue failure to initiate at any internal defect(s) present in the weld metal. Radiographs of all specimens were taken before cycling and were rated according to the Navy standards; the results of this examination are given in Table 4.11. Note that each of the specimens contained porosity, two in amounts exceeding specification limits.

All specimens tested with the reinforcement removed were cycled from zero-to-tension at one of three stress levels: 0 to +80.0 ksi; 0 to +50.0 ksi; or 0 to +43.0 ksi. The results of the fatigue tests are reported in Table 4.11 and plotted in Fig. 4.19. No S-N curve could be determined for these data because of the few tests conducted and the large scatter in results. The locations of fatigue crack initiation in the specimens with the reinforcement removed were the same as for those specimens tested in the as-welded condition; i.e., the failures initiated internally in regions where either porosity or lack of fusion was evident, Tables 4.8, 4.9, and 4.11.

Comparison of the fatigue results for specimens tested in both the as-welded condition and with the reinforcement removed again clearly demonstrates the critical effect of internal defects on the fatigue resistance of welded joints in the HY-130/150 steel.

4.5 Fatigue Crack Initiation and Propagation

In HY-100 weldments prepared with the use of a metal oxide grinding wheel, fatigue cracks often were observed to initiate at internal defects containing either singular pores or porosity clusters. With the introduction of the carbide grinding wheel (1/4 in. radius face), subsequent fatigue failures initiated on the surface as a result of the geometrical stress raiser associated with the toe of the weld reinforcement. Since porosity was present also in the early HY-130/150 MIG welded joints (NB series specimens prepared with an oxide grinding wheel), it was reasoned that the use of the carbide grinding wheel could perhaps eliminate the porosity within the MIG weldments. In addition, several of the early MIG weldments had lines of incomplete fusion along the long axis of the weld. These fusion defects were caused, as concluded in Section 4.3, by inadequate straightening of the MIG welding wire which rotated out of position during the deposition process. When adequate MIG welding equipment and the carbide grinding wheel were used in the fabrication of the NC series weldments, the problems with lack of fusion were eliminated, but internal porosity was still found to be present and was the usual site for the nucleation of fatigue cracks. This would indicate, then, that the metal oxide grinding wheel was not the sole contributing factor to the occurrance of porosity in the HY-130/150 weldments.

In another attempt to decrease the amount of this porosity, several techniques were combined in a new welding procedure. The techniques employed were: carbide grinding, the use of a protective argon atmosphere on the underside of the root pass to keep the metal soft for grinding and to prevent excessive oxidation of the "V" groove, and the requirement that the "V" groove be machined just prior to welding to prevent the machined edges from rusting while in storage. The fatigue results for specimens prepared in this manner were not noticeably better than previous results, and there continued to be a prevalence toward fatigue crack initiation at internal defects.

As a result of the frequency of occurrance of fatigue failures at internal defects in the HY-130/150 joints, a metallurgical investigation of the fracture surface within the weld metal of the fractured specimens was initiated. The main purpose of examining the regions of fatigue crack initiation and propagation in the MIG welded joints was to observe the selectivity of the fatigue crack in following certain paths through the metallurgical structure of the weldment. The examinations of the fracture surfaces were conducted with the aid of an electron microscope using standard methods of microfractography as described below.

In order to investigate the possible causes for initiation of fatigue cracks in the HY-130/150 weldments, and to compare fatigue fracturing to shear fracturing, replicas were first made of the weld metal (AX-140 wire) of a welded joint fractured in static tension. (A static tension test produces a typical shear type fracture.) Both a plastic

replica and a carbon extraction replica were made of this shear fracture and are shown in Fig. 4.20, as they appeared under the electron microscope. The plastic replica was made by placing a viscous acetate film over the fracture surface. After allowing the acetate to harden, the plastic replica was peeled from the fracture surface giving an image of the actual fracture contours. The plastic replica was shadowed with chromium at an angle of 45^{o} in order to emphasize the topography. A second stage carbon replica was then made of the plastic replica; the carbon replica now possessed the same contour as the original specimen.

A second type of replica (carbon extraction replica) was made by evaporating carbon over the sample containing the shear fracture. The carbon replica was removed from the fracture surface by allowing a 10% nital solution to permeate through the porous carbon and dissolve the metal matrix of the fracture surface. The particles on the fracture surface which were not dissolved by the nital solution were frequently left attached to the single stage carbon extraction replica. Thus, the non-metallic particles were extracted by this replication technique. The particles on the top of each dimple, shown in the replica of Fig. 4.20b, are the non-metallic particles which appear as black dots in the photograph.

In contrast to the surface of a typical shear fracture, which was observed to be the same for both the HY-100 and HY-130/150 steels, the surface of a fatigue fracture for each of these steels had fewer dimples and a flatter appearance; this characteristic is shown for the HAZ and base metal of HY-100 steel in Fig. 4.21. Many large particles were observed in the HAZ near the fusion line when polished and etched samples of HY-100 and HY-130/150 steels were examined, but the fatigue fracture did not form

any large dimples around these particles as was the case with shear fractures of these steels. However, very shallow dimples were observed around some of the particles on the surface of the fatigue fracture of the HAZ and around the few particles observed on the surface of the fatigue fracture of the base metal as shown in Fig. 4.21.

When a weld bead from an HY-130/150 weldment was cross-sectioned perpendicular to the long axis of the weld, as shown in Fig. 4.22, the structure at the center line of the weld bead was observed to be similar to the center of a cast ingot with respect to segregation. The elements and compounds which are rejected from the solidifying dendrites of the metal are either trapped between dendrites or left at the center line of the ingot or weld bead, creating a relatively weak metallurgical structure along this center line. A crack along the center line of a weld bead at the bottom of the lobe is shown by the arrow in Fig. 4.22. This lobe crack was present in the as-welded specimen before static testing. When the crack was exposed by the fracturing of the welded joint in static tension, a plastic replica taken of the fracture surface contained small droplets of segregates appearing as hundreds of small dots on the replica in the region of the lobe crack, Fig. 4.22.

Fatigue fractures were frequently observed to propagate along the center line of a weld lobe as shown by the arrows in Figs. 4.23 and 4.24, even though radiography did not indicate a crack in this lobe area prior to fatigue cycling. It is probable, therefore, that such weld lobe areas were also the nucleation points for internal fatigue failure in those specimens which exhibited no physical discontinuity (porosity, lack of fusion, etc.) at the fatigue crack origin (specimens denoted as failing "in weld metal"

in Tables 4.9 and 4.10). The plastic replicas shown in Figs. 4.23 and 4.24 of the fatigue crack in one lobe area indicate that there are many particles of the type mentioned above, both large and small, on the surface. The extraction replica shown in Fig. 4.23, taken directly from the surface of the fatigue fracture, reveals a detailed dendritic structure. The reason that such a detailed dendritic structure was extracted so completely from the surface of the fatigue fracture must be due to the fact that the fatigue crack propagated along the nonmetallic network which outlined the dendritic structure, especially along the center line of the lobe of the weld bead. It should also be noted that the spacing between droplets (dots) shown in the plastic replica of Fig. 4.24 is of the same order of magnitude as the spacing between the non-metallic particles outlining the dendritic structure shown in the extraction replica of Fig. 4.23.

Another type of segregation was observed by the replication of a fatigue crack which propagated along the HAZ of a weld bead created by the subsequent deposition of another weld bead. The areas replicated for the two samples are shown by the arrows in Figs. 4.25 and 4.26. All of the replicas shown in Figs. 4.25 and 4.26 were made with plastic. The segregate particles are clearly seen to outline the grain boundaries in the HAZ of the weld metal shown in Fig. 4.25. A frequent position for segregated particles is on the prior austenite grain boundaries of the HAZ of the base metal. Since the fatigue fracture moves across these grain boundaries outlined in Figs. 4.25 and 4.26, it is assumed they do not represent weak areas for fatigue crack propagation.

Based on observations made by replicating the fracture surfaces of HY-130/150 welded joints, it appears that the metallurgical "zone of

weakness" for fatigue crack initiation and propagation in several specimens was associated with the dendritic structure along the center line of the lobe of the weld bead. Although segregation occurred at grain boundaries in the HAZ of previously deposited weld beads, the fatigue crack did not appear to propagate along the grain boundaries containing the particles. It should also be noted that nucleation of fatigue cracks occurred most often at internal defects such as porosity and lines of incomplete fusion for the defective welded joints of HY-130/150 steel, and not at the zones of metallurgical weakness, Tables 4.8 and 4.9.

4.6 Concluding Remarks

During the course of the investigation, transverse butt-welded specimens of HY-130/150 steel were prepared by each of three laboratories: University of Illinois, U.S. Naval Applied Science Laboratory, and U. S. Steel Corporation. Specimens in the as-welded condition from the three laboratories were tested in axial fatigue at a stress level of 0 to +80.0 ksi. There was considerable scatter of fatigue results for these specimens, with lives varying from a low of 2,200 cycles to a maximum of 38,100 cycles. In general, specimens prepared at each of the laboratories exhibited similar fatigue behavior with the majority initiating failure at internal defects containing porosity, or lack of fusion, or in regions of weakness in the metallurgical structure of the weld. It appears that the presence of flaws such as the ones encountered in these weldments, which were all welded using the same MIG wire, will almost invariably result in internally initiated fatigue failures under high stress axial fatigue. It is necessary, therefore, to recognize the importance of even minute flaws, inasmuch as they affect the fatigue behavior of HY-130/150 welded joints (and, perhaps,

other steels of even higher strength) and to set design criteria accordingly. More important, however, is the continuing need to strive toward increasing the quality of high strength steel weldments by further improving the composition and properties of the MIG welding wire, and by refining and improving the welding techniques and quality control.

V. SUMMARY AND CONCLUSIONS

The studies reported herein are part of a continuing investigation into the development and evaluation of high-strength steels slated for use in the U. S. Navy shipbuilding program. The purposes of the current investigation were to develop welding procedures for HY-100 steel which are consistently high quality (low defect density) and to evaluate the axial fatigue behavior of welded joints prepared in accordance with these procedures. Similar development studies were performed for specimens of HY-130/150 steel welded using two types of MIG wires; preliminary fatigue results for these welded joints have also been obtained.

Observations of the weld quality obtained in joints of both HY-100 and HY-130/150 steel, and the resultant fatigue behavior of these members have been reviewed in Chapters III and IV. The more significant results are briefly summarized and the data evaluated in the following sections.

5.1 Summary

5.1.1 Studies of HY-100 Steel

A previous investigation of the axial fatigue behavior of welded joints in HY-100 steel revealed that, when internal defects were present in these weldments, internally initiated failures were prevalent in tests conducted at cyclic maximum stresses greater than one-half the static yield strength of the material. The defects at which the internal cracks nucleated were often small isolated pores seldom detected by standard radiographic inspection prior to testing. Since the fatigue lives of these welded specimens were low in comparison to the behavior of the base material, it

became evident that new welding procedures were required to insure that virtually defect-free weldments could be fabricated, thus removing the critical points for internal crack initiation. As a result of a re-evaluation of the welding techniques used in this study for the preparation of the initial fatigue test specimens, it was concluded that the bonded metal oxide wheel used in grinding the root pass of the welds was largely responsible for embedding small oxide particles in this root pass. It was suggested that these particles decomposed during subsequent welding and produced the observed isolated pores. To eliminate these defects, a carbide grinding wheel was used in the preparation of all later joints, which were welded with both the MIL-12018 and MIL-11018 electrodes. Metallographic examination of sections cut from these weldments did show a much lower density of pores when the carbide wheel was introduced. In addition, fatigue tests performed on the weldments resulted in externally initiated failures for both as-welded specimens and those with the reinforcement removed, at cyclic stresses approaching the nominal yield strength of the HY-100 steel.

Axial fatigue tests, using a stress cycle of zero-to-tension, were conducted on transverse butt-welded joints of HY-100 steel; the weldments were prepared using both the MIL-12018 and MIL-11018 electrodes. For those as-welded specimens using either electrode and which were considered "sound" weldments (no defects detected by radiography, and corresponding fatigue crack initiation at the toe of the weld), the computed fatigue strength at 100,000 cycles was 43.6 ksi, or approximately 40 percent of the HY-100 static yield strength. The fatigue strength of the plain plate material was 68.6 ksi at 100,000 cycles; thus, at 100,000 cycles, a reduction in axial fatigue strength of 25 ksi (36 percent) may be expected when a

butt-welded joint is present in a structural component. This percent reduction in axial fatigue strength becomes even more pronounced at longer lives as shown in the table below.

Specimen Type	Surface Condition	Fatigue Strength, ksi (Zero-to-Tension)			
		$F_{50,000}$	$F_{100,000}$	$F_{200,000}$	$F_{500,000}$
Plain Plate	As-Received	84.5	68.6	55.7	42.9
Transverse Butt Weld	As-Welded	56.9	43.6	33.6	21.0
(Percent Reduction)		(32.8)	(36.3)	(39.5)	(51.0)

At each of the stress levels examined, there was a large scatter of fatigue lives obtained for the HY-100 specimens which initiated failure at internal defects. At 0 to +50.0 ksi, for example, the lives of the specimens tested with the reinforcement removed ranged from a low of 32,300 cycles to a maximum of 1,108,600 cycles. A variety of defects were found in these specimens, including: clusters of porosity, slag, lack of fusion, and isolated pores. No one type or size of defect was noticeably the most detrimental to the fatigue resistance of the specimens; in several instances, a single small pore was the cause of failure at an earlier life than that obtained in a specimen containing a large porosity cluster which would have been rejected by current radiographic standards.

One HY-100 specimen was examined periodically during fatigue cycling, using both ultrasonic and radiographic techniques to obtain a measure of the number of cycles required to initiate an internal fatigue crack, and to trace the rate of subsequent crack propagation. For this specimen, tested at 0 to

+50.0 ksi, cracking initiated (in a region containing porosity, lack of fusion, and slag) at approximately 20 percent of the total lifetime (41,400 cycles) of the member. There then followed a long stage of slow propagation, occupying over 60 percent of the specimen life, followed by a short stage of rapid growth to failure after the crack had extended to the specimen surface. There is evidence, however, that this failure pattern is not necessarily typical of all welded joints in high-strength steels; several HY-80 specimens similarly examined during a previous investigation were not found to initiate a fatigue crack until well beyond half the total specimen life had expired. Considerably more work is needed in this area, therefore, before the actual mechanisms involved in internal crack nucleation are fully understood.

5.1.2 Studies of HY-130/150 Steel

Studies of the axial fatigue behavior of HY-130/150 plain plate specimens in the as-received condition were included in this investigation. The fatigue strengths obtained from tests at zero-to-tension stress cycles are compared with the strengths of HY-80 and HY-100 plain plate specimens in the following table.

Steel (As-Received)	Thickness (in.)	Fatigue Strength, ksi (Zero-to-Tension)			
		$F_{50,000}$	$F_{100,000}$	$F_{200,000}$	$F_{500,000}$
HY-80	3/4	75.6	65.6	57.1	47.4
HY-80	1-1/2	78.5	67.9	60.9	54.5
HY-100	3/4	84.5	68.6	55.7	42.9
HY-130/150	1; 1/2	83.2	70.7	60.3	51.4

In general, the HY-130/150 specimens exhibited a slightly better fatigue resistance than the other steels, notably at the shorter lives associated with the higher cyclic stresses. As noted in the report, however, the HY-80 steel exhibits the best relative fatigue behavior when the three materials are compared on the basis of the ratio of fatigue strength to either static yield or ultimate strength.

The HY-130/150 plain plates were found to contain a rough oxidized layer located just beneath the thin exterior mill scale surface. When this hard, oxidized layer was machined off the surface of the test section of several specimens, the fatigue lives of these specimens were found to be from four to six times as great as the lives for similar members tested with the mill scale left in place. Thus, it must be recognized that the results reported in the table above represent the fatigue strengths of the composite metal plus surface layer, and not strictly the base metal per se. However, it is indeed this composite, and not the highly polished laboratory test specimen, which approximates the plate as usually found in sevice structures; in this respect the data in the above table may be considered a more appropriate basis for establishing allowable design stresses for base metal.

Numerous HY-130/150 transverse butt-welded joints, in which metal inert gas (MIG) welding was employed, were tested in axial fatigue at a stress cycle of zero-to-tension. The majority of these specimens, tested in the as-welded condition, initiated failure at internal defects containing porosity, lack of fusion, or in regions of weakness in the metallurgical structure of the weld deposit. As a result of the various types and frequency of occurrence of defects in the weldments, several modifications in the welding procedures were adopted which were intended to improve both the quality of the weld and the directly related resistance to internal fatigue

crack nucleation. These modifications included: (1) use of a protective argon atmosphere on the underside of the root pass to keep the metal soft for grinding and to prevent excessive oxidation of the "double V" groove, (2) use of a carbide wheel to backgrind the root pass, (3) careful positioning of each weld bead directly over the cusp formed by prior beads to insure full penetration in the cusp region, and (4) removal of the mill scale on the base plate directly adjacent to the milled "V" groove. When these techniques were introduced into the welding procedures, defects containing severe lack of fusion and large porosity clusters were subsequently held to a minimum. It is recommended, therefore, that these procedures be followed where possible in field welding operations when a high axial fatigue resistance of a transverse butt welded joint is essential to the proper functioning of the structure.

Even when the above techniques were used in the preparation of welded test specimens, there continued to be a prevalence of internal fatigue cracks at pores, and occasionally, in the structure associated with the center line of the lobe protruding from a weld bead. Examination of the fracture surface of a fatigue crack along the center line of such a lobe revealed a chemical segregation which produced non-metallic particles between the dendrites of the solidified weld metal. This evidence of segregation was obtained from transparent replicas of the fractured surface made with the use of plastic replication and extraction replication of the surface, and observed with an electron microscope.

Since the majority of the HY-130/150 welded joints, both in the as-welded condition and with the reinforcement removed, initiated internal fatigue cracks at the various defects discussed above, there was a wide

scatter in their resultant fatigue lives at the zero-to-tension stress levels examined. The range of lives for the as-welded specimens tested at 0 to +80.0 ksi varied from 2,200 cycles to a maximum of 38,100 cycles. The average life for all specimens examined at this 0 to +80.0 ksi stress level was approximately 12,000 cycles as compared to almost 60,000 cycles for the as-received plain plates and 250,000 cycles for the polished plates. There was no conclusive evidence that any one type of flaw was most critical for early fatigue crack initiation; however, those specimens containing regions where lack of fusion extended along most of the length of the weld exhibited, on the average, the lowest lives.

Companion specimens were welded at the U. S. Naval Applied Science Laboratory and U. S. Steel Corporation using the same commercial MIG wires, and were then tested in the as-welded condition at the University of Illinois. The axial fatigue lives for these specimens, tested at 0 to +80.0 ksi, were within the range of lives reported above for those weldments prepared at the University of Illinois; the three NASL specimens had an average life of 18,600 cycles, and the three USS specimens an average of 7,900 cycles. Each of these six weldments initiated internal weld failures, with nucleation occurring at either porosity or in a zone of structural weakness where no physical discontinuity was observed.

Comparison of the data obtained from specimens prepared at the three laboratories indicate that, when current MIG procedures are used in the welding of HY-130/150 specimens, the introduction of certain types of internal defects into the weld deposit will be a common occurrence. The presence of these weld flaws may be expected to result in internally initiated fatigue failures when the welded joints are subjected to large axial cyclic loads.

For the butt welds examined, the low fatigue resistance (relative to that for the plain plate material) and large scatter in the test lives obtained at a particular cyclic stress level demonstrate the need to consider the importance of weld defects when establishing radiographic standards and allowable design stresses. The results also indicate that continued research is required toward the goal of increased weld quality through improvements in the MIG wires and refinements in the welding techniques.

5.2 Conclusions

Based on the studies reported herein, the following conclusions and observations have been reached concerning the axial fatigue behavior of HY-100 and HY-130/150 steels:

1. The presence of small weld defects; i.e., flaws well within current Navy specification limits and often not detected by standard radiographic techniques, can be seriously detrimental to the axial fatigue resistance of butt-welded joints in HY-100 steel. At cyclic maximum stresses approaching the yield strength of the material, such flaws were found to be points of internal fatigue crack initiation with resulting fatigue lives as low as one-fourth the lives anticipated for weldments initiating surface fatigue failures. It is imperative, therefore, that welds of particularly high quality be required in HY-100 weldments which must resist severe axial fatigue loadings.

2. Use of a carbide grinding wheel to back-grind the root pass of butt welds in HY-100 steel has proven successful in significantly reducing the density of small pores invariably found in earlier weldments prepared with a metal oxide grinding wheel. Specimens prepared using the carbide wheel, and otherwise welded in accordance with accepted techniques for the

production of high quality weldments, were found to initiate axial fatigue failures at the toe of the weld reinforcement, and not at internal flaws. It is recommended, therefore, that a carbide grinding wheel be employed in the future preparation of HY-100 weldments which may be subjected in service to severe axial cyclic loading conditions.

The axial fatigue strengths of "sound" HY-100 butt-welded specimens are compared to the strengths for the HY-100 plain plate material and to the corresponding fatigue strengths of HY-80 plain plates and butt-weldments in the following table:

Material (thickness)	Specimen Type	Surface Condition	Fatigue Strength, ksi (Zero-to-Tension)			
			$F_{50,000}$	$F_{100,000}$	$F_{200,000}$	$F_{500,000}$
HY-100 (3/4")	Plain Plate	As-Received	84.5	68.6	55.7	42.9
HY-100 (3/4")	Transverse Butt Weld	As-Welded	56.9	43.6	33.6	21.0
HY-80 (3/4")	Plain Plate	As-Received	75.6	65.6	57.1	47.4
HY-80 (3/4")	Transverse Butt Weld	As-Welded	69.3	57.1	45.0	35.0

3. Under a stress cycle of zero-to-tension, HY-130/150 plain plates tested in the as-received condition (mill scale left in place) exhibited an axial fatigue resistance only slightly higher that the resistance offered by similar specimens of HY-80 and HY-100 steel. The fatigue behavior of the HY-130/150 material was markedly improved, however, when the specimen surfaces were polished to remove the mill scale and underlying hard oxidized layer. The fatigue lives of the polished specimens were from four to six times greater than the lives of the as-received plates for the stress cycles examined.

4. Several modifications in the procedures for MIG welding of HY-130/150 butt-joints were employed in an attempt to produce welds of particularly high quality (low defect density); none, however, was entirely satisfactory in eliminating all those flaws which, throughout this investigation, have proven to be critical points for internal crack initiation under high-stress axial fatigue loading. A wide scatter in fatigue lives was observed for the butt-welded joints, with the average life falling well below the average for the base material at the same stress level. At this time then, it is not possible to compare directly the axial fatigue of butt-welded joints in HY-130/150 with sound weldments of HY-80 and HY-100 steel.

5. Butt-welded specimens of HY-130/150 fabricated at three separate facilities, U. S. Naval Applied Science Laboratory, U. S. Steel Corporation, and the University of Illinois, were adjudged to be of approximately equivalent quality insofar as their resistance to axial fatigue loading is concerned. Fatigue failures were internally initiated in specimens welded at each of the three laboratories. On the average, the joints prepared by NASL, where a manual welding technique was used, exhibited a somewhat higher fatigue resistance than those from the other two sources, where automated processes were employed.

LIST OF REFERENCES

1. Bureau of Ships, U. S. Navy, "Fabrication, Welding and Inspection of HY-80 Submarine Hulls," NAVSHIPS 250-637-3, January 1962.

2. Air Reduction Company, Inc., "HY-130/150 Weldments: Summary Report on the Development of Filler Metals and Joining Procedures," Research and Engineering Department, RE-66-014-CRE-34, 26 January 1966.

3. Munse, W. H., Bruckner, W. H., Radziminski, J. B., Hinton, R. W., and Leibold, J. W., "Fatigue of Plates in Weldments in HY-100 and HY-130/150 Steels," Civil Engineering Studies, Structural Research Series No. 300, University of Illinois, December 1965.

4. Sahgal, R. K., and Munse, W. H., "Fatigue Behavior of Axially Loaded Weldments in HY-80 Steel," University of Illinois, Department of Civil Engineering, Structural Research Series No. 204, September 1960.

5. Hartmann, A. J., Bruckner, W. H., Mooney, J. and Munse, W. H., "Effect of Weld Flaws on the Fatigue Behavior of Butt-Welded Joints in HY-80 Steel," University of Illinois, Department of Civil Engineering, Structural Research Series No. 275, December 1963.

6. Hartmann, A. J., and Munse, W. H., "Fatigue Behavior of Welded Joints and Weldments in HY-80 Steel Subjected to Axial Loadings," University of Illinois, Department of Civil Engineering, Structural Research Series No. 250, July 1962.

7. Bureau of Ships, U. S. Navy, "Radiographic Standards for Production and Repair Welds," NAVSHIPS 0900-003-9000, August 1965.

8. Munse, W. H., Bruckner, W. H., Hartmann, A. J., Radziminski, J. B., Hinton, R. W., and Mooney, J. L., "Studies of the Fatigue Behavior of Butt-Welded Joints in HY-80 and HY-100 Steel", University of Illinois, Department of Civil Engineering, Structural Research Series No. 285, November 1964.

9. Bureau of Ships, U. S. Navy, "Military Standard Mechanical Tests for Welded Joints," MIL-STD-418A, 26 March 1965.

10. "Crack Growth Properties of Welds in HY-80, HY-100, and HY-130/150 High Strength Steels in a Sea Water Environment," Lab. Project 9300-1, Technical Memo. #39, U. S. Naval Applied Science Laboratory, Brooklyn, N. Y., 16 September 1965.

11. Letter to Prof. W. H. Munse, University of Illinois, from M. W. Lightner, U. S. Steel Corporation, Pittsburgh, Pa., 4 March 1966.

TABLE 2.1

MECHANICAL PROPERTIES OF BASE METAL

(Data Supplied by Manufacturer)

Heat Number	Designation	Thickness (inches)	Properties in the Longitudinal Direction				
			Yield Strength* (ksi)	Tensile Strength (ksi)	Elong. in 2 inches (percent)	Reduction in Area (percent)	Charpy V-Notch** (ft-lbs)
N15423	HY(HY-100)†	3/4	110.0	127.5	23.0	71.1	83 (a)
73A661	HY(HY-100)††	3/4	105.9	121.6	22.5	71.5	93 (a)
3P0074	NA;NB(HY-130/150)	1/2; 1	138.0	144.0	20.0	69.8	102 (b)
5P0540***	NC(HY-130/150)	1	138.5	149.0	20.5	67.5	83 (b)

* 0.2 percent offset

** (a) @ -120°F
(b) @ 0°F

*** Properties are average values for two plates

† Material used for fabrication of fatigue specimens HY-1 through HY-61

†† Material used for fabrication of fatigue specimens HY-62 through HY-90

TABLE 2.2

CHEMICAL COMPOSITION OF BASE METAL

(Data Supplied by Manufacturer)

Chemical Composition (percent)	Heat Number			
	N15423	73A661	3P0074	5P0540
Base Metal Designation	HY(HY-100)	HY(HY-100)	NA;NB(HY-130/150)	NC(HY-130/150)
C	0.20	0.15	0.110	0.12
Mn	0.30	0.31	0.78	0.79
P	0.010	0.012	0.008	0.004
S	0.014	0.016	0.006	0.003
Si	0.21	0.22	0.29	0.35
Ni	3.00	2.49	5.03	4.96
Cr	1.67	1.53	0.56	0.57
Mo	0.50	0.36	0.42	0.41
Cu	0.11	0.04	----	----
V	----	0.01	0.05	0.057
Al*	----	----	0.008	0.044
Al**	----	----	0.015	0.048
Ti	----	0.001	----	----
N	----	----	0.011	0.013
O	----	----	0.0029	0.0019

* acid soluble

** total

TABLE 2.3

CHEMICAL COMPOSITION OF MIG ELECTRODES

Chemical Composition (percent)	Heat Number	
	OR0440*	IP0047**
MIG Wire Designation	Linde X-150	Airco AX-140
C	0.11	0.097
Mn	1.60	1.85
P	0.008	0.006
S	0.007	0.007
Si	0.34	0.30
Ni	2.75	2.10
Cr	0.62	0.91
Mo	0.89	0.54
Cu	0.34	----
V	0.02	----
Al	0.020	0.018
Ti	0.010	0.01
Zr	0.006	----
N	----	0.013
O	----	0.015

* Data supplied by U. S. Steel Applied Research Lab.

** Data from Ref. 2

TABLE 3.1

MICROHARDNESS SURVEY OF THE WELD METAL FOR HY-100 SPECIMENS PREPARED WITH VARIOUS WELDING PROCEDURES*

Welding Procedure	Number of Weld Passes	Avg. Energy Imput During Each Pass (joules/in.)	Avg. HAZ Hardness DPH**	Average Weld Hardness, DPH**		
				Parallel to Plate Surface		Center Line of Weld Through Plate Thickness
				Mid-Thickness***	Near Surface***	
P100-11018-J	6	40,000	409±7(a)	286±11(a)	274±8(a)	283±12(b)
P100-11018-J50	6	50,000	463±12	276±11	300±12	280±12
P100-11018-J30	12	30,000	416±15	276±10	285±11	278±15
P100-12018-A	6	40,000	---	284±10	314±7	302±17
P100-12018-C	12	30,000	---	288±12	310±25	297±17

* Minimum preheat and interpass temperatures for all samples were 150°F and 200°F, respectively.

** The Diamond Pyramid Hardness values were obtained with a 1 kg. load. The average base metal hardness obtained from a large number of determinations was 270 DPH.

*** Mid-thickness trace was parallel to the rolling direction and located at the geometrical mid-thickness of the plate.
Near surface trace was parallel to the rolling direction and located 1.25 mm below the plate surface.

(a) Standard deviation for a minimum of six hardness indentations.

(b) Standard deviation for a minimum of sixteen hardness indentations.

TABLE 3.2

SUMMARY OF POROSITY IN HY-100 WELDED JOINTS*

Welded Sample or Fatigue Specimen	Electrode	Type of Grinding Wheel	Number of Pores	Size of Pore(s) (mm)	Location of Pore(s)
2D-3	MIL-11018	Metal Oxide	none		
2D-4	"	" "	none		
2D-5	"	" "	2	0.023	In 4th or 5th weld pass
				0.035	Near root just outside fusion line.
2D-7	"	" "	none		
2D-8	"	" "	none		
2D-13	"	" "	1	0.184	In HAZ just outside 3rd weld pass fusion line.
4D-2	"	" "	none		
4D-7	"	" "	1	0.06	In the 1st weld pass near fusion line.
4D-8	"	" "	2	0.035	In 5th or 6th weld pass near fusion line.
				0.161	At fusion line of 3rd weld pass.
4D-12	"	" "	1	0.95	At fusion line of the 1st weld pass.
DR-3	"	" "	1	0.184	At fusion line and in 1st weld pass.
P-2	"	" "	1	1.83	Slag inclusion at base of 2nd weld pass.
P-4	"	" "	none		
P4-A	"	" "	none		
SA2-D	"	" "	1	0.195	In 2nd weld pass just inside fusion line.
UA	"	" "	none		
W-2	"	" "	3	0.115	In the 4th weld pass.
				0.081	Near 4th weld pass just outside fusion line.
				0.184	In middle of 5th weld pass.
5E	"	" "	1	0.115	In weld metal of 6th weld pass.
1W	"	" "	none		
2W	"	" "	none		

TABLE 3.2 (continued)

SUMMARY OF POROSITY IN HY-100 WELDED JOINTS*

Welded Sample or Fatigue Specimen	Electrode	Type of Grinding Wheel	Number of Pores	Size of Pore(s) (mm)	Location of Pore(s)
3W	MIL-11018	Metal Oxide	none		
4W	"	" "	none		
8W	"	" "	none		
2	"	" "	none		
6-B	"	" "	none		
HY-34Sec.1	"	" "	1	0.057	In HAZ outside 5th or 6th weld pass.
HY-34Sec.2	"	" "	none		
70	"	Carbide	none		
71	"	"	none		
71A	"	"	none		
72	"	"	none		
73X	"	"	none		
73XX	"	"	none		
74	"	"	none		
75	"	"	none		
76	"	"	none		
77	"	"	none		

*Notes: a - 3/4" thick, 6 pass weld specimens.
b - Only pores greater than 0.020mm are reported.

TABLE 3.3

RESULTS OF FATIGUE TESTS OF HY-100 TRANSVERSE BUTT WELDS IN THE AS-WELDED CONDITION*

(Zero-to-Tension)

Specimen Number**	Welding Procedure (see Figs. 3.1 & 3.4)	Stress Cycle (ksi)	Life (cycles)	Location of Fracture ***
HY-10	P100-11018-J	0 to +80.0	8,200	in weld, initiation at small isolated pores
HY-8	P100-11018-J	0 to +80.0	5,400	in weld, initiation at small isolated pores
HY-9	P100-11018-J	0 to +80.0	4,700	in weld, initiation at small isolated pores
HY-12	P100-11018-J	0 to +50.0	61,800	at edge of weld reinforcement
HY-11	P100-11018-J	0 to +50.0	61,500	at edge of weld reinforcement
HY-13	P100-11018-J	0 to +50.0	24,100	in weld, initiation at small isolated pores
HY-15	P100-11018-J	0 to +30.0	240,600	at edge of weld reinforcement
HY-14	P100-11018-J	0 to +30.0	212,500	at edge of weld reinforcement
HY-63	P100-12018-A	0 to +80.0	23,300	at edge of weld reinforcement
HY-64	P100-12018-A	0 to +80.0	7,700	in weld, initiation at single small pore
HY-65	P100-12018-A	0 to +80.0	5,500	in weld, initiation at single small pore
HY-67	P100-12018-A	0 to +50.0	87,500	at edge of weld reinforcement
HY-66	P100-12018-A	0 to +50.0	49,300	in weld, initiation at lack of fusion
HY-69	P100-12018-A	0 to +30.0	231,000	at edge of weld reinforcement
HY-68	P100-12018-A	0 to +30.0	181,000	at edge of weld reinforcement

* Bonded metal oxide wheel used to grind root pass of weld

** Data for specimens HY-8 through HY-15 reported in Ref. 3

*** Internal defects not detected by radiography

TABLE 3.4

RESULTS OF FATIGUE TESTS OF HY-100 TRANSVERSE BUTT WELDS
IN THE AS-WELDED CONDITION*

(Zero-to-Tension)

Specimen Number	Welding Procedure (see Figs. 3.1,3.4,3.5)	Stress Cycle (ksi)	Life (cycles)	Location of Fracture***
HY-71**	P100-12018-A	0 to +80.0	17,000	at edge of weld reinforcement
HY-70**	P100-12018-A	0 to +80.0	10,500	in weld, initiation at lack of fusion
HY-73**	P100-12018-A	0 to +80.0	6,200	in weld, initiation at single small pore
HY-72**	P100-12018-A	0 to +80.0	4,400	in weld, initiation at lack of fusion
HY-75	P100-12018-A	0 to +80.0	21,600	at edge of weld reinforcement
HY-74	P100-12018-A	0 to +80.0	21,200	at edge of weld reinforcement
HY-76	P100-12018-A	0 to +50.0	96,800	at edge of weld reinforcement
HY-77	P100-12018-A	0 to +50.0	94,200	at edge of weld reinforcement with secondary crack at porosity
HY-90	P100-12018-C	0 to +50.0	92,800	at edge of weld reinforcement
HY-84	P100-11018-J	0 to +80.0	15,900	at edge of weld reinforcement
HY-85	P100-11018-J	0 to +80.0	15,800	at edge of weld reinforcement

* Carbide wheel used to grind root pass of weld.

** 3/8" carbide wheel used; 1/4" carbide wheel used in preparation of other specimens.

*** Internal defects not detected by radiography.

TABLE 3.5

ANALYSIS OF FATIGUE DATA FOR SOUND HY-100 TRANSVERSE BUTT WELDS IN THE AS-WELDED CONDITION*

(Zero-to-Tension)

Specimen Number	Welding Procedure (See Figs. 3.1,3.4,3.5)	Stress Cycle (ksi)	Life (cycles)	Computed Fatigue Strength, ksi**				
				$F_{20,000}$	$F_{50,000}$	$F_{100,000}$	$F_{200,000}$	$F_{500,000}$
HY-63	P100-12018-A	0 to +80.0	23,300	85.3	57.9	43.3	---	---
HY-75	P100-12018-A	0 to +80.0	21,600	82.6	56.1	41.9	---	---
HY-74	P100-12018-A	0 to +80.0	21,200	82.0	55.7	41.6	---	---
HY-71	P100-12018-A	0 to +80.0	17,000	74.7	50.7	--	---	---
HY-84	P100-11018-J	0 to +80.0	15,900	72.6	49.3	--	---	---
HY-85	P100-11018-J	0 to +80.0	15,800	72.4	49.2	--	---	---
HY-76	P100-12018-A	0 to +50.0	96,800	97.2	66.1	49.3	36.8	---
HY-77	P100-12018-A	0 to +50.0	94,200	96.2	65.3	48.8	36.4	---
HY-90	P100-12018-C	0 to +50.0	92,800	95.5	64.9	48.2	36.2	---
HY-67	P100-12018-A	0 to +50.0	87,500	93.2	63.3	47.2	35.2	---
HY-12	P100-11018-J	0 to +50.0	61,800	90.6	54.7	40.8	34.3	---
HY-11	P100-11018-J	0 to +50.0	61,500	90.4	54.6	40.7	34.2	---
HY-15	P100-11018-J	0 to +30.0	240,600	--	58.2	43.5	32.4	22.0
HY-69	P100-12018-A	0 to +30.0	231,000	--	57.3	42.7	31.4	21.7
HY-14	P100-11018-J	0 to +30.0	212,500	--	55.3	41.2	30.8	20.9
HY-68	P100-12018-A	0 to +30.0	181,000	--	51.6	38.5	28.8	19.5
			Average	86.0	56.9	43.6	33.6	21.0

* Specimens failing at edge of weld reinforcement considered "sound" weldments; those failing at internal flaws considered defective weldments and are not included in analysis.

** K = 0.422

TABLE 3.6

RESULTS OF FATIGUE TESTS OF HY-100 TRANSVERSE BUTT WELDS WITH WELD REINFORCEMENT REMOVED*

(Zero-to-Tension)

Specimen Number**	Welding Procedure (See Figs. 3.1,3.2,3.3,3.4)	Stress Cycle (ksi)	Life (cycles)	Location of Fracture***
HY-41	P100-11018-J	0 to +80.0	14,800	in weld, initiation at single small pore
HY-42	P100-11018-J	0 to +80.0	13,700	in weld, initiation at single small pore
HY-25	P100-11018-J	0 to +50.0	1,108,600	in weld
HY-43	P100-11018-J	0 to +50.0	198,100	in weld, initiation at single small pore
HY-39	P100-11018-J	0 to +50.0	88,100	in weld, initiation at single small pore
HY-60	P100-11018-J	0 to +50.0	57,900	in weld, initiation at 3 isolated pores
HY-57	P100-11018-J30	0 to +50.0	412,300	at weld undercut
HY-52	P100-11018-J30	+10.0 to +60.0	85,400	in weld, initiation at single small pore
HY-53	P100-11018-J50	+10.0 to +60.0	318,600	in weld, initiation at single small pore
HY-56	P100-11018-J50	0 to +50.0	137,900	in weld, initiation at single small pore
HY-61	P100-12018-A	0 to +50.0	607,600	in weld, initiation at single small pore

* Bonded metal oxide wheel used to grind root pass of weld

** Data initially reported in Ref. 3

*** Internal defects not detected by radiography

TABLE 3.7

RESULTS OF FATIGUE TESTS OF HY-100 TRANSVERSE BUTT WELDS
WITH WELD REINFORCEMENT REMOVED*
(Zero-to-Tension)

Specimen	Welding Procedure (See Fig. 3.4)	Stress Cycle (ksi)	Life (cycles)	Location of Fracture
HY-79	P100-12018-A	0 to +80.0	148,600	at mill scale surface of plain plate near radius of test section
HY-78	P100-12018-A	0 to +80.0	87,600	at mill scale surface of plain plate near radius of test section
HY-81	P100-12018-A	0 to +50.0	1,567,000 +	in specimen pull-head

* Carbide wheel used to grind root pass of weld

TABLE 3.8

COMPARISON OF FATIGUE BEHAVIOR OF HY-100 AND HY-80 STEELS

(Zero-to-Tension)

Specimen Type	Surface Condition	K	Computed Fatigue Strength, ksi				
			$F_{20,000}$	$F_{50,000}$	$F_{100,000}$	$F_{200,000}$	$F_{500,000}$
(a) 3/4 In. Thick HY-100 Steel[1]							
Plain Plate	As-Received	0.301	---	84.5	68.6	55.7	42.9
Transverse Butt Weld	As-Welded	0.422	86.0	56.9	43.6	33.6	21.0
(b) 3/4 In. Thick HY-80 Steel[2]							
Plain Plate	As-Received	0.201	91.0	75.6	65.6	57.1	47.4
Transverse Butt Weld	As-Welded	0.279	---	69.3	57.1	45.0	35.0
Transverse Butt Weld	Reinforcement Removed	0.229	---	80.7	69.0	58.9	47.9
(c) 1-1/2 In. Thick HY-80 Steel[3]							
Plain Plate	As-Received	0.149	89.9	78.5	67.9	60.9	54.5
Transverse Butt Weld	As-Welded	0.340	77.3	56.3	44.6	35.0	25.6
Transverse Butt Weld	Reinforcement Removed	0.146	82.0	71.2	64.3	58.2	50.8

(1) Data for plain plates reported in Ref. 3

(2) Data reported in Ref. 5

(3) Data reported in Ref. 6

TABLE 3.9

RESULTS OF DEFECT EXAMINATION AND FATIGUE TESTS OF HY-100 TRANSVERSE BUTT WELDS CONTAINING INTENTIONAL WELD DEFECTS

(Zero-to-Tension)

Specimen Number*	Stress Cycle (ksi)	Life (cycles)	Percent Defect Area (Based on Radiography)	Radiographic Rating**	Description of Defects (Observed on Fracture Surface)	Location of Fracture***
HY-54	0 to +50.0	134,700	0.12	Failed	one porosity cluster + single pore, 0.02" dia.	a
HY-55	0 to +50.0	32,200	0.11	Failed	one porosity cluster + single pore, 0.05" dia.	a
HY-86	0 to +50.0	229,000	0.64	Failed	Several Isolated pores 0.04", 0.03", 0.02", 0.01"(3) dia.	b
HY-87	0 to +50.0	41,400	2.27	Failed	slag inclusions, lack of fusion, and porosity cluster	c

* Data for specimens HY-54, HY-55, reported in Ref. 3

** Based on radiographic requirements of Navy Specifications (7)

*** a: initiation in weld at single isolated pore
b: initiation in weld at several isolated pores
c: initiation in weld at combination of defects

TABLE 3.10

RESULTS OF FATIGUE CRACK INITIATION AND PROPAGATION STUDY OF HY-100 TRANSVERSE BUTT WELD CONTAINING INTENTIONAL WELD DEFECTS

(1)	(2)	(3)	(4)	(5)	(6)	(7)	(8)
Specimen Number	Stress Cycle (ksi)	Cycles to Start of Crack Growth (*)	Cycles at Which Crack Length Equal to Specimen Thickness	Total Life (cycles)	Ratio Column 3/ Column 5	Ratio Column 3/ Column 4	Type of Defect
HY-87	0 to +50.0	7,500	24,000	41,400	0.181	0.312	lack of fusion, slag, & porosity

(*) estimated as average of number of cycles between last x-ray showing no fatigue crack and first x-ray showing crack.

TABLE 4.1

RESULTS OF FATIGUE TESTS AND ANALYSIS OF DATA FOR
AS-RECEIVED HY-130/150 PLAIN PLATE SPECIMENS

(Zero-to-Tension)

Specimen Number*	Material Thickness (inches)	Stress Cycle (ksi)	Life** (cycles)	Location of Fracture***	Computed Fatigue Strength, ksi****				
					$F_{20,000}$	$F_{50,000}$	$F_{100,000}$	$F_{200,000}$	$F_{500,000}$
NA-8	1/2	0 to +100.0	26,800	g	106.7	87.3	74.8	---	---
NA-7	1/2	0 to +100.0	21,000	g	101.1	82.7	70.9	---	---
NA-1	1/2	0 to +80.0	64.200	a	103.4	84.5	72.6	62.2	---
NA-2	1/2	0 to +80.0	60,900	g	102.2	83.8	71.7	61.6	---
NC-13	1	0 to +80.0	59,800	g	101.8	83.2	71.4	61.3	---
NA-5	1/2	0 to +80.0	51,100	h	98.3	80.6	69.0	59.4	---
NC-14	1	0 to +80.0	50,500	g	98.1	80.0	68.8	59.1	---
NA-9	1/2	0 to +50.0	345,500	g	---	---	65.5	56.7	46.3
NA-3	1/2	0 to +50.0	280,900	a	---	---	62.8	53.8	44.1
NA-10	1/2	0 to +50.0	1,247,800+	j	---	---	---	---	61.3
NA-6	1/2	0 to +50.0	712,000+	j	---	---	77.0	66.1	54.0
NA-4	1/2	0 to +50.0	555,000±(1)	g	---	---	72.8	62.6	51.2
				Average	101.7	83.2	70.7	60.3	51.4

* Data for all specimens except NC-13, NC-14 reported in Ref. 3

** (1) Cycle counter on fatigue machine broke during test-failure occurred between 484,000 and 627,000 cycles

*** a: Failure initiated at radius of test section
g: Failure initiated at mill scale surface in test section
h: Failure initiated at polished edge of specimen test section
j: Failure in pull-head

**** K = 0.22

TABLE 4.2

COMPARISON OF FATIGUE STRENGTHS FOR
HY-130/150, HY-100, AND HY-80 STEELS
(Zero-to-Tension)

Material	Plate Thickness (inches)	Specimen Type	Surface Condition	K	Computed Fatigue Strength, ksi				
					$F_{20,000}$	$F_{50,000}$	$F_{100,000}$	$F_{200,000}$	$F_{500,000}$
HY-130/150	1/2, 1	Plain Plate	As-Received	0.22	101.7	83.2	70.7	60.3	51.4
HY-100	3/4	Plain Plate	As-Received	0.30	---	84.5	68.6	55.7	42.9
HY-80	3/4	Plain Plate	As-Received	0.20	91.0	75.6	65.6	57.1	47.4
HY-80	1-1/2	Plain Plate	As-Received	0.15	89.9	78.5	67.9	60.9	54.5

TABLE 4.3

FATIGUE STRENGTH-ULTIMATE STRENGTH RATIO FOR
HY-130/150, HY-100, AND HY-80 STEELS
(Zero-to-Tension)

Material	Plate Thickness (inches)	Specimen Type	Surface Condition	Ultimate Strength* (ksi)	Fatigue Strength-Ultimate Strength Ratio at Various Lives				
					@ 20,000 cycles	50,000	100,000	200,000	500,000
HY-130/150	1/2, 1	Plain Plate	As-Received	144.0	0.71	0.58	0.49	0.42	0.36
HY-100	3/4	Plain Plate	As-Received	127.5	--	0.66	0.54	0.44	0.34
HY-80	3/4	Plain Plate	As-Received	109.2	0.83	0.69	0.60	0.52	0.43
HY-80	1-1/2	Plain Plate	As-Received	108.3	0.83	0.73	0.63	0.56	0.50

* Properties in longitudinal direction

TABLE 4.4

FATIGUE STRENGTH-YIELD STRENGTH RATIO FOR
HY-130/150, HY-100, AND HY-80 STEELS

Material	Plate Thickness (inches)	Specimen Type	Surface Condition	Yield Strength 0.2% Offset* (ksi)	Fatigue Strength-Yield Strength Ratio at Various Lives				
					@ 20,000 cycles	50,000	100,000	200,000	500,000
HY-130/150	1/2, 1	Plain Plate	As-Received	138.0	0.74	0.60	0.51	0.44	0.37
HY-100	3/4	Plain Plate	As-Received	110.0	--	0.77	0.62	0.51	0.39
HY-80	3/4	Plain Plate	As-Received	90.0	1.0	0.84	0.73	0.63	0.53
HY-80	1-1/2	Plain Plate	As-Received	88.5	1.0	0.89	0.77	0.69	0.62

* Properties in longitudinal direction

TABLE 4.5

RESULTS OF FATIGUE TESTS OF HY-130/150 PLAIN PLATE SPECIMENS
WITH MILL SCALE REMOVED
(Zero-to-Tension)

Specimen Number	Stress Cycle (ksi)	Life (cycles)	Location of Fracture
NA-11	0 to +100.0	176,000	initiation at radius of test section
NA-14	0 to +100.0	110,500	initiation at radius of test section
NA-13	0 to +80.0	304,300	initiation at radius of test section
NA-15	0 to +80.0	208,800	initiation at two points on polished edge of test section

TABLE 4.6

MICROHARDNESS SURVEY OF THE WELD METAL FOR HY-130/150 SPECIMENS PREPARED WITH VARIOUS MIG WELDING PROCEDURES

Sample Number	Condition	Welding Procedure	Number of Weld Passes	Avg. Energy Input (joules/in.)	Average Weld Metal Hardness, DPH*		
					Parallel to Plate Surface		Center Line of Weld Through Plate Thickness
					Mid-Thickness**	Near Surface**	
NB-1-D	As-Welded	P150-X150-A	13	45,000	361±12(a)	413±16	362±22
NB-1-E	As-Welded	P150-X150-B	10	45,000	368±22	384±23	364±36
NB-1-A	As-Welded	P150-AX140-C	12	45,000	350±18	380±25	365±25
NB-7	Tested in Fatigue	P150-X150-A	13	45,000	346±6	390±6	365±25
USS-1	As-Welded	AX-140 wire	12	-	-	-	376±27
NASL	As-Welded	AX-140 wire	17	45,000	-	-	382±20

* Diamond Pyramid Hardness values were obtained with a 1 kg. load. The average base metal hardness obtained from a large number of determinations in the NB series plate was 320 DPH.

** Mid-thickness trace was parallel to the rolling direction and located at the geometrical mid-thickness of the plate.

Near-surface trace was parallel to the rolling direction and located 1.25 mm below the plate surface.

(a) The standard deviation was for a minimum of 10 indentations in all cases except for the mid-thickness trace of NB-1-D.

TABLE 4.7

COMPARISON OF HY-130/150 MIG WELDING PROCEDURES USED AT USS, NASL, AND U of I

Welding Procedure	Source		
	University of Illinois P150-Ax140-D	NASL*	USS**
1. HY-130/150 Base Material			
heat number	5P0540	5P0540	5P0540
plate thickness	1 in.	1 in.	1 in.
2. Joint Geometry			
double 'V' angle	60°	80°	60°
land	none	none	none
root opening	none	1/8 in.	none
no. weld passes	12	17	12
welding position	flat	flat	flat
3. Weld Metal			
wire designation	AX-140	AX-140	AX-140
wire heat no.	1P0047	1P0047	1P0047
wire diameter	1/16 in.	1/16 in.	1/16 in.
4. Shielding Gas			
Argon	98%	99%	98%
Oxygen	2%	1%	2%
flow rate	50 cfh	50 cfh	50 cfh
5. Temperature Control			
preheat temperature	275°F	250-300°F	200-225°F
interpass temperature	225°F	250-300°F	200-225°F
6. Equipment Control			
current (DC, reversed polarity)	310-330amps	320-350amps	300-340amps
voltage	29 volts	30 volts	28 volts
heat imput, joules/in.	45,000	45,000	---
7. Weld Gun Manipulation	automatic	manual	automatic
Gun Travel Speed	12-15 in/min	15 in/min	10-14 in/min

* Data from Ref. 10

** Data from Ref. 11

TABLE 4.8

RESULTS OF DEFECT EXAMINATION AND FATIGUE TESTS OF HY-130/150 TRANSVERSE BUTT WELDS IN THE AS-WELDED CONDITION*

(Zero-to-Tension)

Specimen Number	Welding Procedure (See Figs. 4.5 and 4.6)	Defective Area, percent (Based on Radiographic Examination)	Radiographic Rating***	Stress Cycle (ksi)	Life (cycles)	Location of Fracture
NB-6	P150-X150-A	0.637 (porosity)	F	0 to +80.0	19,900	at 3 separate internal pores; 0.025", 0.02", 0.015" dia.
NB-7	P150-X150-A	none	P	0 to +80.0	5,100	at single internal flaw
NB-8	P150-X150-A	0.031 (single flaw)	P	0 to +80.0	3,000	at lack of fusion; 2.25" long
NB-4	P150-X150-B	0.122 (single flaw)	P	0 to +80.0	10,100	at several minute internal flaws
NB-2	P150-X150-B	none	P	0 to +80.0	2,200	at lack of fusion; 0.45" long
NB-3	P150-X150-B	none	P	0 to +50.0	6,900	at lack of fusion; 2.75" long
NB-10	P150-X150-B**	0.370 (porosity)	P	0 to +80.0	38,100	at edge of weld reinforcement
NB-9	P150-X150-B**	none in test section; 0.577 (porosity) at ends of weld	P	0 to +80.0	10,100	at lack of fusion, 0.23" long

* Bonded metal oxide wheel used to grind root pass of weld

** All interior weld passes ground with metal oxide wheel before placing subsequent passes.

*** Based on requirements of Navy Specifications [7] (P: passed; F: failed)

TABLE 4.9

RESULTS OF DEFECT EXAMINATION AND FATIGUE TESTS OF HY-130/150 TRANSVERSE BUTT WELDS IN THE AS-WELDED CONDITION*

(Zero-to-Tension)

Specimen Number	Welding Procedure (See Figs. 4.7 and 4.8)	Defective Area, percent (Based on Radiographic Examination)	Radiographic Rating**	Stress Cycle (ksi)	Life (cycles)	Location of Fracture
NC-2	P150-AX140-C	0.34 (porosity)	P	0 to +80.0	17,500	at toe of weld & at internal pore; 0.06" dia.
NC-4	P150-AX140-C	1.26 (porosity)	F	0 to +80.0	13,400	at lack of fusion & at 4 internal pores; 0.02", 0.04"(2), 0.06" dia.
NC-5	P150-AX140-C	0.28 (porosity)	P	0 to +80.0	10,600	at lack of fusion; 2.25" long
NC-3	P150-AX140-C	1.20 (porosity)	F	0 to +80.0	5,400	at lack of fusion & isolated pores
NC-7	P150-AX140-D	0.44 (porosity)	P	0 to +80.0	9,900	in weld metal
NC-6	P150-AX140-D	none	P	0 to +80.0	4,050	in weld metal
NC-15	P150-AX140-D	0.07 (porosity)	P	0 to +50.0	34,200	at isolated pores; 0.02"(2); 0.03"(2); 0.04" dia.
NC-11	P150-AX140-D	0.12 (porosity)	P	0 to +50.0	14,800	in weld metal
NC-12	P150-AX140-D	none	P	0 to +50.0	12,400	in weld metal
NC-16	P150-AX140-D	0.32 (porosity)	P	0 to +40.0	223,600	at edge of weld reinforcement

* Carbide wheel used to grind root pass of weld

** Based on requirements of Navy Specifications[7] (P: passed; F: failed)

TABLE 4.10

RESULTS OF FATIGUE TESTS OF COMPARISON HY-130/150
TRANSVERSE BUTT WELDS IN THE AS-WELDED CONDITION

(Zero-to-Tension)

Specimen Number	Welding Procedure (See Table 4.7)	Stress Cycle (ksi)	Life (cycles)	Location of Fracture
USS-2*	AX-140 wire	0 to +80.0	9,950	in weld metal
USS-3*	AX-140 wire	0 to +80.0	9,800	in weld metal
USS-1*	AX-140 wire	0 to +80.0	3,850	in weld metal
NC-10B**	AX-140 wire	0 to +80.0	27,900	at single internal pore; 0.04" dia.
NC-9B**	AX-140 wire	0 to +80.0	17,300	at two internal pores; 0.02", 0.04" dia.
NC-8B**	AX-140 wire	0 to +80.0	10,650	in weld metal

* Specimens welded by U. S. Steel Corporation, Pittsburgh, Pennsylvania

** Specimens welded by U. S. Naval Applied Science Lab., Brooklyn, New York

TABLE 4.11

RESULTS OF FATIGUE TESTS OF HY-130/150 TRANSVERSE BUTT WELDS WITH WELD REINFORCEMENT REMOVED*

(Zero-to-Tension)

Specimen Number	Welding Procedure (See Fig. 4.8)	Defective Area, percent (Based on Radiographic Examination)	Radiographic Rating**	Stress Cycle (ksi)	Life (cycles)	Location of Fracture
NC-22	P150-AX140-D	1.78 (porosity)	F	0 to +80.0	9,500	at isolated pores; 0.02", 0.04", 0.045", 0.05" dia.
NC-21	P150-AX140-D	0.21 (single flaw)	F	0 to +80.0	3,900	at lack of fusion 0.9" long
NC-20	P150-AX140-D	0.41 (porosity)	P	0 to +50.0	6,600	at lack of fusion 2.4" long
NC-19	P150-AX140-D	0.75 (porosity)	P	0 to +43.0	2,272,500	at isolated pore 0.08" dia.

* Carbide wheel used to grind root pass of weld

** Based on requirements of Navy Specifications[7] (P: passed; F: failed)

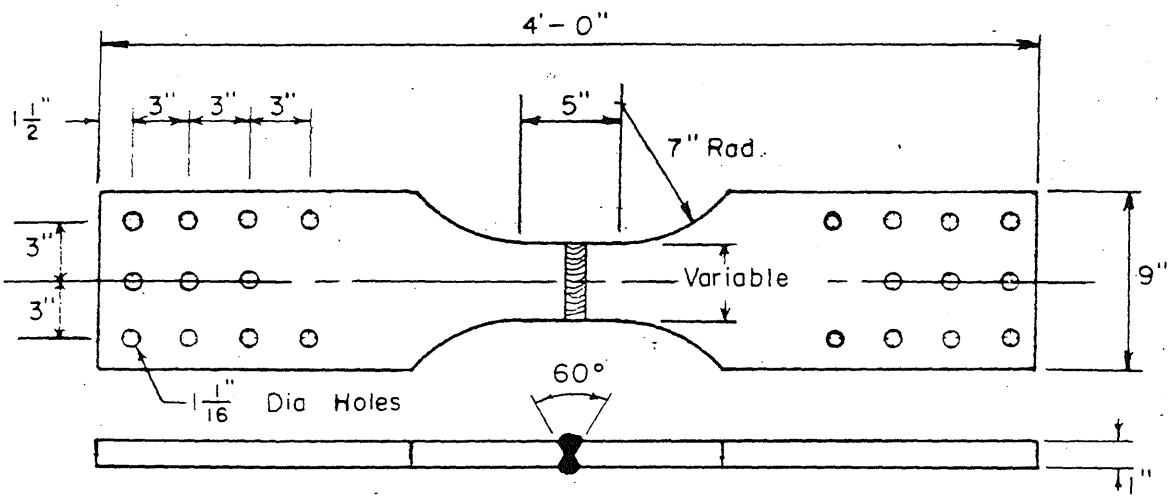

(a) Transverse Butt Weld (HY-130/150 Material)

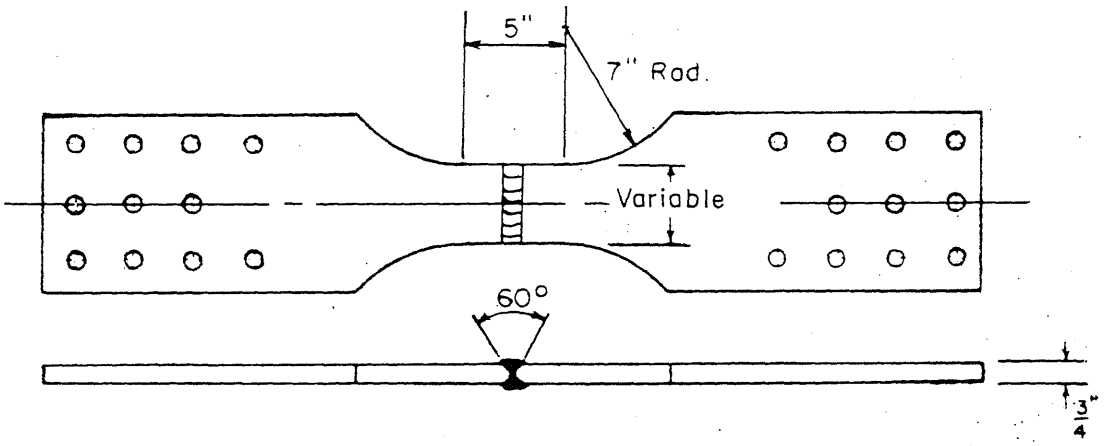

(b) Transverse Butt Weld (HY-100 Material)

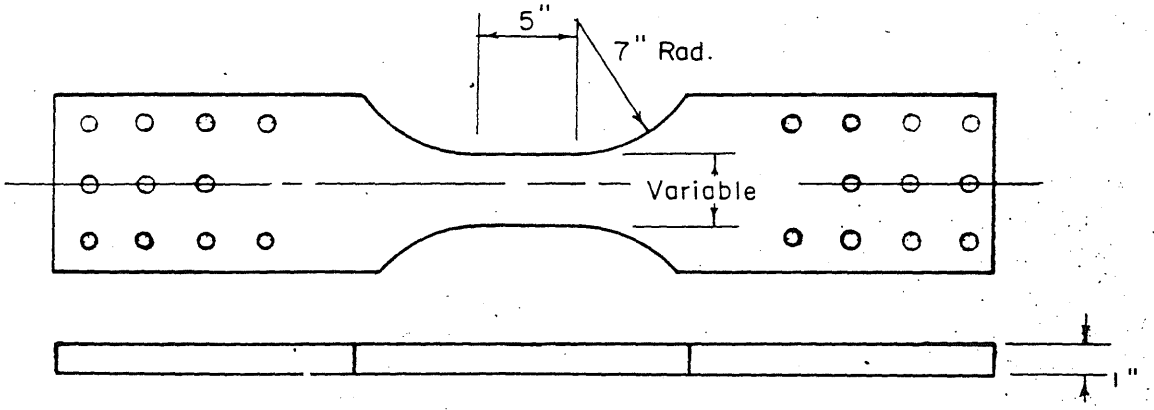

(c) Plain Plate (HY-130/150 Material)

FIG. 2.1 DETAILS OF TEST SPECIMENS

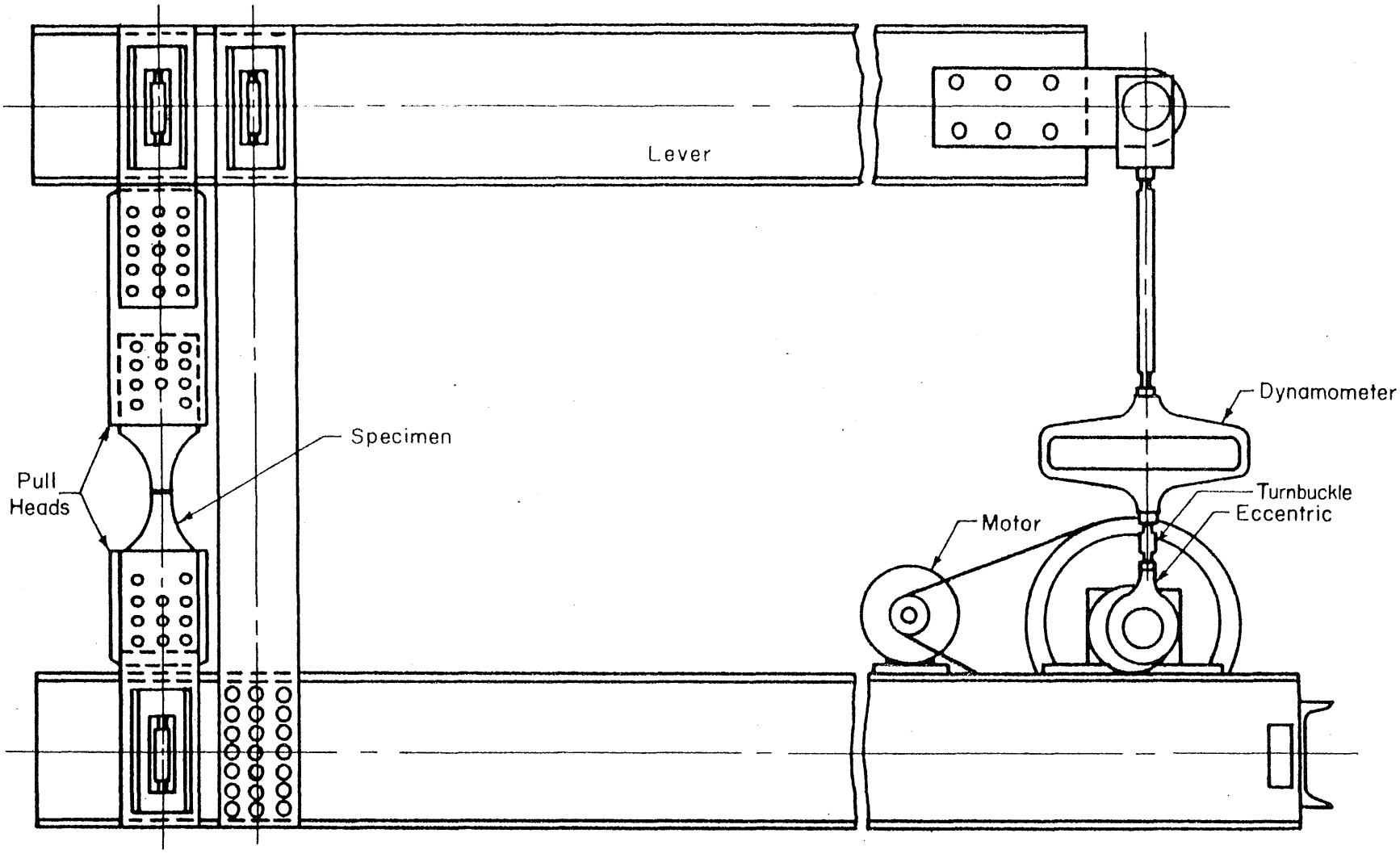

FIG. 2.2 ILLINOIS' FATIGUE TESTING MACHINE AS USED FOR AXIAL LOADING OF WELDED JOINTS

D IN POSITION

R

STUDY OF

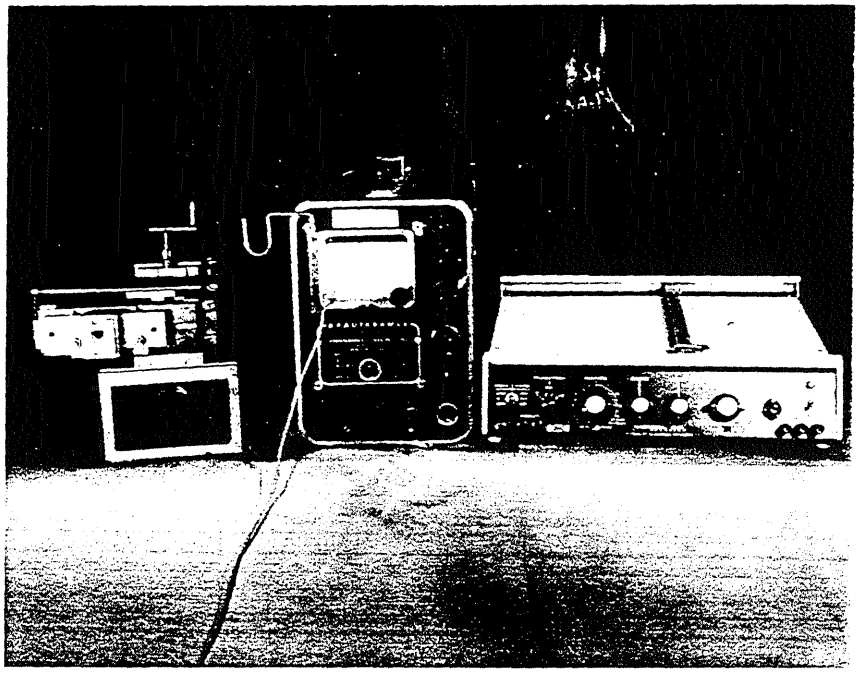

a) Probe Support, Detector And X-Y Recorder

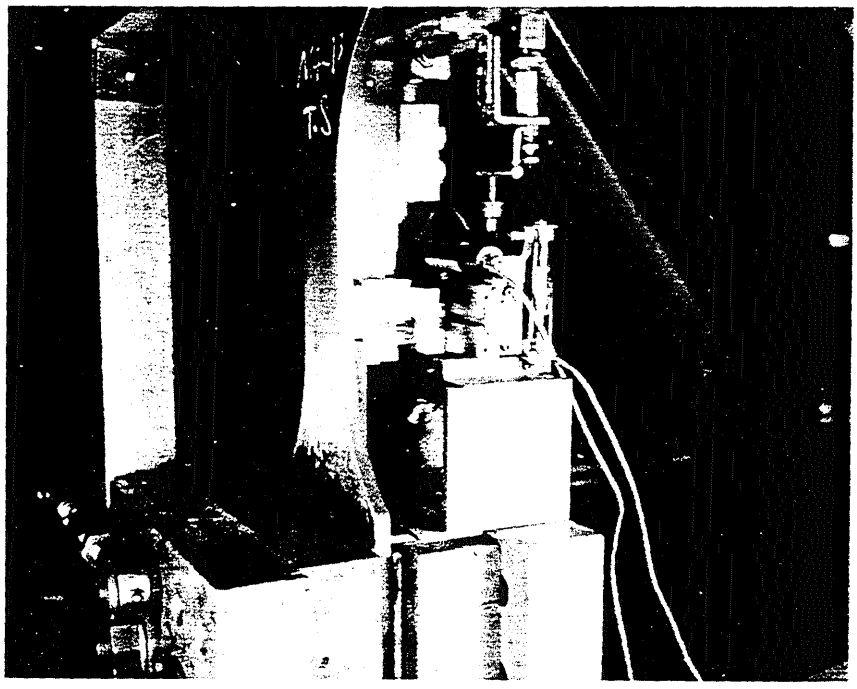

b) Unit In Position For Testing

FIG. 2.4 ULTRASONIC TESTING EQUIPMENT

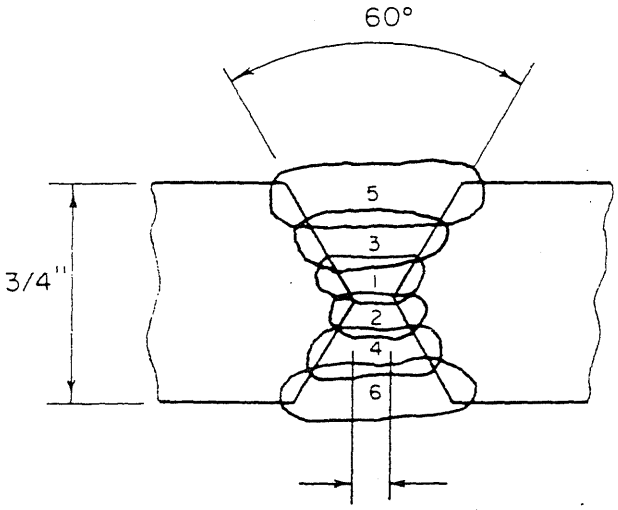

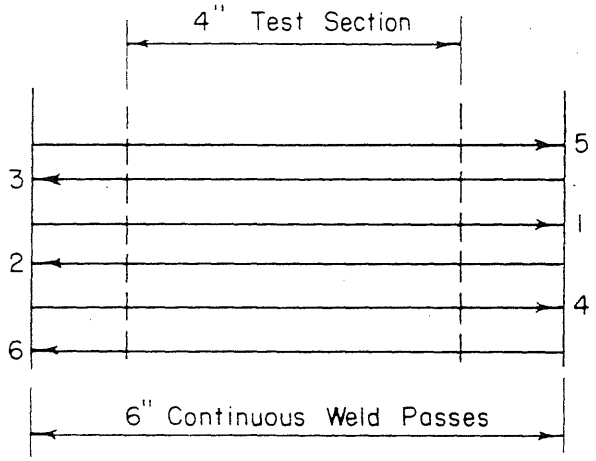

Arrows indicate direction of welding.

Surface of plate adjacent to weld cleaned by grinding before welding.

Pass	Electrode size, in.	Current, amps.	Rate of travel, in./min.
1	5/32	130	5
2	5/32	140	5
3	3/16	230	8
4	3/16	220	7
5	3/16	210	7
6	3/16	210	7

Voltage: 21 Volts
Polarity: D C Reversed
Preheat: 150°F
Electrode: MIL 11018
Interpass Temperature: 200°F (Maximum)
Heat Input: 40,000 Joules/in. (Maximum)
All welding in flat position
Underside of pass 1 ground before placing pass 2

FIG. 3.1 WELDING PROCEDURE P100-11018-J
(Transverse Butt Welds in HY-100)

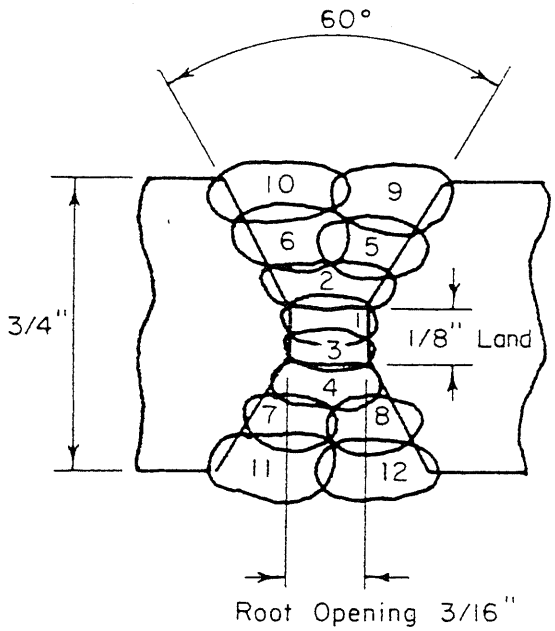

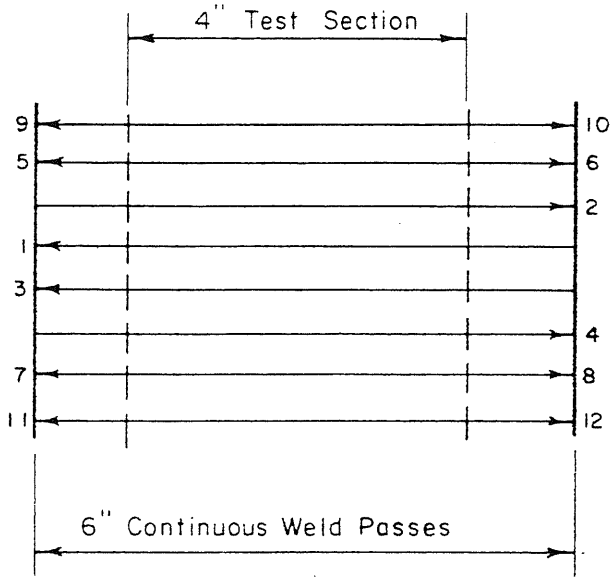

Arrows indicate direction of welding.

Surface of plate adjacent to weld cleaned by grinding before welding.

Pass	Electrode Size, in.	Current, amps	Rate of Travel, in./min.
1	1/8	110	4
2 – 12	5/32	175	8

Voltage : 21 volts
Polarity : D.C. Reversed
Preheat : 150 ° F
Electrode : MIL 11018
Interpass Temperature : 200° F (Maximum)

Heat Input : 30,000 Joules/in. (Maximum)
All welding in flat position.
Underside of pass 1 ground before placing pass 2.

FIG. 3.2 WELDING PROCEDURE P100-11018-J30
(Transverse Butt Welds in HY-100)

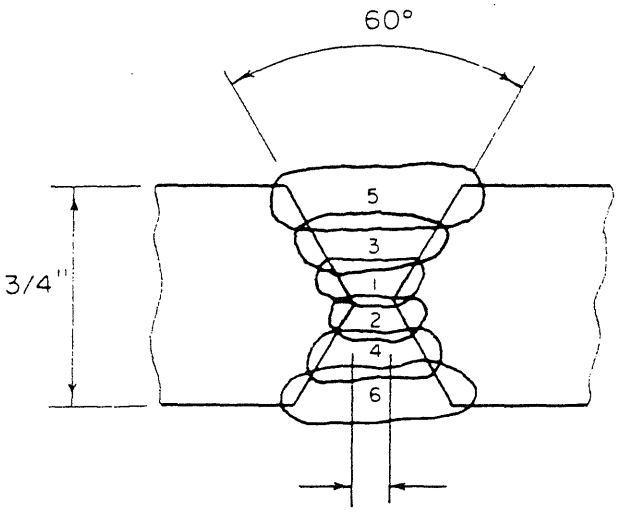

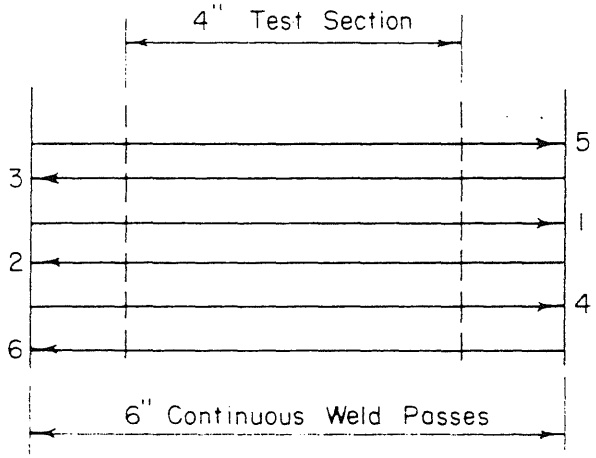

Arrows indicate direction of welding.

Surface of plate adjacent to weld cleaned by grinding before welding.

Pass	Electrode size, in.	Current, amps.	Rate of travel, in./min.
1	5/32	150	5
2	5/32	150	5
3	3/16	220	6
4	3/16	220	6
5	3/16	220	6
6	3/16	220	6

Voltage: 21 Volts
Polarity: D C Reversed
Preheat: 150°F
Electrode: MIL 11018
Interpass Temperature: 200°F (Maximum)
Heat Input: 50,000 Joules/in (Maximum)
All welding in flat position
Underside of pass 1 ground before placing pass 2

FIG.3.3 WELDING PROCEDURE P100-11018-J50
(Transverse Butt Welds in HY-100)

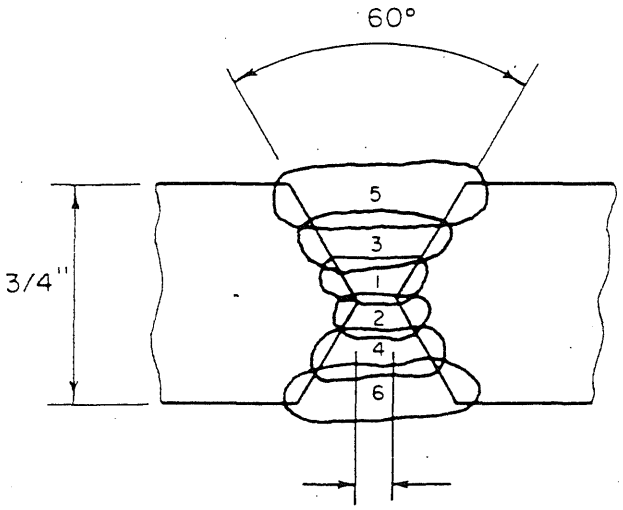

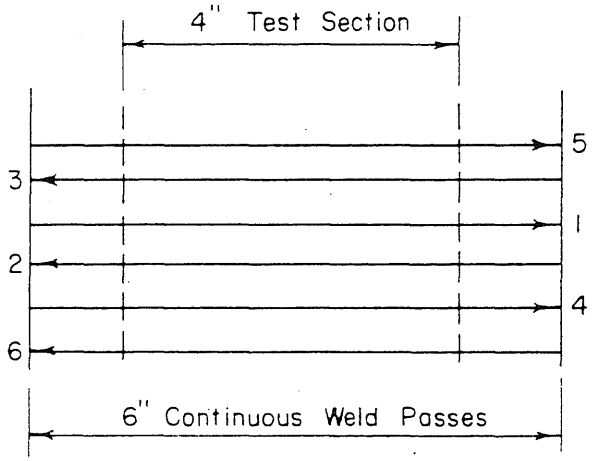

Arrows indicate direction of welding.

Surface of plate adjacent to weld cleaned by grinding before welding.

Pass	Electrode size, in.	Current, amps.	Rate of travel, in /min
1	5/32	130	5
2	5/32	140	5
3	3/16	230	8
4	3/16	220	7
5	3/16	210	7
6	3/16	210	7

Voltage: 21 Volts
Polarity: D C Reversed
Preheat: 150°F
Electrode: MIL 12018
Interpass Temperature: 200°F (Maximum)
Heat Input: 40,000 Joules/in. (Maximum)
All welding in flat position
Underside of pass 1 ground before placing pass 2

FIG.3.4 WELDING PROCEDURE P100-12018-A
(Transverse Butt Welds in HY-100)

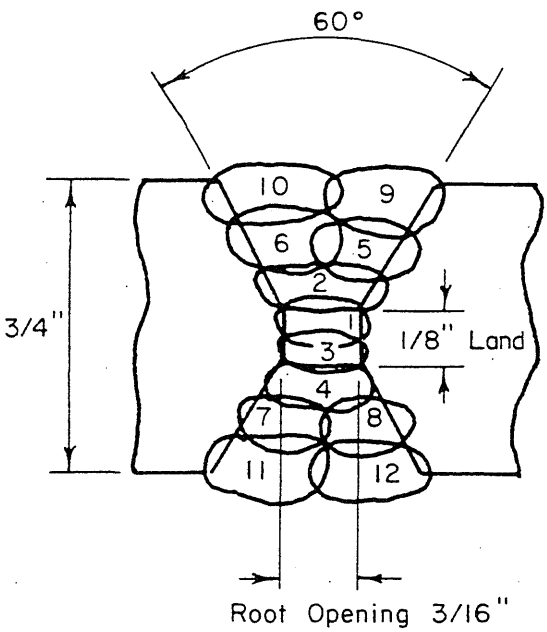

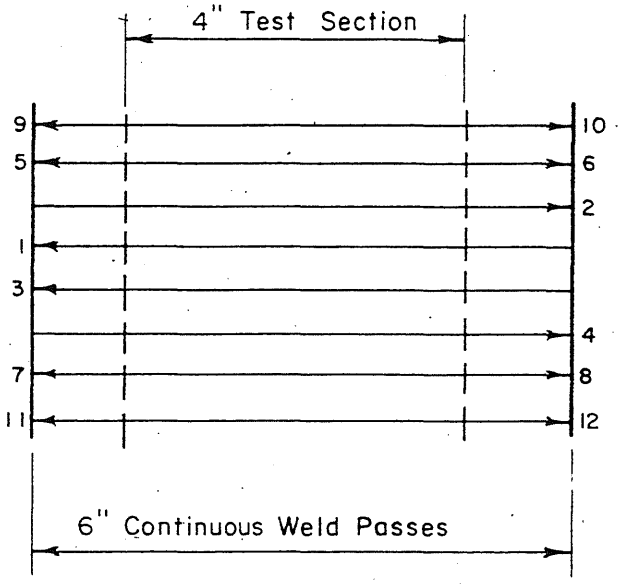

Arrows indicate direction of welding.

Surface of plate adjacent to weld cleaned by grinding before welding.

Pass	Electrode Size, in.	Current, amps	Rate of Travel, in./min.
1	1/8	110	4
2-12	5/32	175	8

Voltage: 21 volts
Polarity: D.C. Reversed
Preheat: 150° F
Electrode: MIL 12018
Interpass Temperature: 200° F (Maximum)

Heat Input: 30,000 Joules/in. (Maximum)
All welding in flat position.
Underside of pass 1 ground before placing pass 2.

FIG. 3.5 WELDING PROCEDURE P100-12018-C
(Transverse Butt Weld in HY-100)

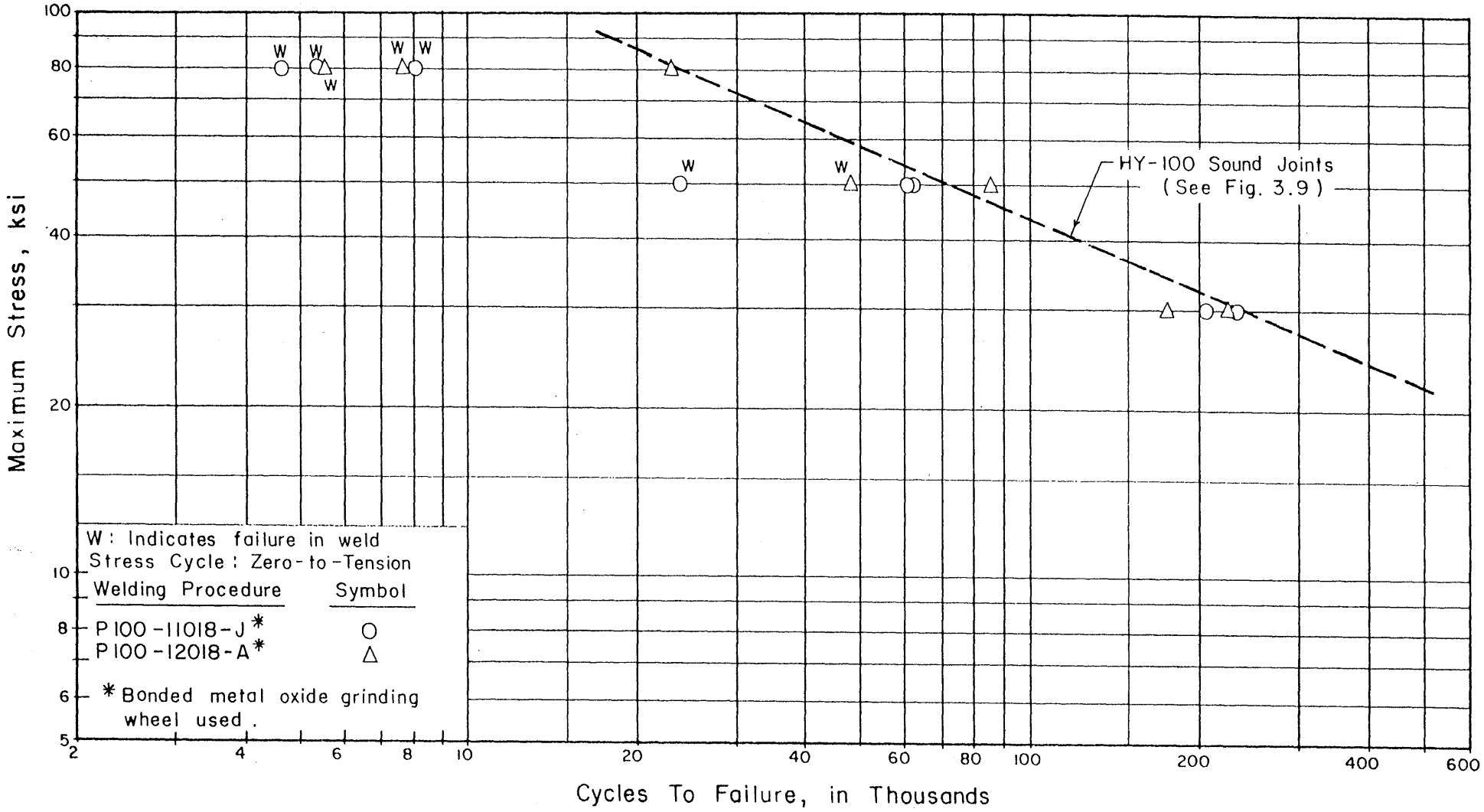

FIG. 3.6 RESULTS OF FATIGUE TESTS OF HY-100 TRANSVERSE BUTT WELDS IN THE AS-WELDED CONDITION

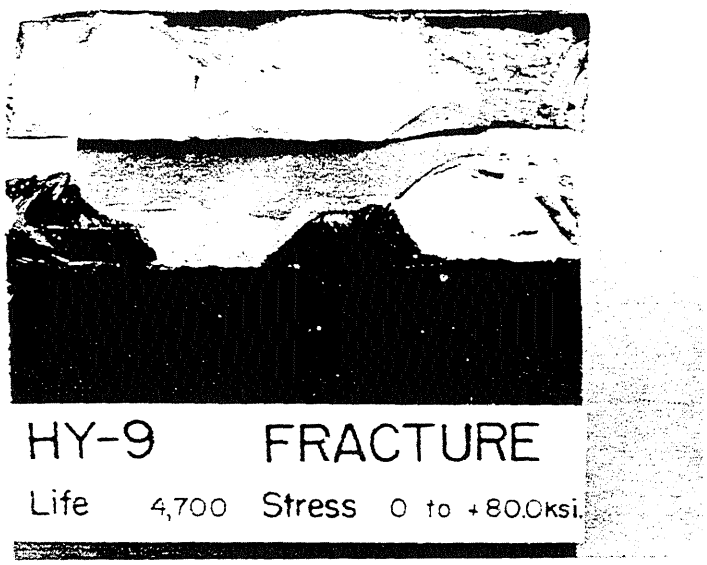

(a) Failure Initiated At Internal Flaws

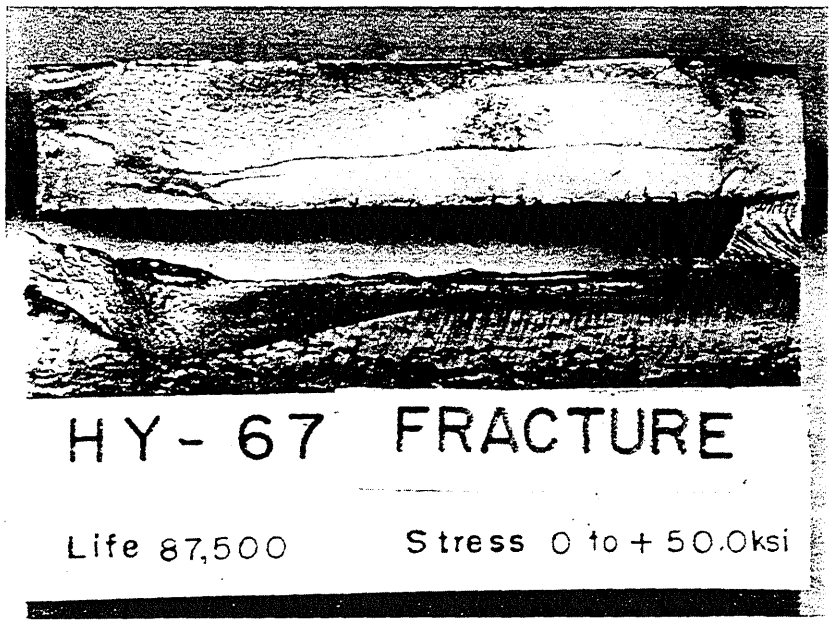

(b) Failure Initiated At Toe Of Weld

FIG. 3.7 FRACTURE SURFACES OF HY-100 TRANSVERSE BUTT WELDS IN THE AS-WELDED CONDITION

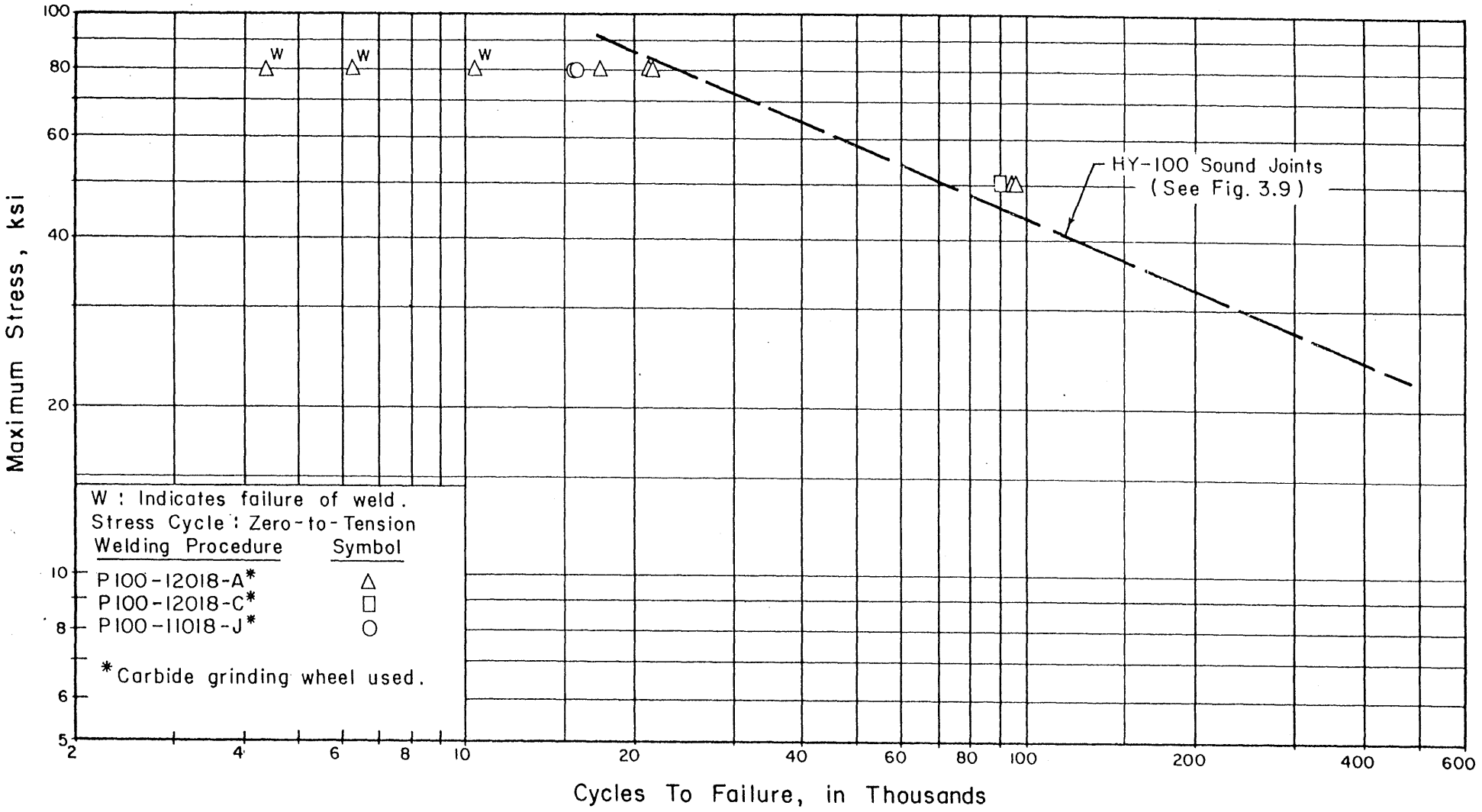

FIG. 3.8 RESULTS OF FATIGUE TESTS OF HY-100 TRANSVERSE BUTT WELDS IN THE AS-WELDED CONDITION

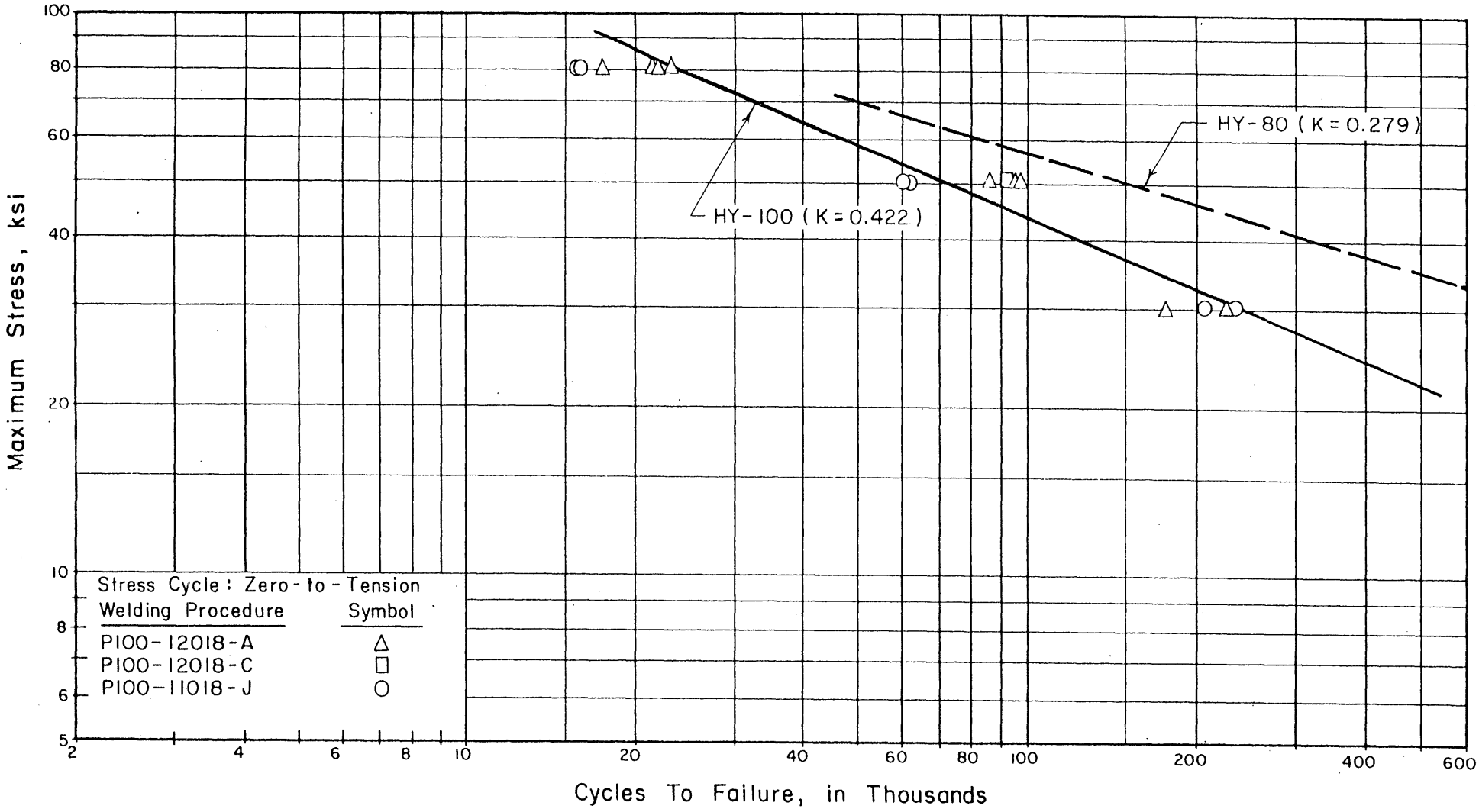

FIG. 3.9 RESULTS OF FATIGUE TESTS OF SOUND HY-100 TRANSVERSE BUTT WELDS IN THE AS-WELDED CONDITION

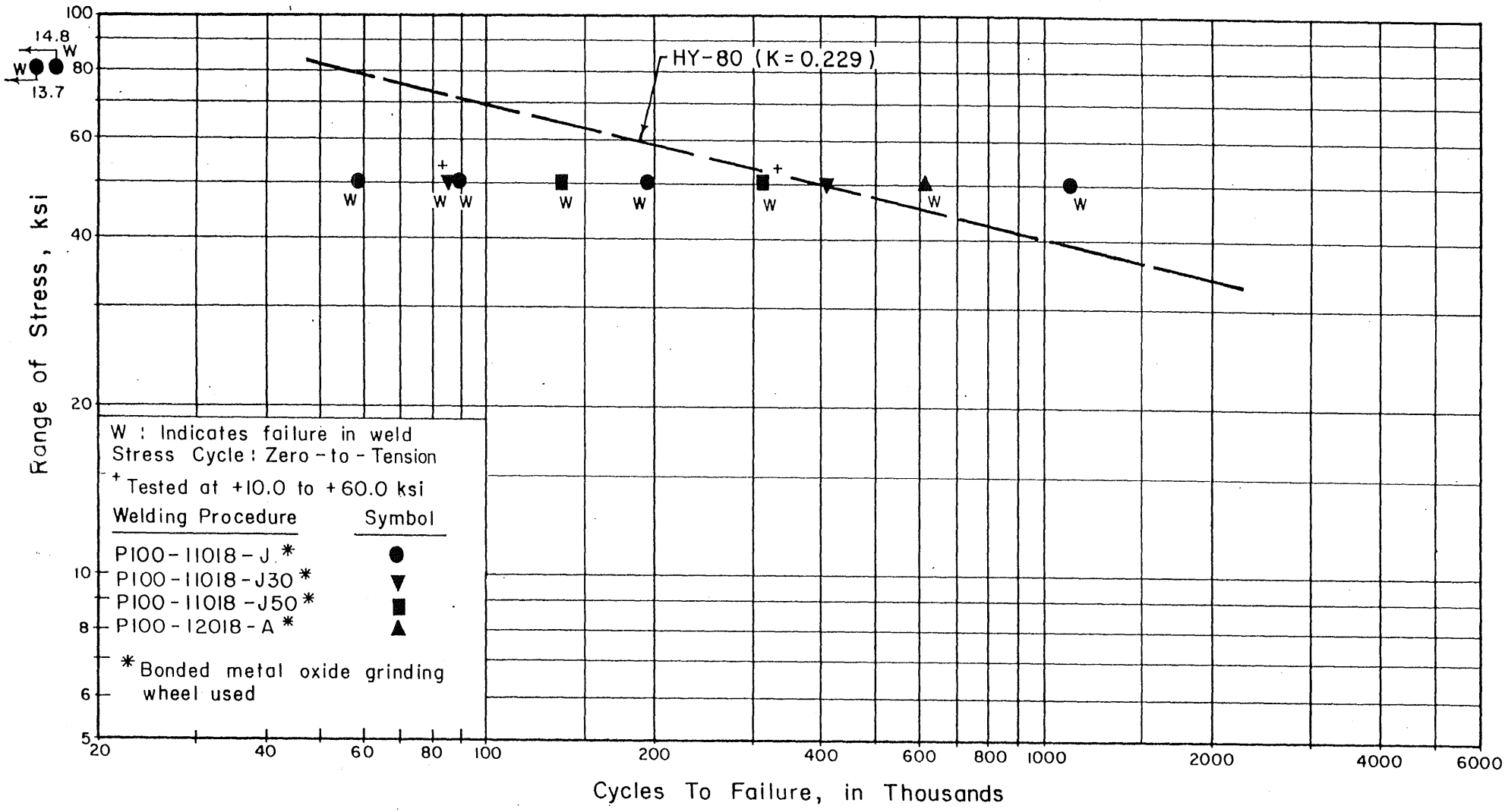

FIG. 3.10 RESULTS OF FATIGUE TESTS OF HY-100 TRANSVERSE BUTT WELDS WITH REINFORCEMENT REMOVED

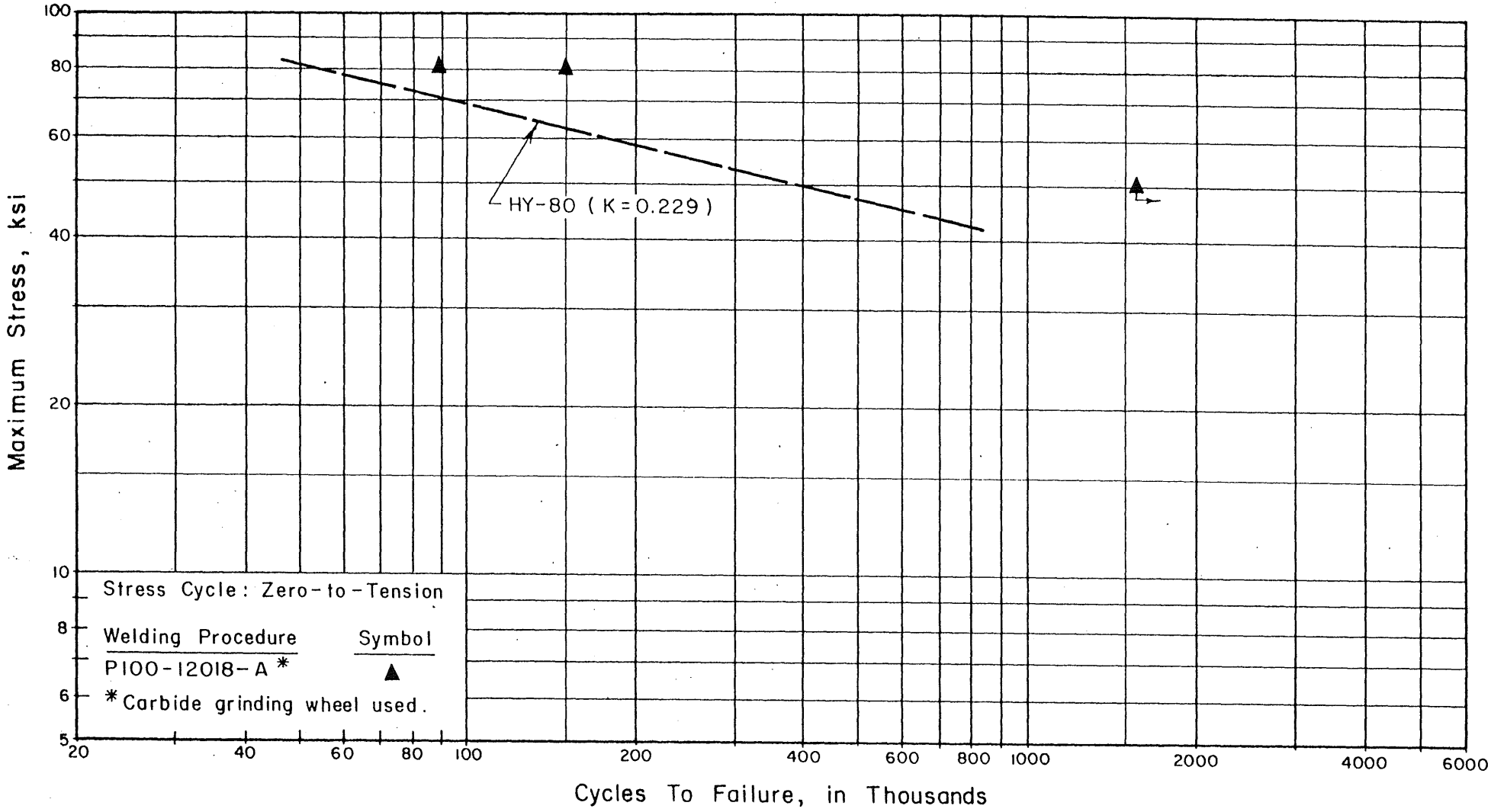

FIG. 3.11 RESULTS OF FATIGUE TESTS OF SOUND HY-100 TRANSVERSE BUTT WELDS WITH REINFORCEMENT REMOVED

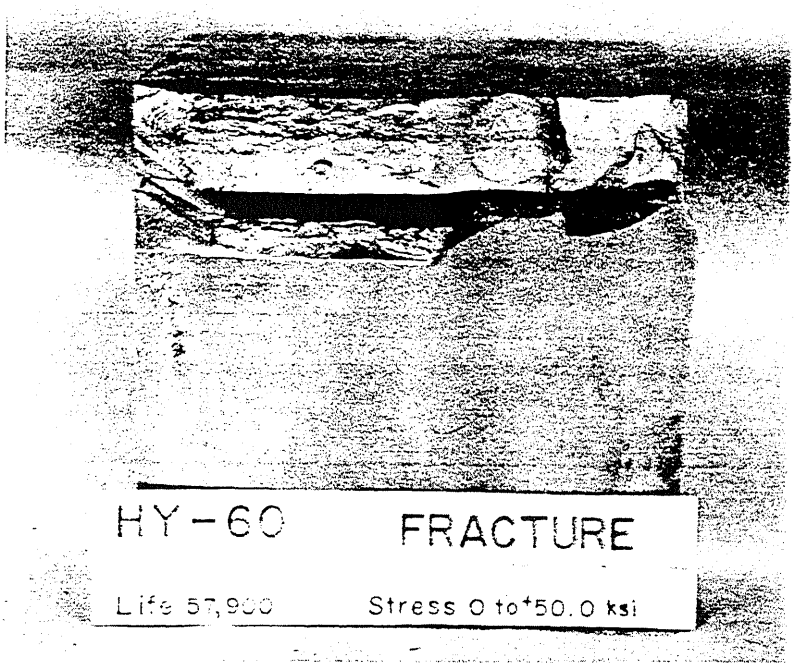

(a) Failure Initiated At Internal Flaws

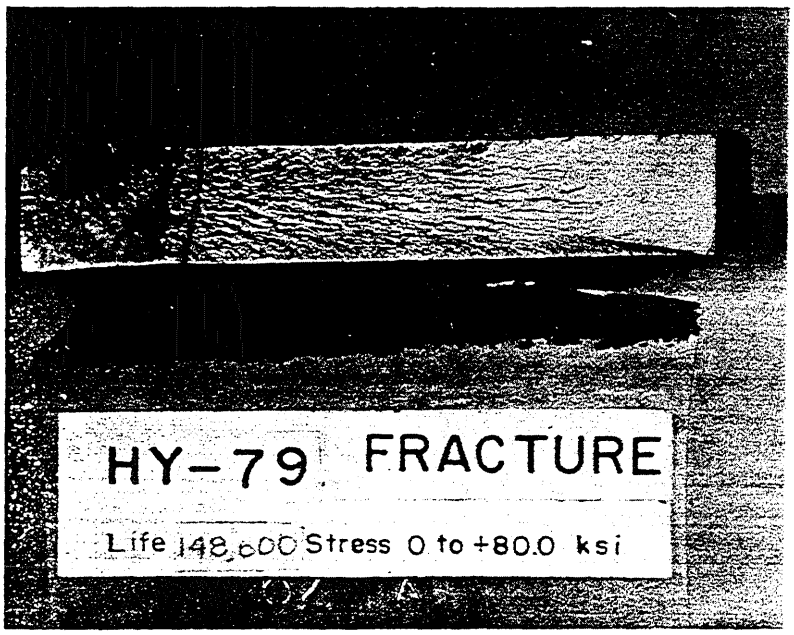

(b) Failure Initiated At Radius Of Test Section

FIG. 3.12 FRACTURE SURFACES OF HY-100 TRANSVERSE BUTT WELDS WITH REINFORCEMENT REMOVED

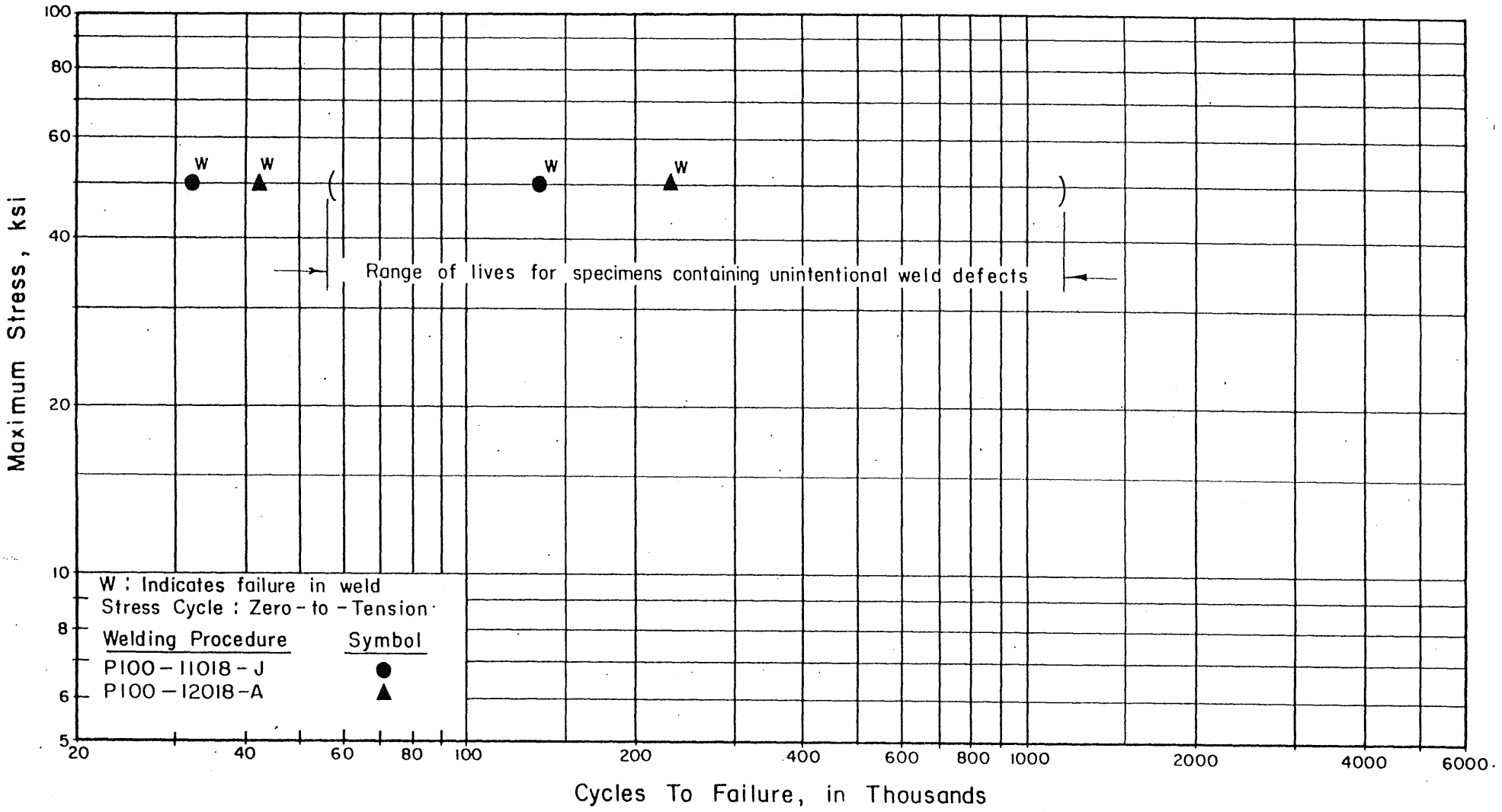

FIG. 3.13 RESULTS OF FATIGUE TESTS OF HY-100 TRANSVERSE BUTT WELDS CONTAINING INTENTIONAL POROSITY (REINFORCEMENT REMOVED)

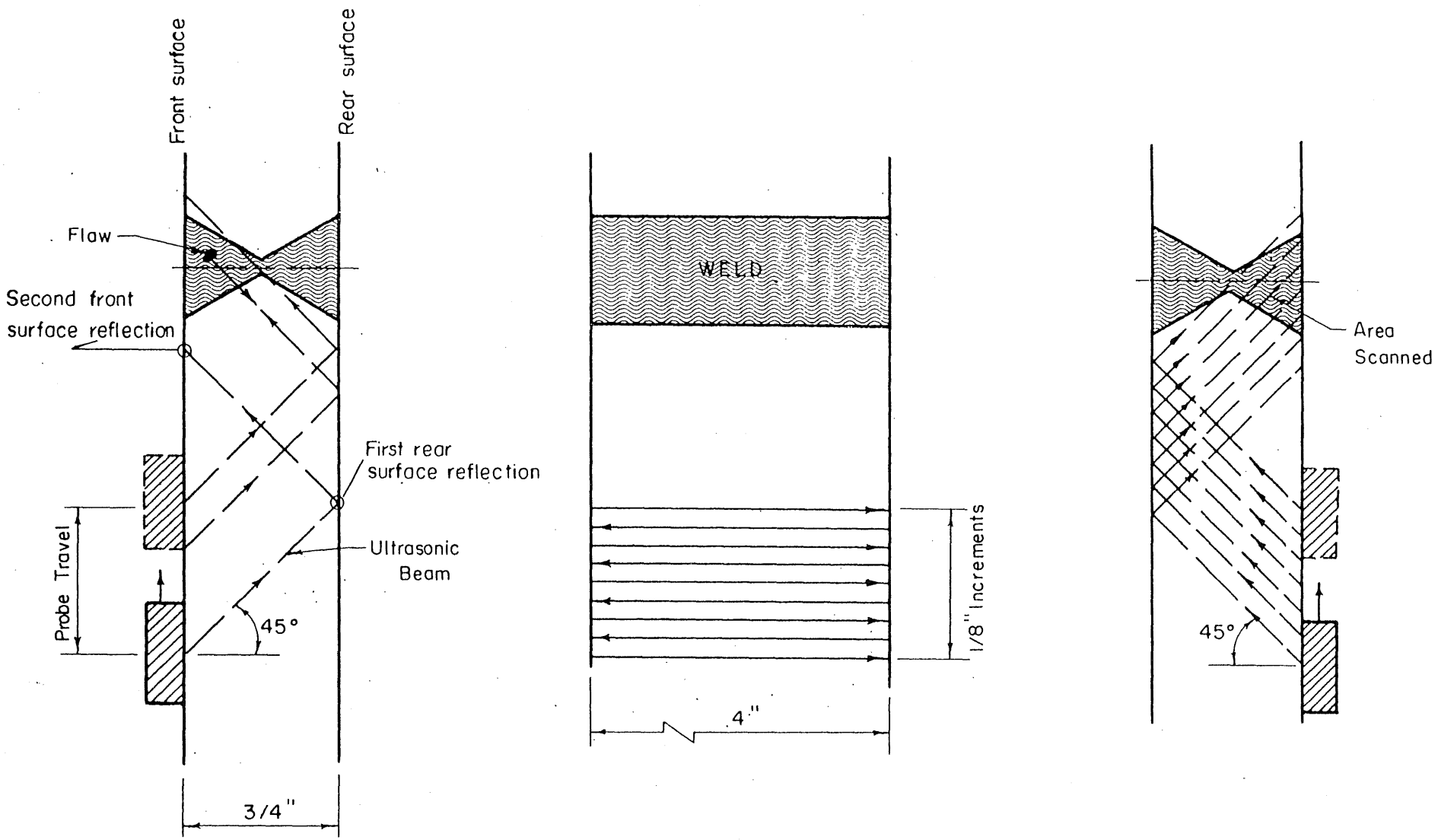

FIG. 3.14 SCANNING PROCEDURE FOR ULTRASONIC EXAMINATION.

Specimen HY-87

Stress Cycle: 0 to +50.0 ksi Life: 41,400

KEY:

FRACTURE SURFACE

1) Internal weld flaws visible on fracture surface . . . . . •

2) Extent of fatigue crack propagation at intersection with surface. . . . . 

ULTRASONIC READINGS

1) Location and extent of responses as indicated on detector scope . . . . . +

2) a. Number designation corresponds to magnitude of peak response as indicated on detector scope.

b. Letter designation corresponds to location along the length of the specimen and with respect to the weld. (Section A and E are at the toes of the weld). . . . . 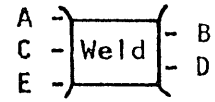

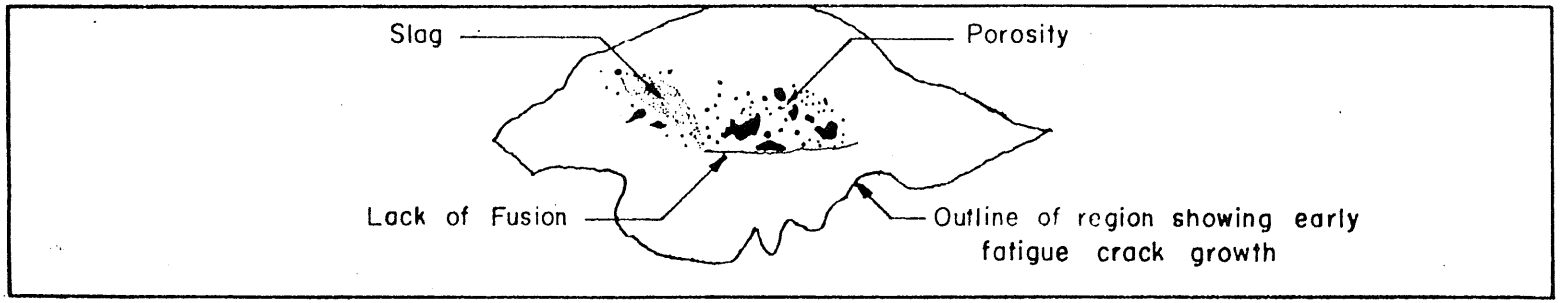

FRACTURE SURFACE

ULTRASONIC READINGS (Projection on a plane perpendicular to longitudinal axis of specimen)

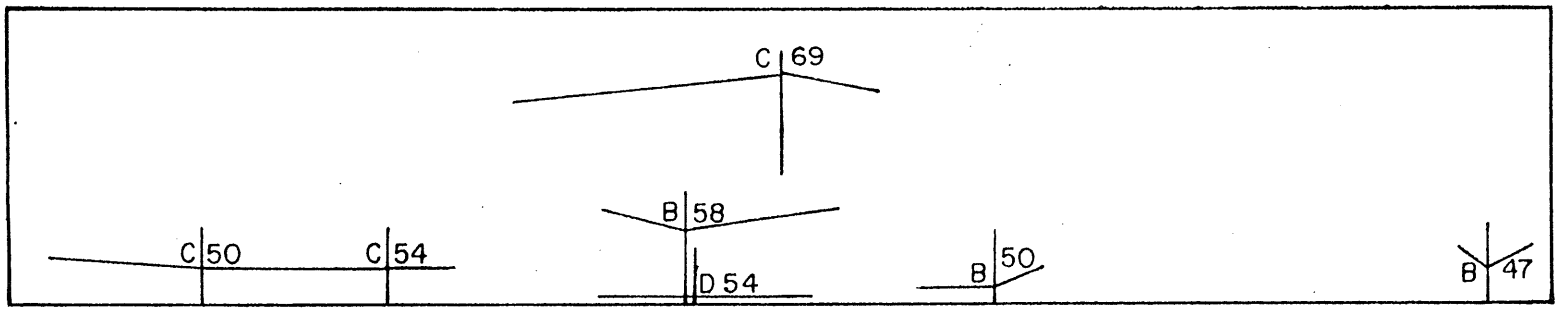

0 Cycles

FIG. 3.15 SKETCH OF FRACTURE SURFACE AND ULTRASONIC READINGS FOR FLAWS IN WELD OF SPECIMEN HY-87

Specimen HY-87 (cont.)

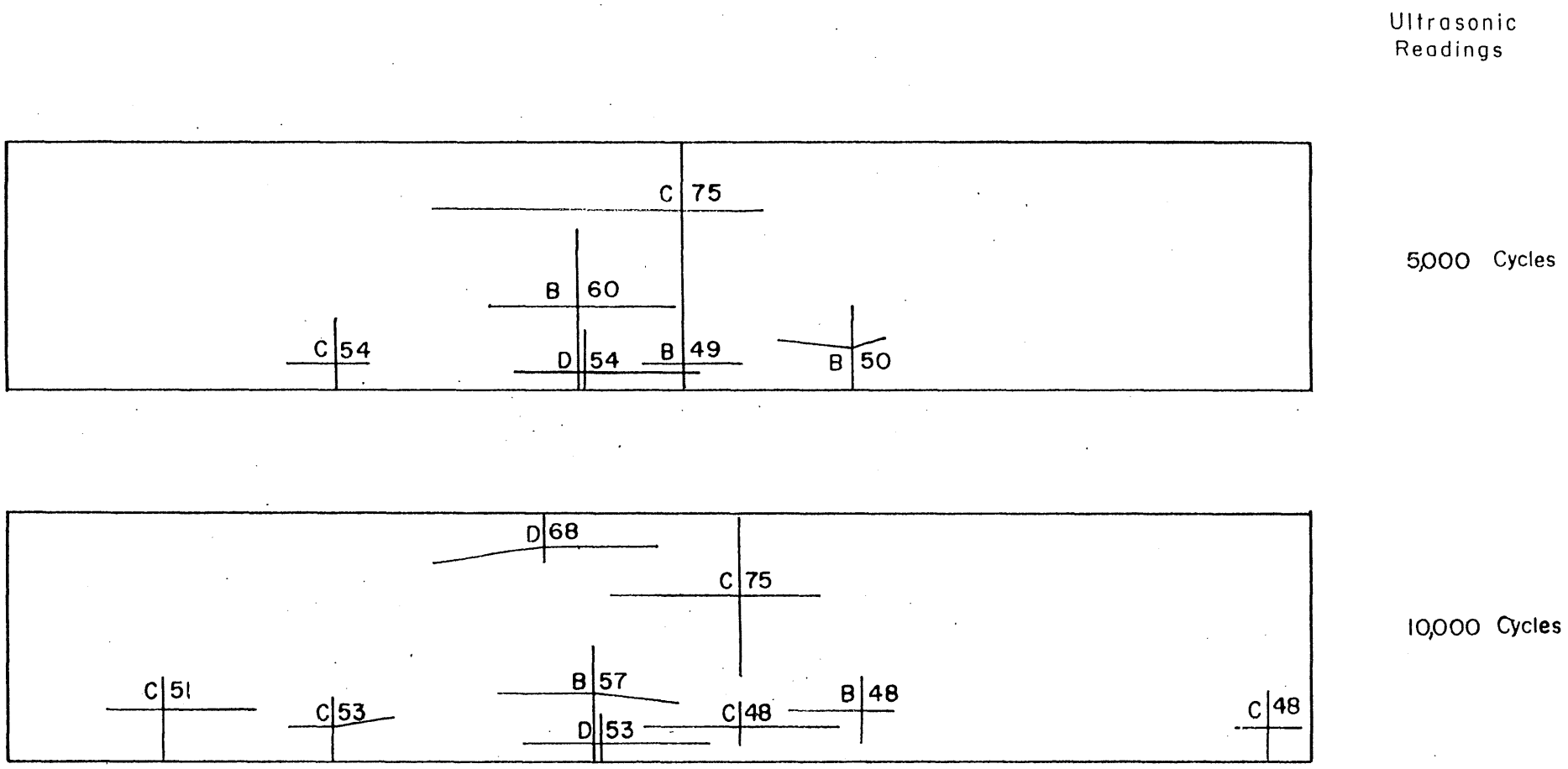

FIG. 3.15 (cont.) SKETCH OF FRACTURE SURFACE AND ULTRASONIC READINGS FOR FLAWS IN WELD OF SPECIMEN HY-87

Specimen HY-87 (cont.)

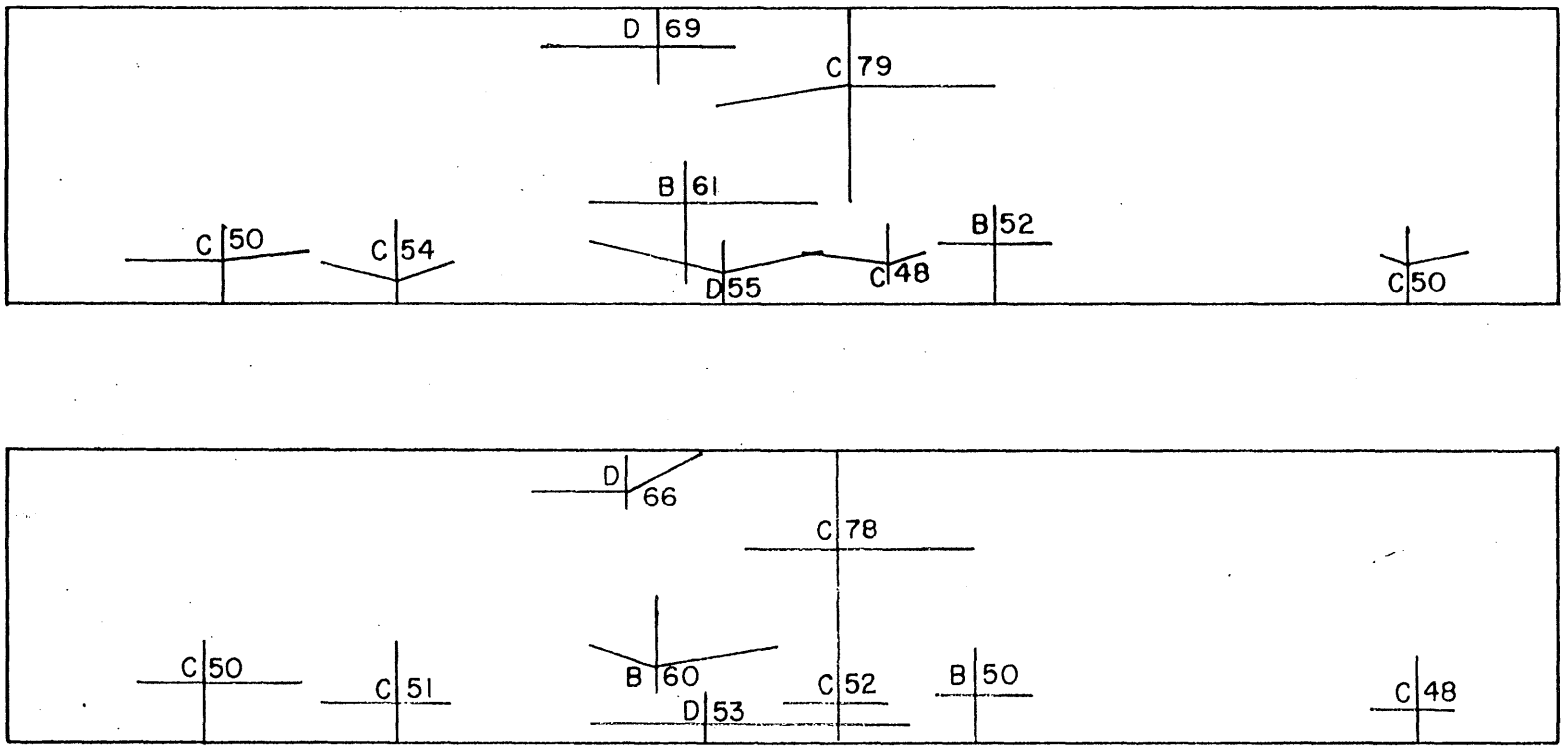

FIG. 3.15 (cont.) SKETCH OF FRACTURE SURFACE AND ULTRASONIC READINGS FOR FLAWS IN WELD OF SPECIMEN HY-87

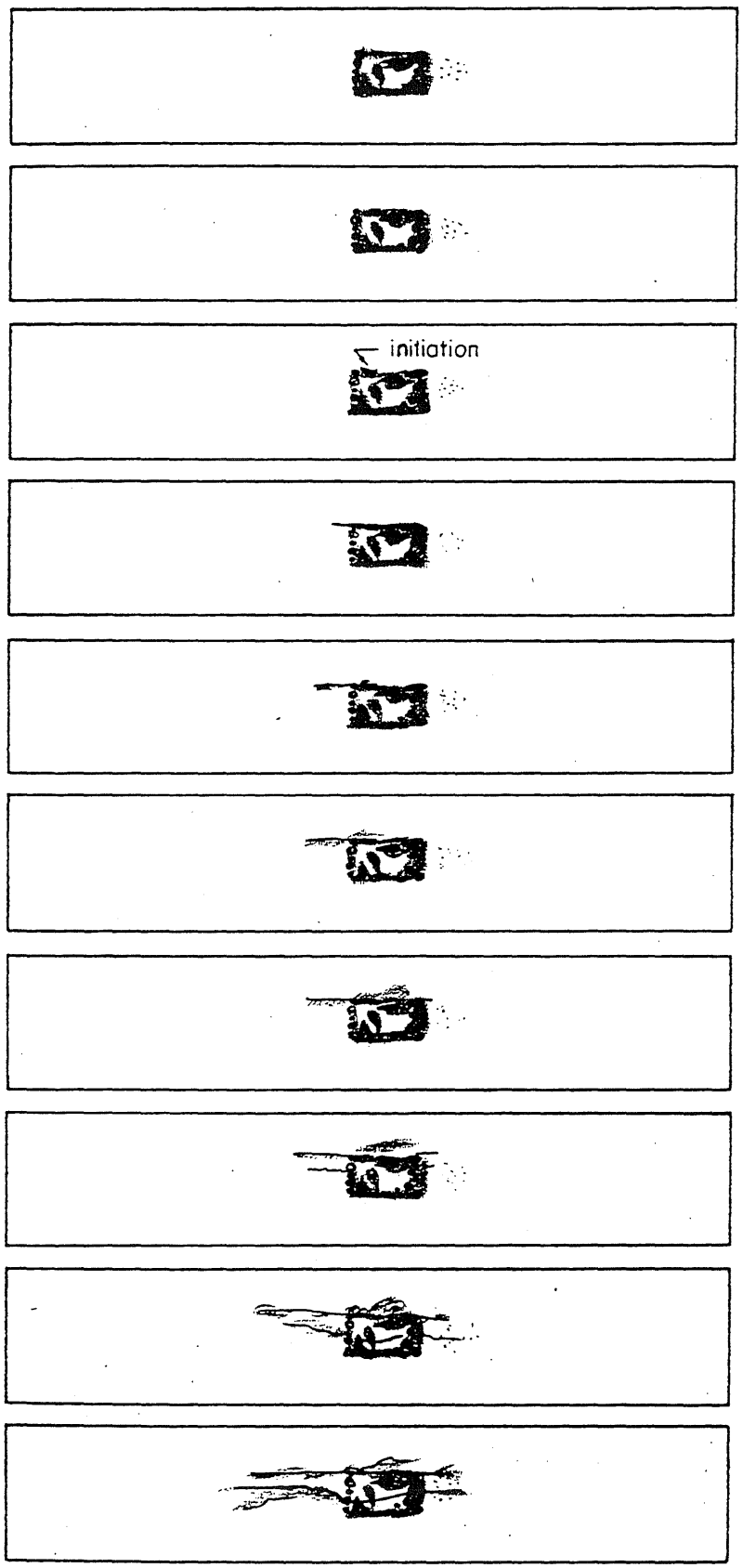

FIG. 3.16 SKETCHES OF RADIOGRAPHS OF SPECIMEN HY-87 TAKEN AT VARIOUS TIMES DURING THE FATIGUE TEST

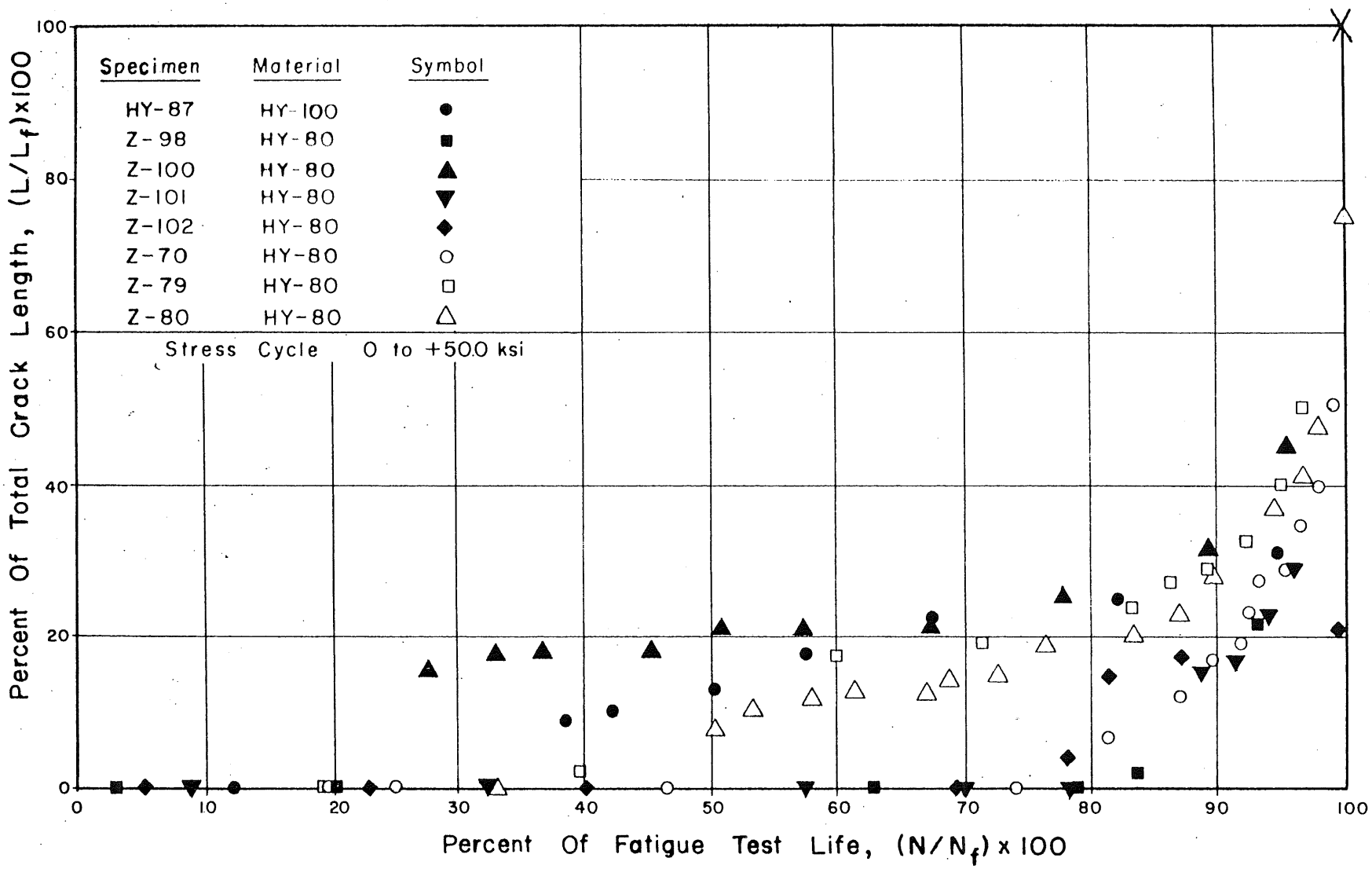

FIG. 3.17 RATE OF CRACK PROPAGATION IN 3/4 IN. HY-80 AND HY-100 TRANSVERSE BUTT-WELDED SPECIMENS

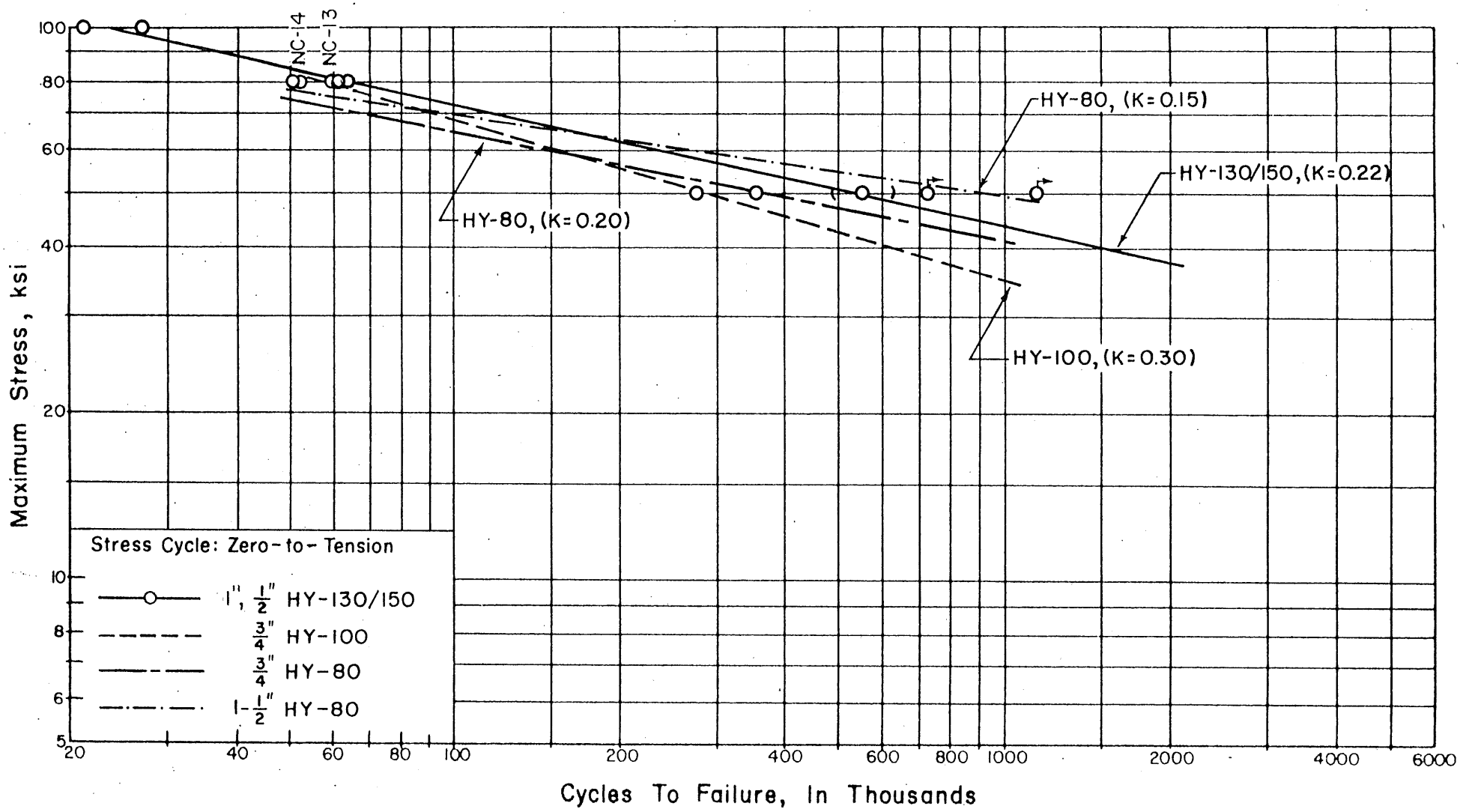

FIG. 4.1 RESULTS OF FATIGUE TESTS OF AS-RECEIVED HY-130/150 PLAIN PLATE SPECIMENS (ZERO-TO-TENSION)

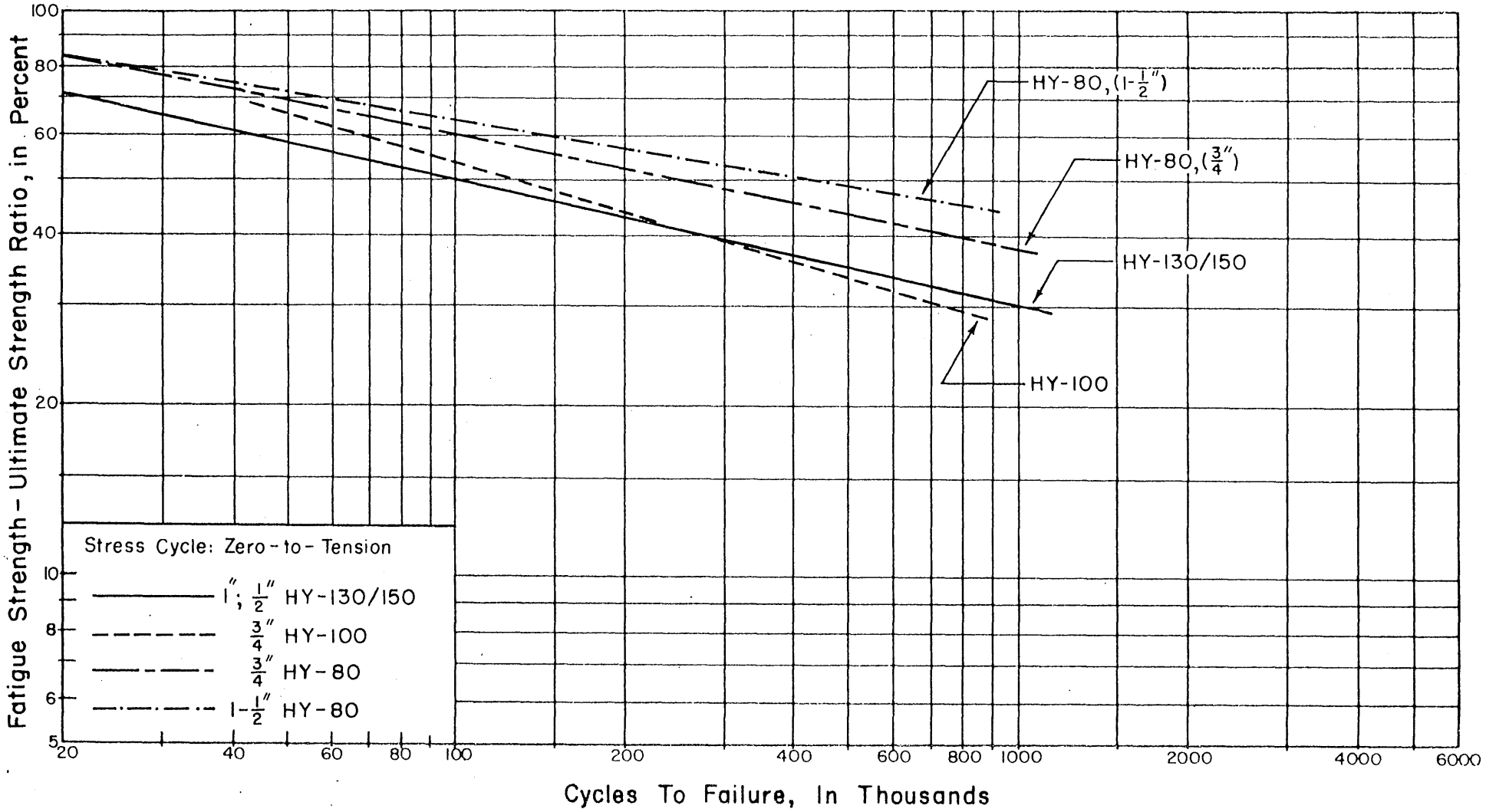

FIG. 4.2 COMPARISON OF FATIGUE STRENGTH TO ULTIMATE STRENGTH FOR AS-RECEIVED PLAIN PLATE SPECIMENS OF HIGH STRENGTH STEELS

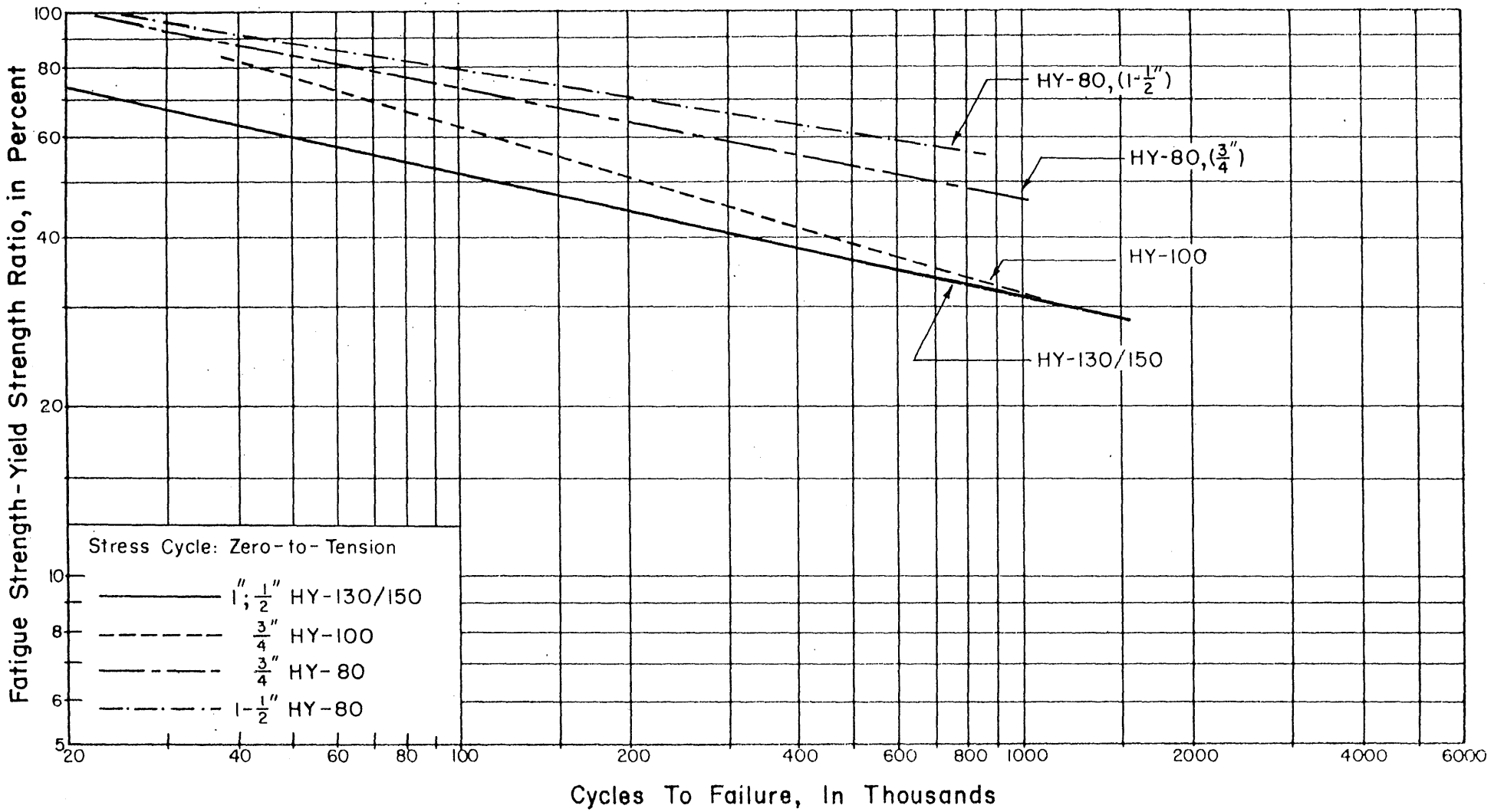

FIG. 4.3 COMPARISON OF FATIGUE STRENGTH TO YIELD STRENGTH FOR AS-RECEIVED PLAIN PLATE SPECIMENS OF HIGH STRENGTH STEELS

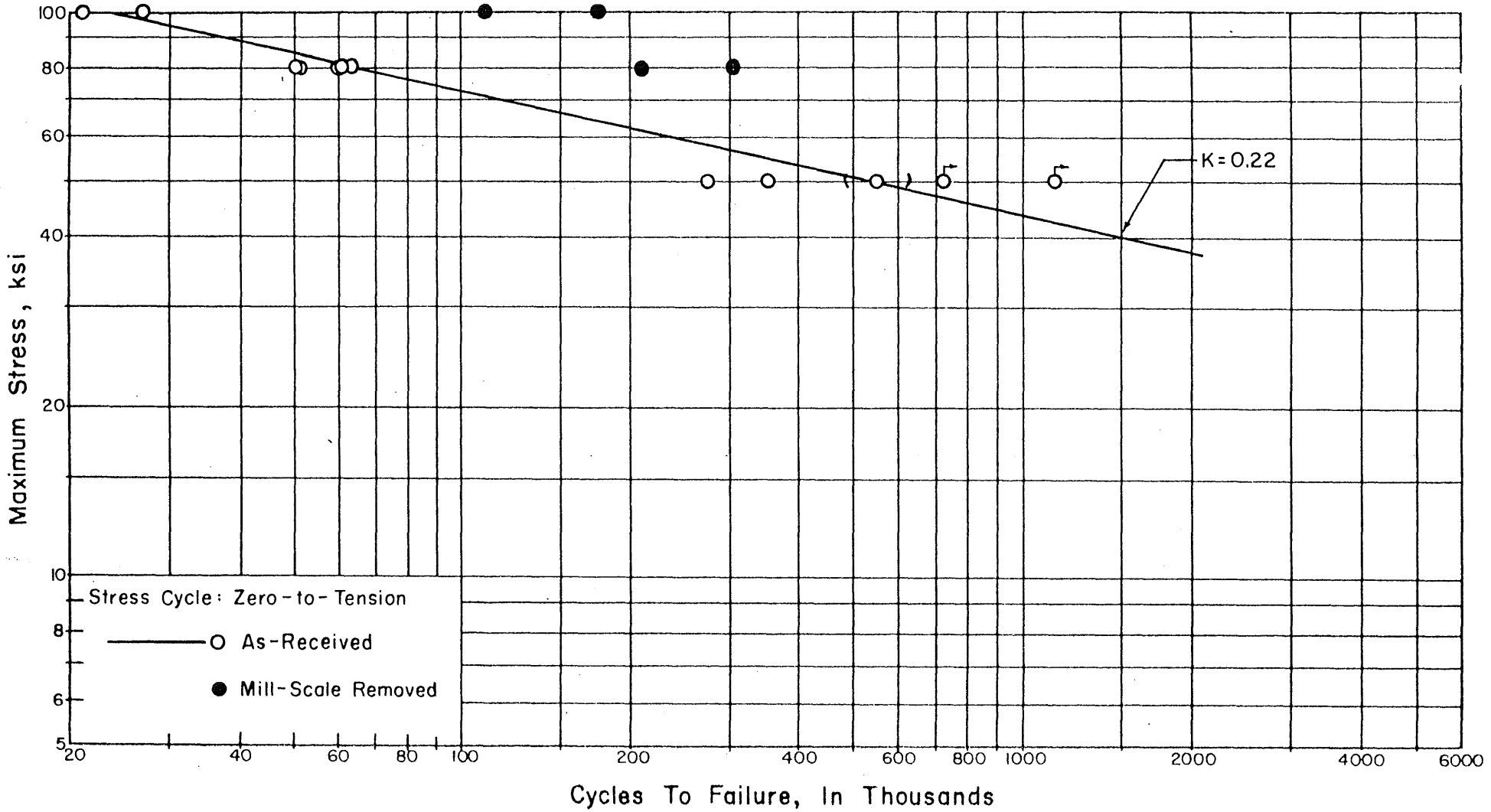

FIG. 4.4. RESULTS OF FATIGUE TESTS OF HY-130/150 PLAIN PLATE SPECIMENS WITH MILL SCALE REMOVED (ZERO-TO-TENSION)

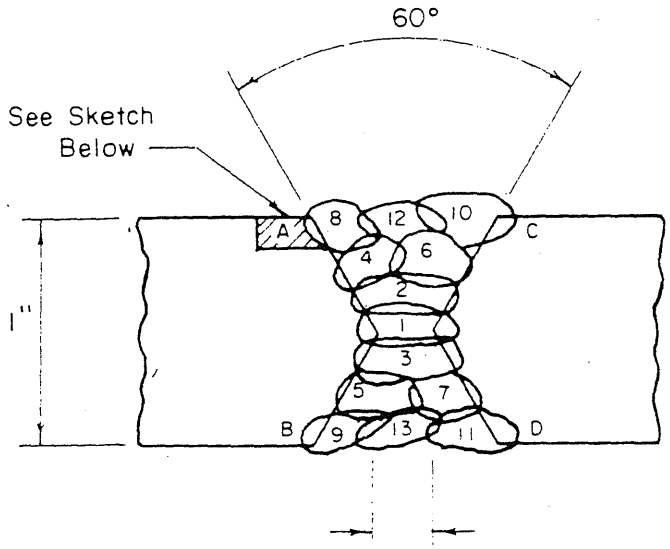

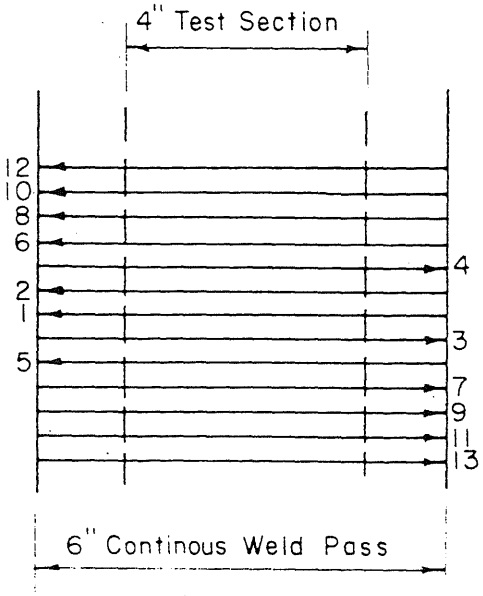

Arrows indicate direction of welding.

Pass	Electrode size, in	Current, amps.	Rate of travel, in./min.
1 – 13	1/16	340	13

Voltage: 29 Volts

Polarity: DC Reversed

Preheat: 275 °F

Wire: Linde X-150

Interpass Temperature: 225 °F (Maximum)

Heat Input: 45,000 Joules/in. (Maximum)

All welding in flat position.

Underside of pass 1 and 2 ground before placing pass 3.

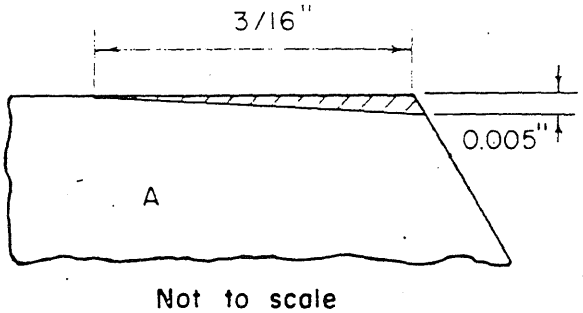

Not to scale

Preparation of joint before welding. Cross hatched area removed by milling on corners A, B, C, D. Rest of joint surface cleaned by grinding.

FIG. 4.5. WELDING PROCEDURE P150-X150-A (Transverse Butt Welds in HY-130/150)

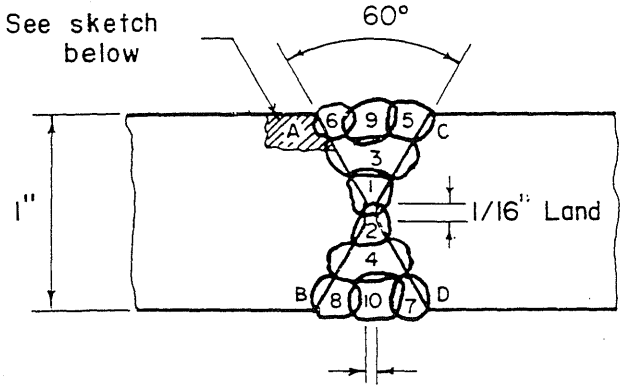

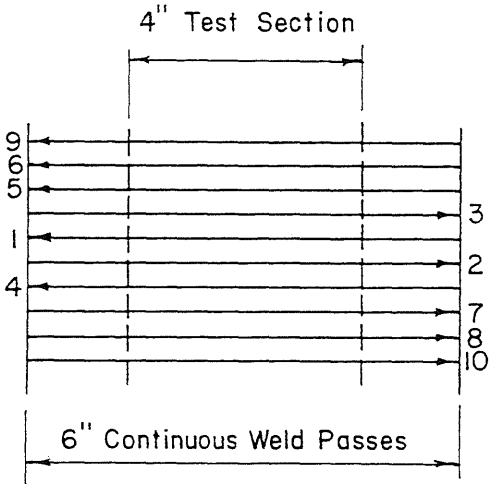

Arrows indicate direction of welding.

Pass	Electrode size, in.	Current, amps.	Rate of travel, in./min.
1-4	1/16	340	13
5-10	1/16	340	16

Voltage 29 Volts

Polarity DC Reversed

Preheat 275 °F

Wire Linde X-150

Interpass Temperature 225 °F (Maximum)

Heat Input 45,000 Joules/in. (Maximum)

All welding in flat position.

Underside of pass 1 and 2 ground before placing pass 3.

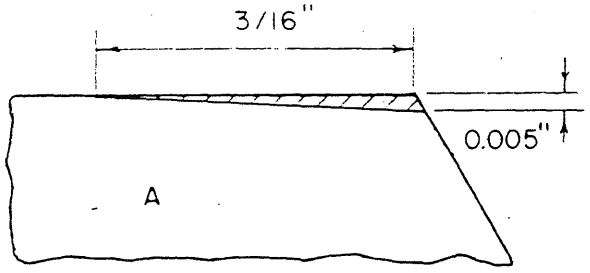

Not to scale

Preparation of joint before welding. Cross hatched area removed by milling on corners A, B, C, D. Rest of joint surface cleaned by grinding.

FIG. 4.6 WELDING PROCEDURE P150-X150-B
(Transverse Butt Welds in HY-130/150)

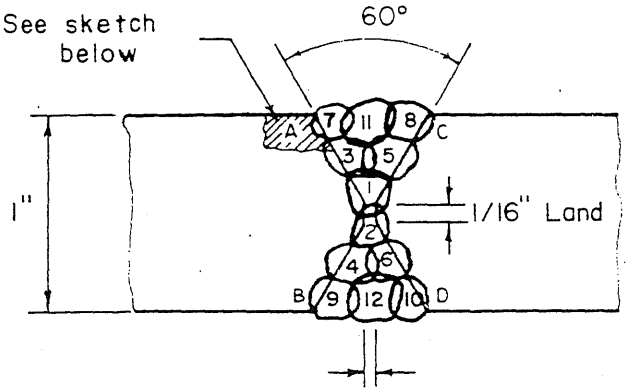

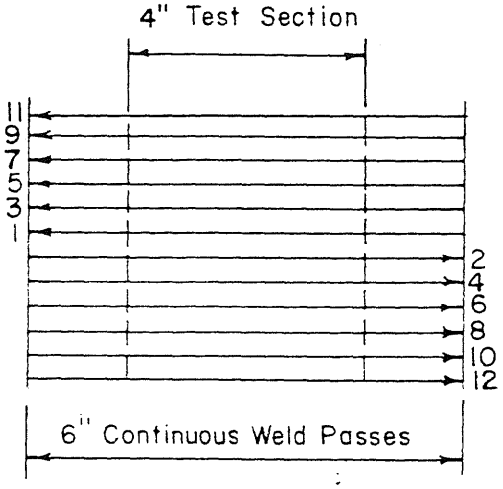

Arrows indicate direction of welding.

Pass	Electrode size, in.	Current, amps.	Rate of travel, in./min.
1-12	1/16	290-340	13-16

Voltage: 29 Volts

Polarity: DC Reversed

Preheat: 275 °F

Wire: Airco AX-140

Interpass Temperature: 225 °F (Maximum)

Heat Input: 45,000 Joules/in (Maximum)

All welding in flat position

Underside of pass 1 ground before placing pass 2.

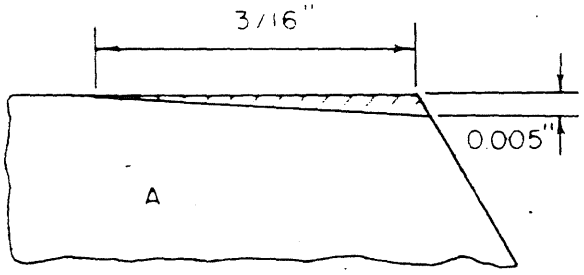

Not to scale

Preparation of joint before welding
Cross hatched area removed by milling on corners A, B, C, D
Rest of joint surface cleaned by grinding

FIG. 4.7 WELDING PROCEDURE P150-AX140-C
(Transverse Butt Welds in HY-130/150)

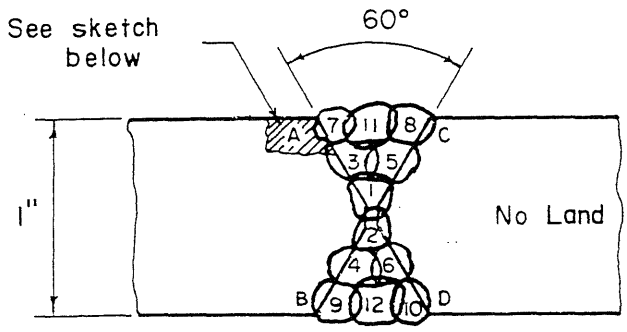

No Root Opening

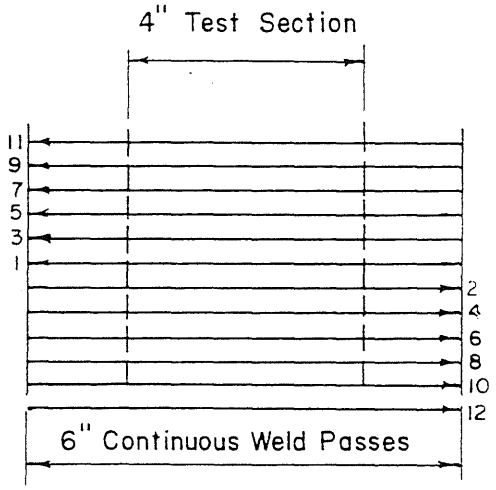

Arrows indicate direction of welding.

Pass	Electrode size, in.	Current, amps.	Rate of travel, in./min.
1-12	1/16	310-330	12-15

Voltage: 29 Volts

Polarity: DC Reversed

Preheat: 275 °F

Wire: Airco AX-140

Interpass Temperature: 225 °F (Maximum)

Heat Input: 45,000 Joules/in (Maximum)

All welding in flat position.

Underside of pass 1 ground before placing pass 2.

Argon shield used on underside of pass 1.

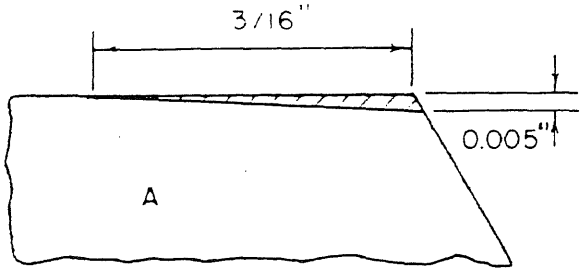

Not to scale

Preparation of joint before welding
Cross hatched area removed by milling on corners A, B, C, D.
Rest of joint surface cleaned by grinding. Root pass and in between passes 7-8 and 9-10 were ground with a carbide grinding wheel.

FIG. 4.8 WELDING PROCEDURE P150-AX-140-D
(Transverse Butt Welds in HY-130/150)

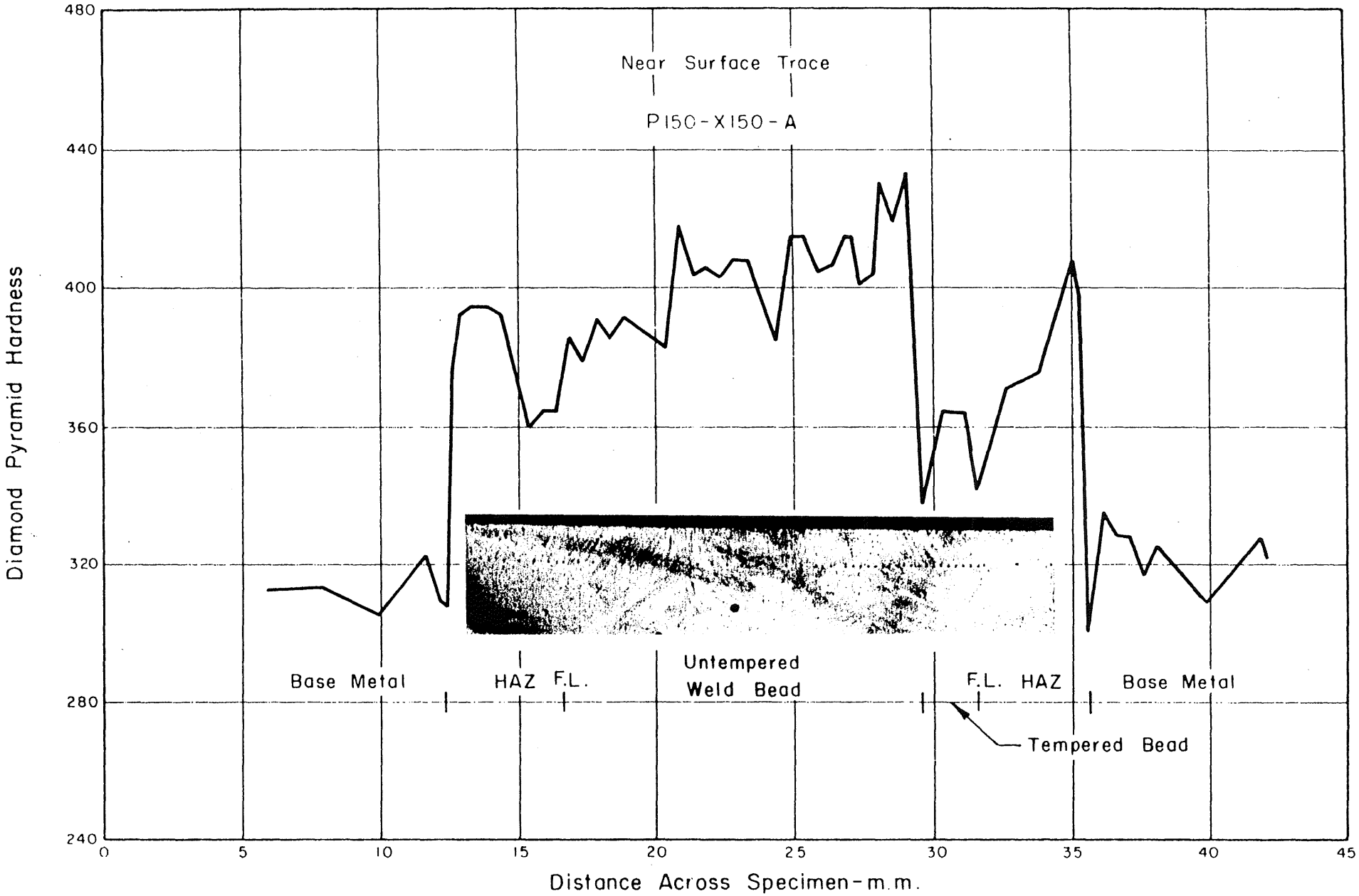

FIG. 4.9 MICRO-HARDNESS SURVEY OF 1 IN. THICK HY-130/150 STEEL WELDED JOINT

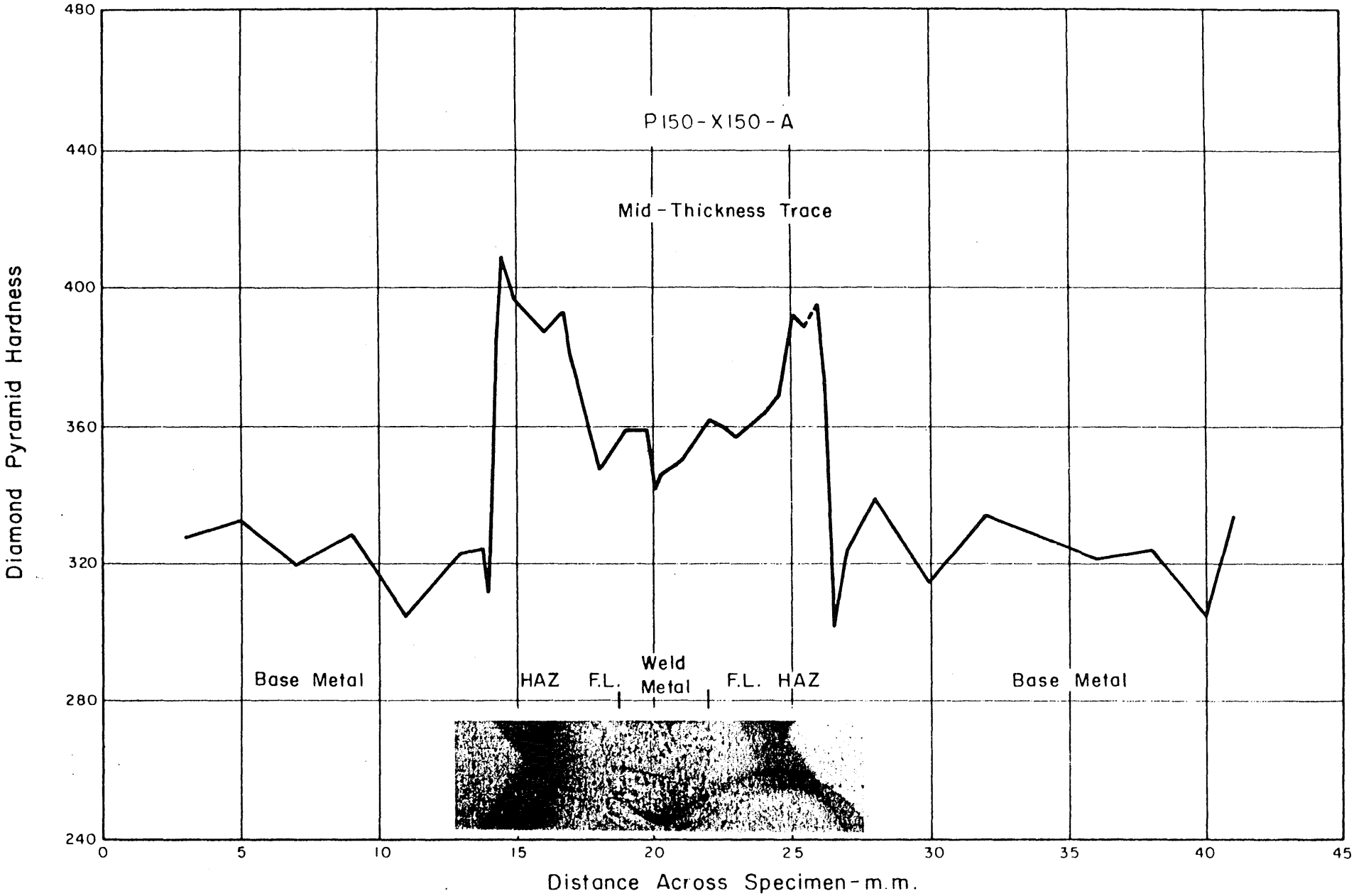

FIG. 4.10 MICRO-HARDNESS SURVEY OF 1 IN. THICK HY-130/150 STEEL WELDED JOINT

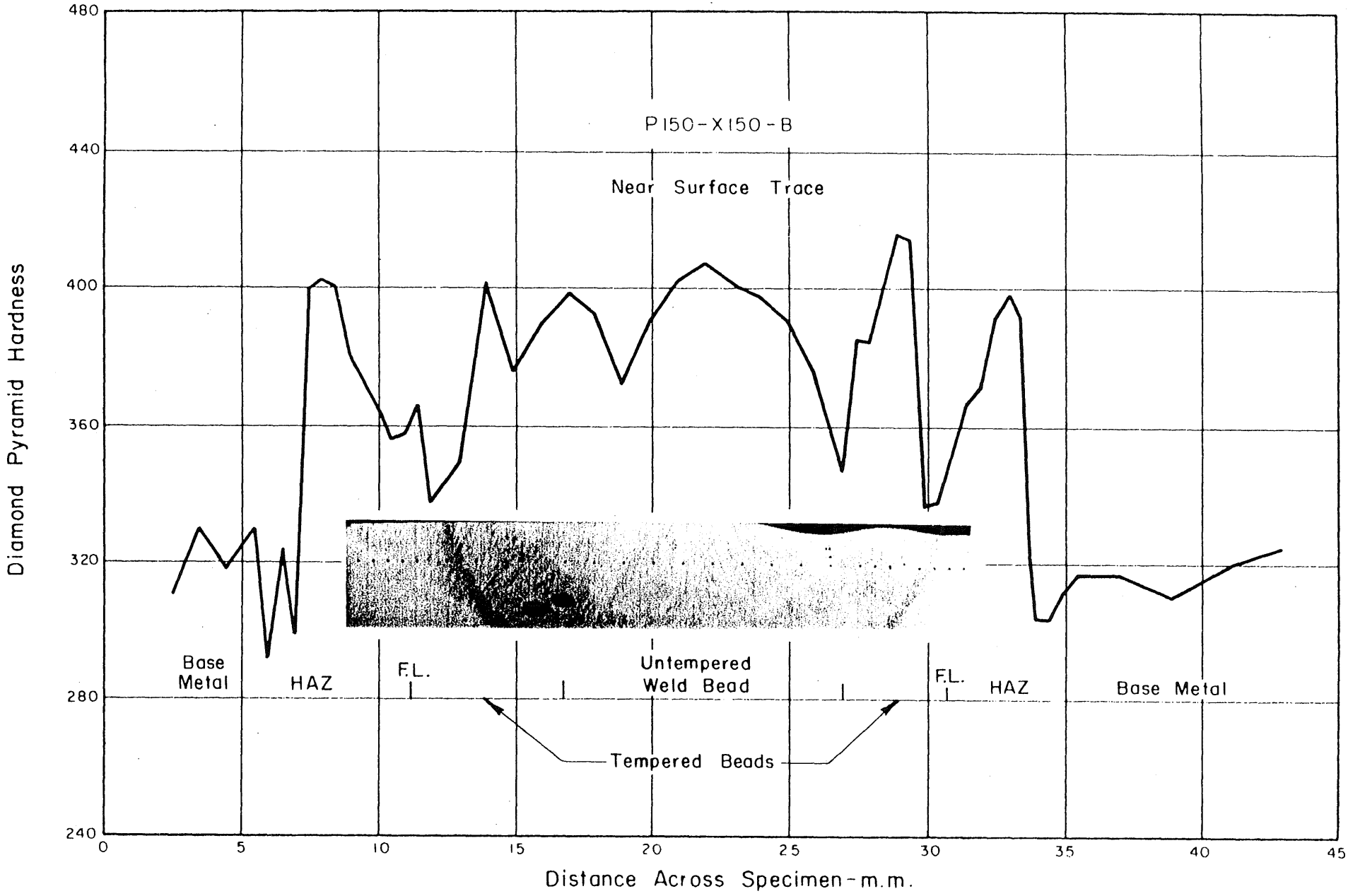

FIG. 4.11 MICRO-HARDNESS SURVEY OF 1 IN. THICK HY-130/150 STEEL WELDED JOINT

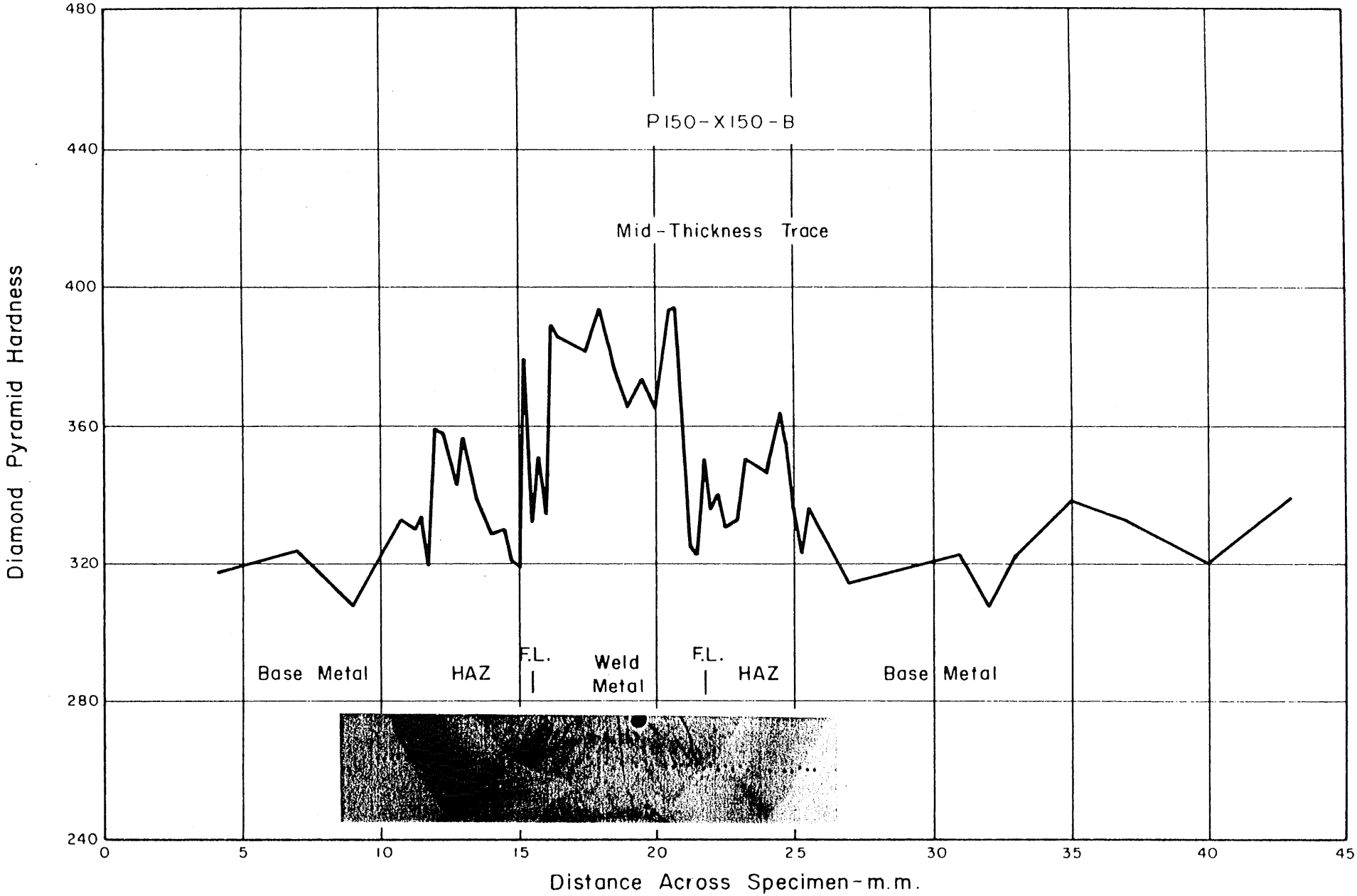

FIG. 4.12 MICRO-HARDNESS SURVEY OF 1 IN. THICK HY-130/150 STEEL WELDED JOINT

100X

(a) PROCEDURE P150-X150-A

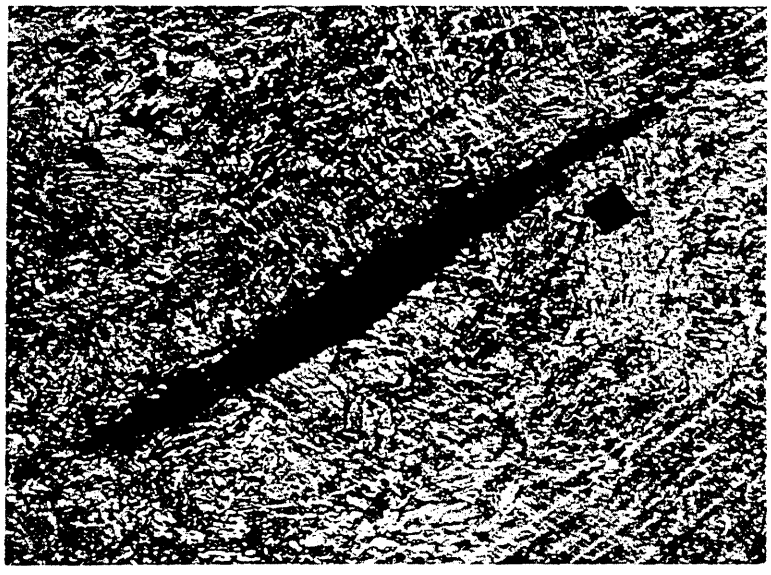

100X

(b) PROCEDURE P150-X150-B

FIG.4.13 HOT CRACKS LOCATED IN WELD METAL DEPOSITED IN ACCORDANCE WITH PROCEDURES P150-X150-A & P150-X150-B

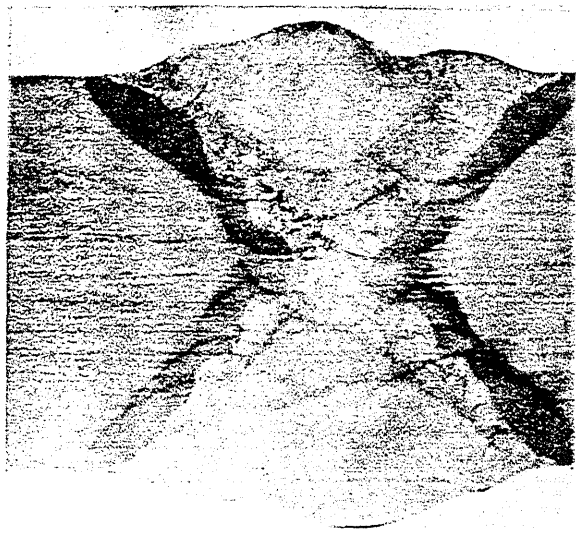

(a) U.S. Naval Applied Science Lab. 2x

(b) U.S. Steel Corporation 2x

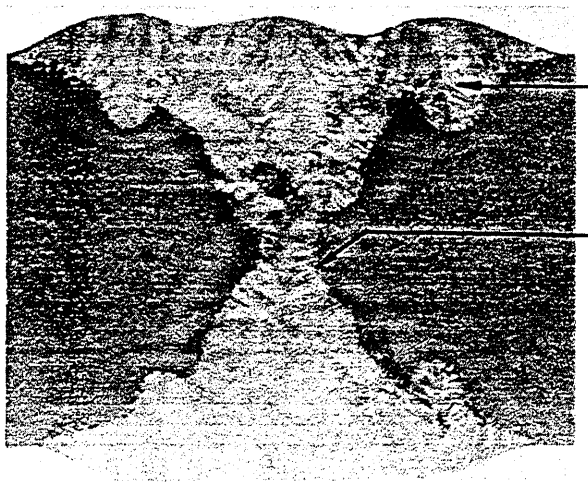

(c) University of Illinois 2x

FIG. 4.14 COMPARISON OF TRANSVERSE SECTIONS OF HY-130/150 WELDED JOINTS FROM N.A.S.L., U.S.S. CORP., & U. OF I.

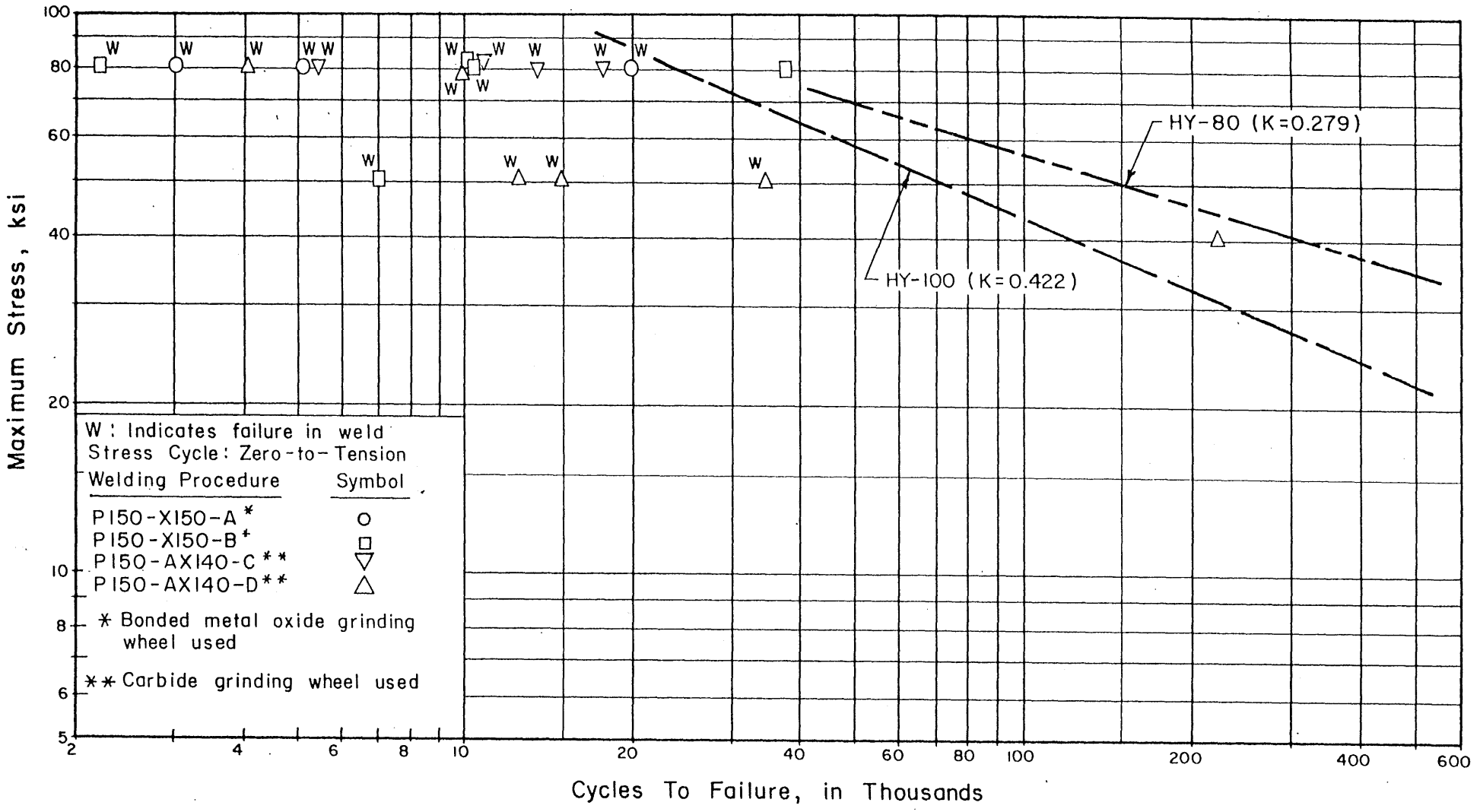

FIG. 4.15 RESULTS OF FATIGUE TESTS OF HY-130/150 TRANSVERSE BUTT WELDS IN THE AS-WELDED CONDITION

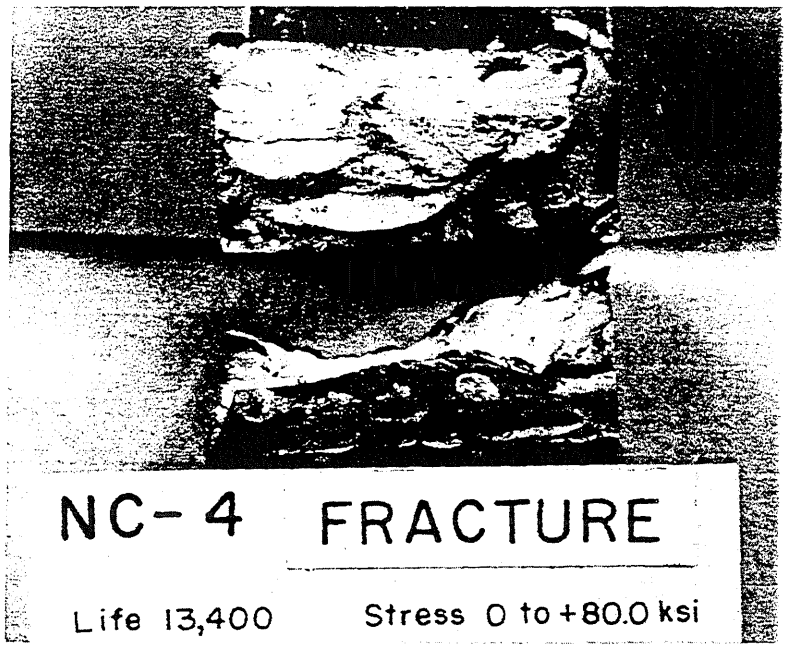

(a) Failure Initiated At Porosity

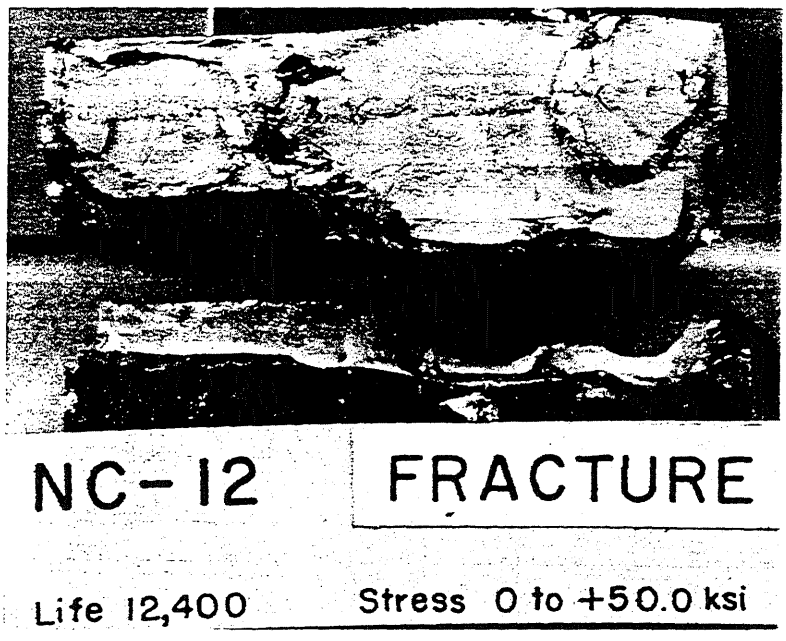

(b) Failure Initiated In The Lobe Of A Weld Bead

FIG. 4.16 FRACTURE SURFACES OF HY-130/150 TRANSVERSE BUTT WELDS IN THE AS-WELDED CONDITION

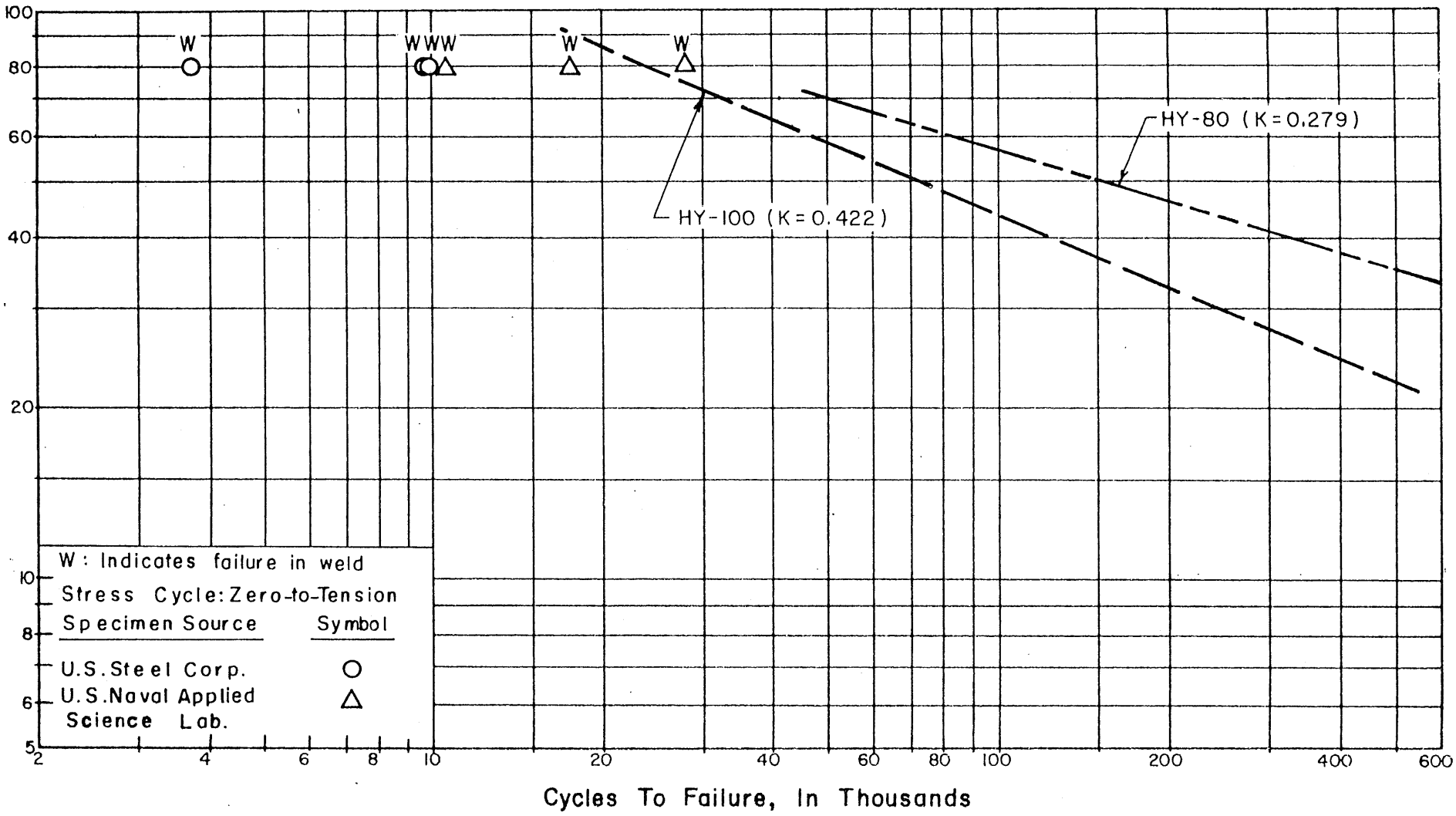

FIG. 4.17 RESULTS OF FATIGUE TESTS OF HY-130/150 TRANSVERSE BUTT WELDS IN THE AS-WELDED CONDITION

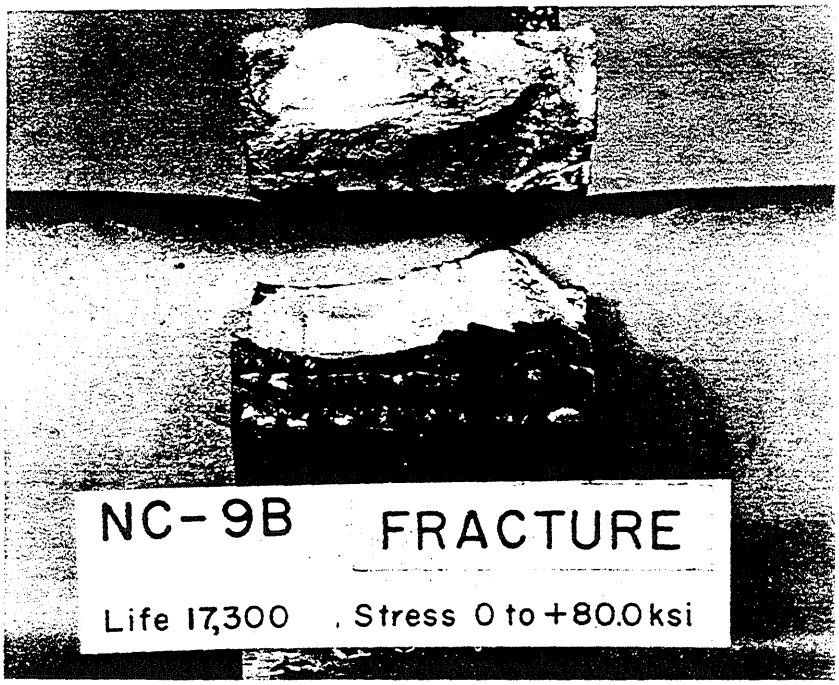

(a) Specimen Prepared By NASL

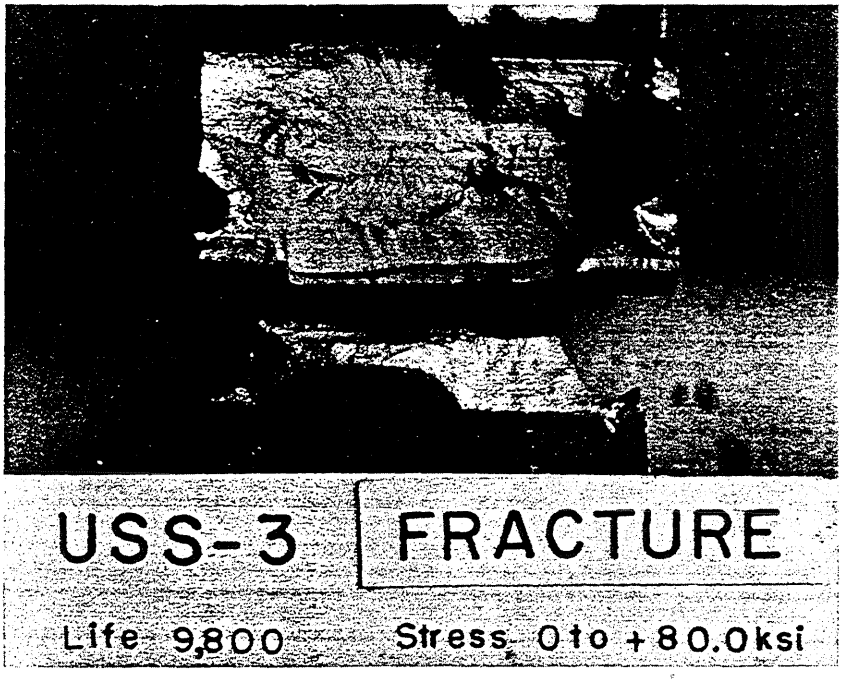

(b) Specimen Prepared By U.S. Steel

FIG. 4.18 FRACTURE SURFACES OF HY-130/150 TRANSVERSE BUTT WELDS IN THE AS-WELDED CONDITION

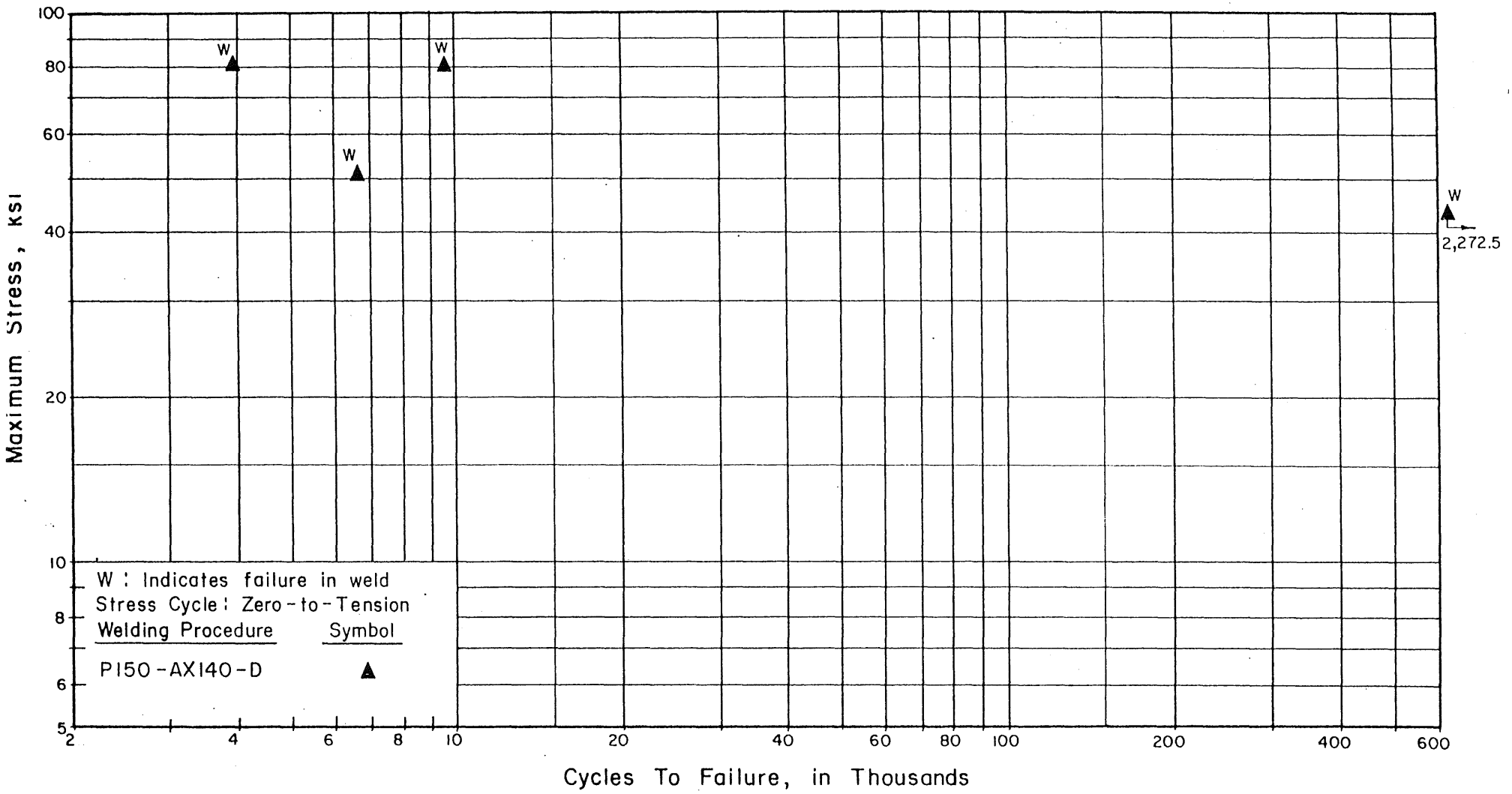

FIG. 4.19 RESULTS OF FATIGUE TESTS OF HY-130/150 TRANSVERSE BUTT WELDS WITH REINFORCEMENT REMOVED

(a) Plastic Replica (b) Carbon Extraction Replica

(Dimension lines are 10 microns long)

FIG. 4.20 DUCTILE FRACTURE IN THE WELD METAL OF A WELDED JOINT OF HY-130/150 TESTED IN STATIC TENSION

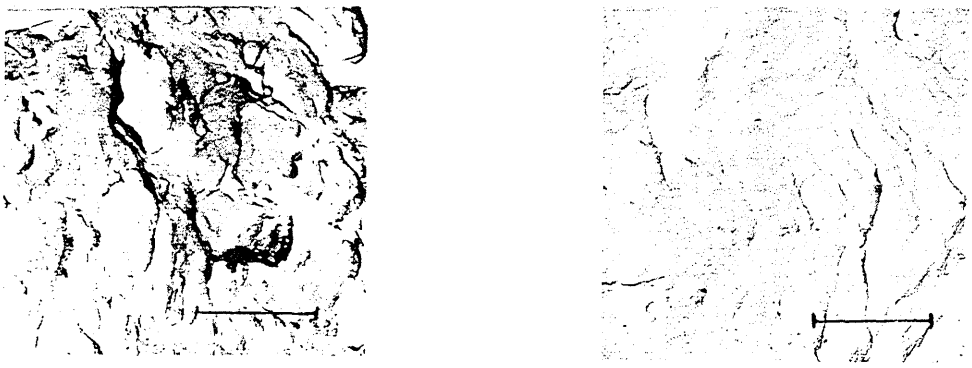

HAZ Base Metal

(Dimension lines are 10 microns long)

FIG. 4.21 PLASTIC REPLICA OF A FATIGUE FRACTURE IN THE HAZ AND THE BASE METAL OF A WELDED JOINT OF HY-100 STEEL

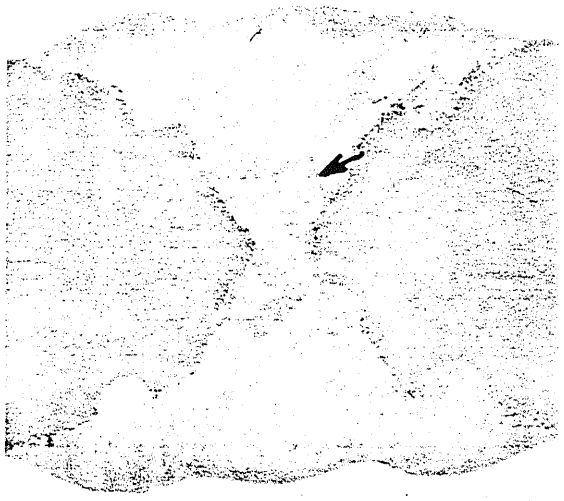

Macro 2X

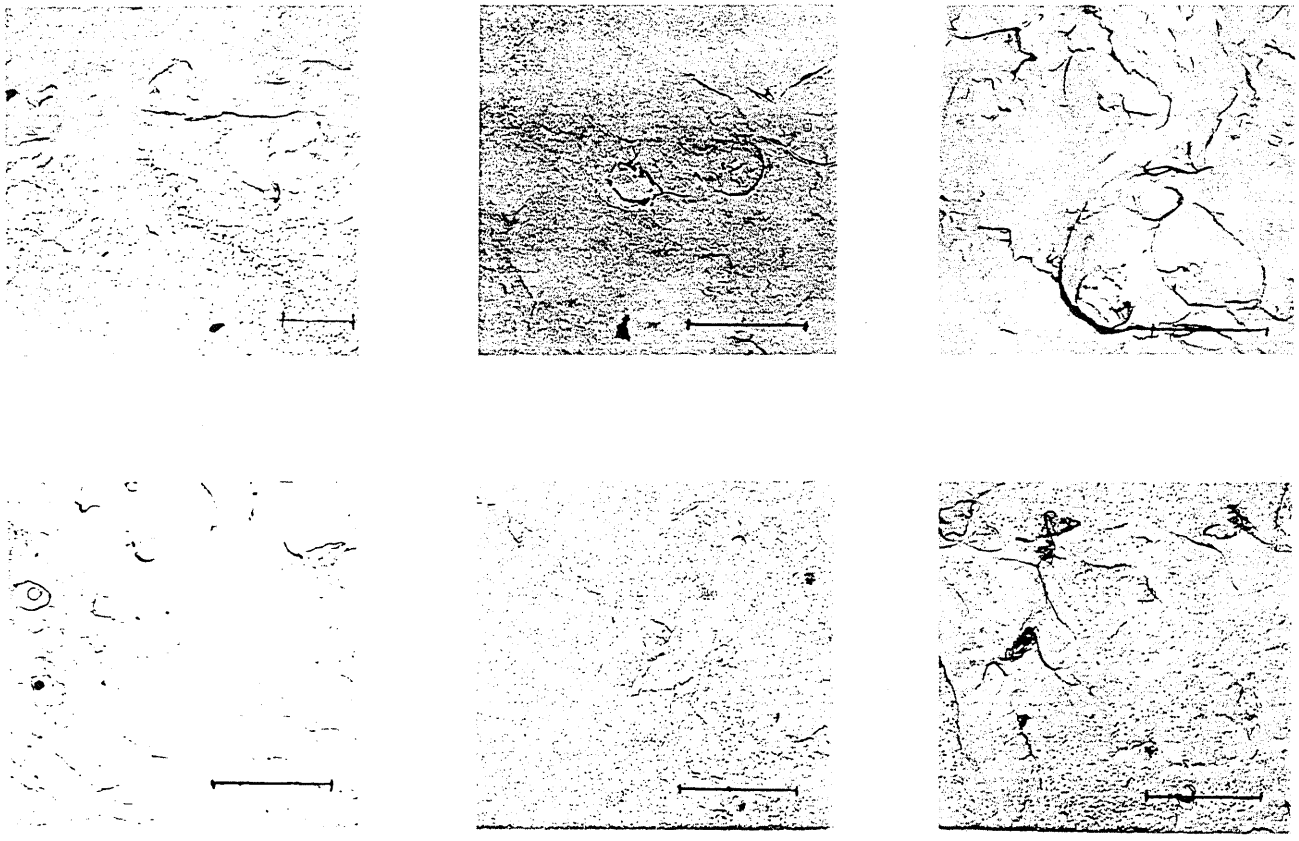

(Dimension lines are 2 microns long)

FIG. 4.22 PLASTIC REPLICA OF A LOBE CRACK (ARROW) EXPOSED BY THE STATIC FRACTURE OF WELDED SAMPLE NC-I-D

Macro 2X

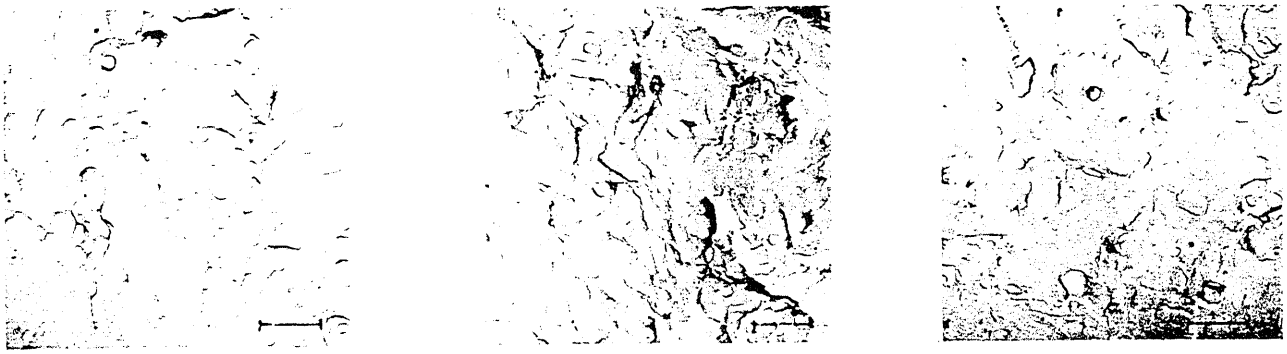

Plastic Replica
(Dimension lines are 2 microns long)

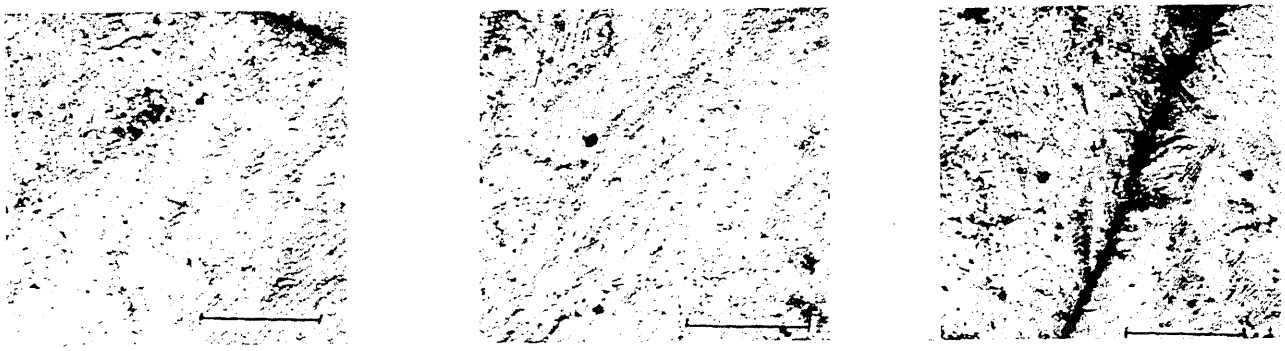

Carbon Extraction Replica
(Dimension lines are 10 microns long)

FIG. 4.23 REPLICAS OF THE FATIGUE FRACTURE ALONG THE CENTER OF A LOBE (ARROW) OF SAMPLE NC-2

Macro 2X

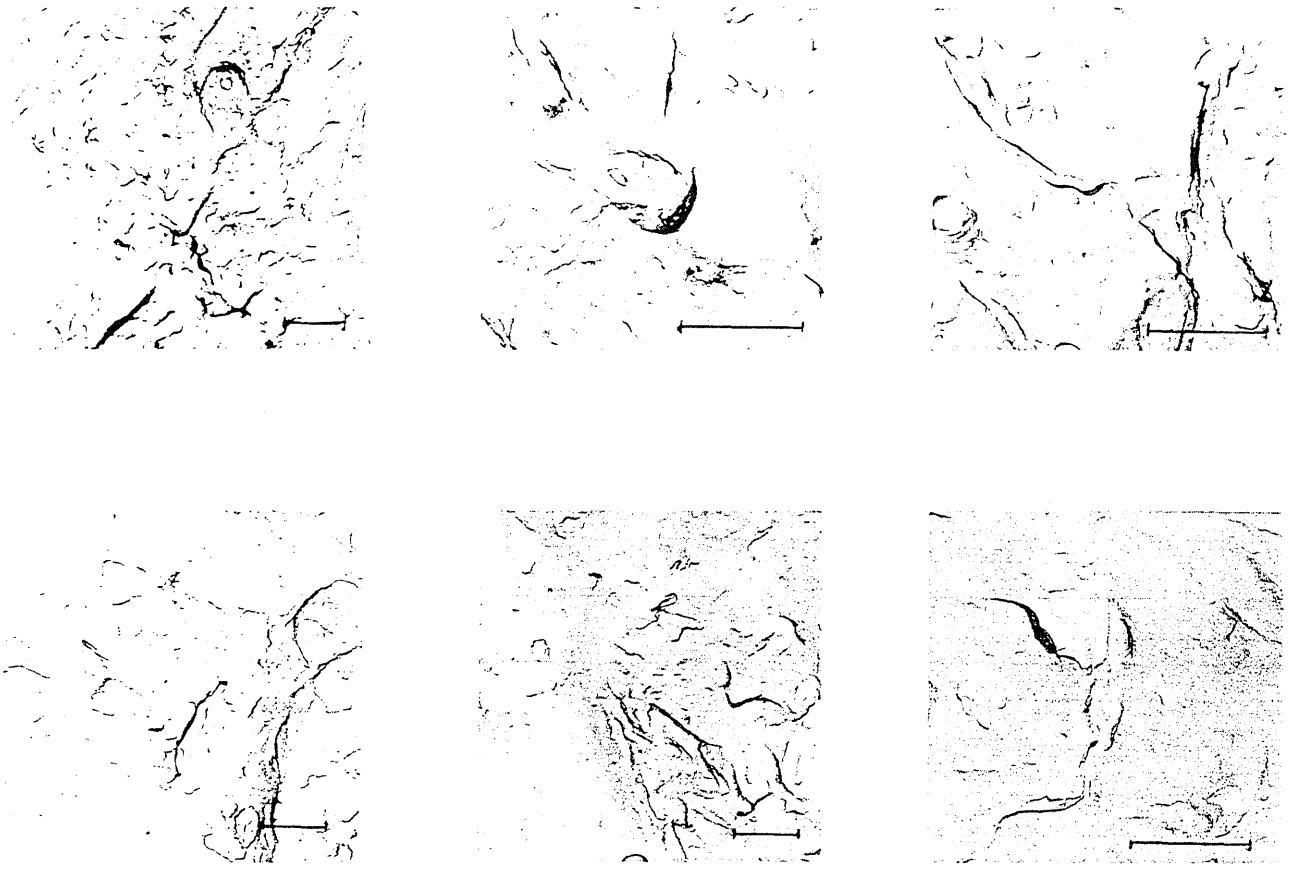

(Dimension lines are 2 microns long)

FIG. 4.24 PLASTIC REPLICA OF THE FATIGUE FRACTURE IN SAMPLE NC-6 ALONG THE CENTER LINE OF THE LOBE (ARROW)

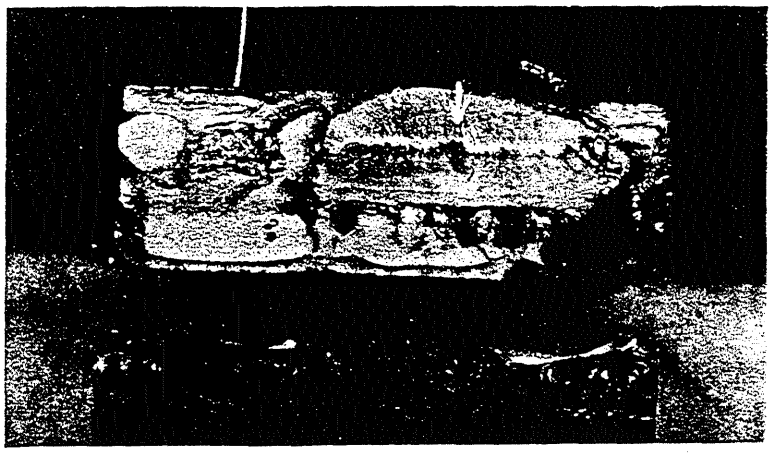

Macro IX

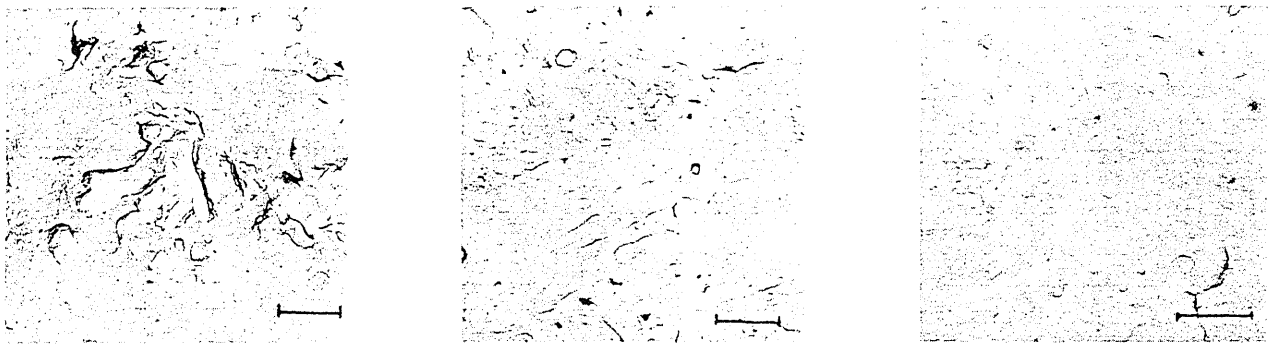

(Dimension lines are 2 microns long except when noted)

FIG. 4.25 PLASTIC REPLICA OF THE FATIGUE FRACTURE IN SAMPLE NC-11 IN THE WELD METAL (ARROW)

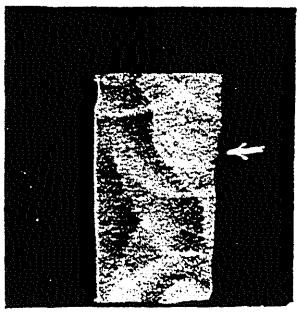

Macro 2X

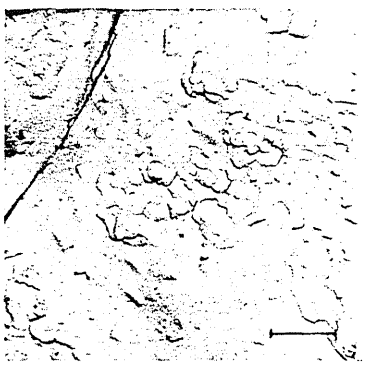

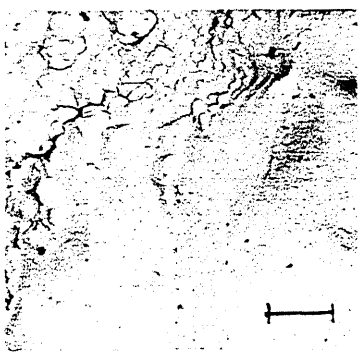

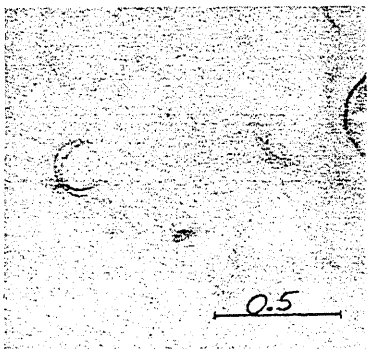

(Dimension lines are 2 microns long except when noted)

FIG. 4.26 PLASTIC REPLICA OF THE FATIGUE FRACTURE IN SAMPLE NC-12 ALONG THE SIDE OF THE LOBE (ARROW)

ILLINOIS UNIVERSITY, URBANA. DEPARTMENT OF CIVIL ENGINEERING

FATIGUE OF PLATES AND WELDMENTS IN HIGH STRENGTH STEELS, by J. B. Radziminski, R. W. Hinton, D. F. Meinheit, H. A. Osman, W. H. Bruckner, and W. H. Munse

February 1967, 143 pp.

Structural Research Series No. 318

Contract NObs 94232, Project Serial No. SF-020-01-05, Task 729-0

AN EVALUATION OF THE AXIAL FATIGUE BEHAVIOR OF TRANSVERSE BUTT-WELDED JOINTS IN HY-100 STEEL IS PRESENTED. WELDING PROCEDURES, USING MIL-12018 AND MIL-11018 ELECTRODES, HAVE BEEN DEVELOPED IN WHICH THE DEFECT DENSITY IS HELD TO A MINIMUM. SPECIMENS WELDED IN ACCORDANCE WITH THESE PROCEDURES INITIATED FATIGUE FAILURES ON THE SURFACE AT THE STRESS RAISER CREATED BY THE GEOMETRY AT THE TOE OF THE WELD. FOR THOSE MEMBERS, THE S-N CURVE FOR THE LIFE RANGE FROM 10^4 TO 10^6 CYCLES IS PRESENTED FOR A STRESS CYCLE OF ZERO-TO-TENSION. RADIOGRAPHIC AND ULTRASONIC INSPECTIONS WERE USED TO STUDY FATIGUE CRACK INITIATION AND PROPAGATION ORIGINATING AT AN INTERNAL WELD FLAW.

A PRELIMINARY INVESTIGATION OF THE AXIAL FATIGUE BEHAVIOR OF MIG WELDMENTS IN HY-130/150 STEEL IS REPORTED. THE MAJORITY OF THE TRANSVERSE BUTT-WELDED SPECIMENS PREPARED AT EACH OF THREE LABORATORIES INITIATED FATIGUE FAILURES AT A VARIETY OF INTERNAL DEFECTS WHEN SUBJECTED TO A CYCLIC MAXIMUM STRESS OF APPROXIMATELY HALF THE ULTIMATE STRENGTH OF THE BASE METAL. SEVERAL ALTERATIONS IN THE STANDARD MIG WELDING PROCEDURES WERE STUDIED IN AN EFFORT TO IMPROVE THE WELD QUALITY; HOWEVER NO MODIFICATION HAS BEEN ENTIRELY SUCCESSFUL IN ELIMINATING ALL THE DEFECTS WHICH HAVE PROVEN TO BE CRITICAL POINTS FOR FATIGUE CRACK NUCLEATION.

KEYWORDS:

Axial Fatigue Testing, HY-100 Steel, HY-130/150 Steel, Weldments, Non-Destructive Testing, Radiography, Ultrasonics, Crack Initiation, Crack Propagation

ILLINOIS UNIVERSITY, URBANA. DEPARTMENT OF CIVIL ENGINEERING

FATIGUE OF PLATES AND WELDMENTS IN HIGH STRENGTH STEELS, by J. B. Radziminski, R. W. Hinton, D. F. Meinheit, H. A. Osman, W. H. Bruckner, and W. H. Munse

February 1967, 143 pp.

Structural Research Series No. 318

Contract NObs 94232, Project Serial No. SF-020-01-05, Task 729-0

AN EVALUATION OF THE AXIAL FATIGUE BEHAVIOR OF TRANSVERSE BUTT-WELDED JOINTS IN HY-100 STEEL IS PRESENTED. WELDING PROCEDURES, USING MIL-12018 AND MIL-11018 ELECTRODES, HAVE BEEN DEVELOPED IN WHICH THE DEFECT DENSITY IS HELD TO A MINIMUM. SPECIMENS WELDED IN ACCORDANCE WITH THESE PROCEDURES INITIATED FATIGUE FAILURES ON THE SURFACE AT THE STRESS RAISER CREATED BY THE GEOMETRY AT THE TOE OF THE WELD. FOR THOSE MEMBERS, THE S-N CURVE FOR THE LIFE RANGE FROM 10^4 TO 10^6 CYCLES IS PRESENTED FOR A STRESS CYCLE OF ZERO-TO-TENSION. RADIOGRAPHIC AND ULTRASONIC INSPECTIONS WERE USED TO STUDY FATIGUE CRACK INITIATION AND PROPAGATION ORIGINATING AT AN INTERNAL WELD FLAW.

A PRELIMINARY INVESTIGATION OF THE AXIAL FATIGUE BEHAVIOR OF MIG WELDMENTS IN HY-130/150 STEEL IS REPORTED. THE MAJORITY OF THE TRANSVERSE BUTT-WELDED SPECIMENS PREPARED AT EACH OF THREE LABORATORIES INITIATED FATIGUE FAILURES AT A VARIETY OF INTERNAL DEFECTS WHEN SUBJECTED TO A CYCLIC MAXIMUM STRESS OF APPROXIMATELY HALF THE ULTIMATE STRENGTH OF THE BASE METAL. SEVERAL ALTERATIONS IN THE STANDARD MIG WELDING PROCEDURES WERE STUDIED IN AN EFFORT TO IMPROVE THE WELD QUALITY; HOWEVER NO MODIFICATION HAS BEEN ENTIRELY SUCCESSFUL IN ELIMINATING ALL THE DEFECTS WHICH HAVE PROVEN TO BE CRITICAL POINTS FOR FATIGUE CRACK NUCLEATION.

KEYWORDS:

Axial Fatigue Testing, HY-100 Steel, HY-130/150 Steel, Weldments, Non-Destructive Testing, Radiography, Ultrasonics, Crack Initiation, Crack Propagation

ILLINOIS UNIVERSITY, URBANA. DEPARTMENT OF CIVIL ENGINEERING

FATIGUE OF PLATES AND WELDMENTS IN HIGH STRENGTH STEELS, by J. B. Radziminski, R. W. Hinton, D. F. Meinheit, H. A. Osman, W. H. Bruckner, and W. H. Munse

February 1967, 143 pp.

Structural Research Series No. 318

Contract NObs 94232, Project Serial No. SF-020-01-05, Task 729-0

AN EVALUATION OF THE AXIAL FATIGUE BEHAVIOR OF TRANSVERSE BUTT-WELDED JOINTS IN HY-100 STEEL IS PRESENTED. WELDING PROCEDURES, USING MIL-12018 AND MIL-11018 ELECTRODES, HAVE BEEN DEVELOPED IN WHICH THE DEFECT DENSITY IS HELD TO A MINIMUM. SPECIMENS WELDED IN ACCORDANCE WITH THESE PROCEDURES INITIATED FATIGUE FAILURES ON THE SURFACE AT THE STRESS RAISER CREATED BY THE GEOMETRY AT THE TOE OF THE WELD. FOR THOSE MEMBERS, THE S-N CURVE FOR THE LIFE RANGE FROM 10^4 TO 10^6 CYCLES IS PRESENTED FOR A STRESS CYCLE OF ZERO-TO-TENSION. RADIOGRAPHIC AND ULTRASONIC INSPECTIONS WERE USED TO STUDY FATIGUE CRACK INITIATION AND PROPAGATION ORIGINATING AT AN INTERNAL WELD FLAW.

A PRELIMINARY INVESTIGATION OF THE AXIAL FATIGUE BEHAVIOR OF MIG WELDMENTS IN HY-130/150 STEEL IS REPORTED. THE MAJORITY OF THE TRANSVERSE BUTT-WELDED SPECIMENS PREPARED AT EACH OF THREE LABORATORIES INITIATED FATIGUE FAILURES AT A VARIETY OF INTERNAL DEFECTS WHEN SUBJECTED TO A CYCLIC MAXIMUM STRESS OF APPROXIMATELY HALF THE ULTIMATE STRENGTH OF THE BASE METAL. SEVERAL ALTERATIONS IN THE STANDARD MIG WELDING PROCEDURES WERE STUDIED IN AN EFFORT TO IMPROVE THE WELD QUALITY; HOWEVER NO MODIFICATION HAS BEEN ENTIRELY SUCCESSFUL IN ELIMINATING ALL THE DEFECTS WHICH HAVE PROVEN TO BE CRITICAL POINTS FOR FATIGUE CRACK NUCLEATION.

KEYWORDS:

Axial Fatigue Testing, HY-100 Steel, HY-130/150 Steel, Weldments, Non-Destructive Testing, Radiography, Ultrasonics, Crack Initiation, Crack Propagation

ILLINOIS UNIVERSITY, URBANA. DEPARTMENT OF CIVIL ENGINEERING

FATIGUE OF PLATES AND WELDMENTS IN HIGH STRENGTH STEELS, by J. B. Radziminski, R. W. Hinton, D. F. Meinheit, H. A. Osman, W. H. Bruckner, and W. H. Munse

February 1967, 143 pp.

Structural Research Series No. 318

Contract NObs 94232, Project Serial No. SF-020-01-05, Task 729-0

AN EVALUATION OF THE AXIAL FATIGUE BEHAVIOR OF TRANSVERSE BUTT-WELDED JOINTS IN HY-100 STEEL IS PRESENTED. WELDING PROCEDURES, USING MIL-12018 AND MIL-11018 ELECTRODES, HAVE BEEN DEVELOPED IN WHICH THE DEFECT DENSITY IS HELD TO A MINIMUM. SPECIMENS WELDED IN ACCORDANCE WITH THESE PROCEDURES INITIATED FATIGUE FAILURES ON THE SURFACE AT THE STRESS RAISER CREATED BY THE GEOMETRY AT THE TOE OF THE WELD. FOR THOSE MEMBERS, THE S-N CURVE FOR THE LIFE RANGE FROM 10^4 TO 10^6 CYCLES IS PRESENTED FOR A STRESS CYCLE OF ZERO-TO-TENSION. RADIOGRAPHIC AND ULTRASONIC INSPECTIONS WERE USED TO STUDY FATIGUE CRACK INITIATION AND PROPAGATION ORIGINATING AT AN INTERNAL WELD FLAW.

A PRELIMINARY INVESTIGATION OF THE AXIAL FATIGUE BEHAVIOR OF MIG WELDMENTS IN HY-130/150 STEEL IS REPORTED. THE MAJORITY OF THE TRANSVERSE BUTT-WELDED SPECIMENS PREPARED AT EACH OF THREE LABORATORIES INITIATED FATIGUE FAILURES AT A VARIETY OF INTERNAL DEFECTS WHEN SUBJECTED TO A CYCLIC MAXIMUM STRESS OF APPROXIMATELY HALF THE ULTIMATE STRENGTH OF THE BASE METAL. SEVERAL ALTERATIONS IN THE STANDARD MIG WELDING PROCEDURES WERE STUDIED IN AN EFFORT TO IMPROVE THE WELD QUALITY; HOWEVER NO MODIFICATION HAS BEEN ENTIRELY SUCCESSFUL IN ELIMINATING ALL THE DEFECTS WHICH HAVE PROVEN TO BE CRITICAL POINTS FOR FATIGUE CRACK NUCLEATION.

KEYWORDS:

Axial Fatigue Testing, HY-100 Steel, HY-130/150 Steel, Weldments, Non-Destructive Testing, Radiography, Ultrasonics, Crack Initiation, Crack Propagation